Assessing the paleoclimatic utility of the Indo-Pacific coral genus *Diploastrea* in a 225-year oxygen isotope record from Fiji

Abstract of a thesis presented to the Faculty

of the University at Albany, State University of New York

in partial fulfillment of the requirements

for the degree of

Master of Science

College of Arts and Sciences

Department of Earth and Atmospheric Sciences

Stefan Bagnato

2003

ABSTRACT

In the Western Pacific there remains, both spatially and temporally, a sparse record of surface ocean conditions and very few long paleoclimate records able to extend our understanding of this important region. The coral genus *Porites* is the common coral currently used for Pacific paleoclimate studies and has proven to be very useful. The massive coral *Diploastrea*, due to its slow growth rate and dense structure, may preserve temporally longer geochemical proxy records than *Porites* colonies of the same length. Its long lifespan and fossil history give this genus great potential, however no assessment has been made of the paleoclimatic utility of *Diploastrea* skeletons.

Presented here are *Diploastrea* $\delta^{18}O$ time series from Savusavu, Fiji, a region sensitive to combined SST and precipitation changes due to activity of the El Ni o Southern Oscillation (ENSO) and the South Pacific Convergence Zone (SPCZ). Sampling of a single skeletal element and/or a narrow sample track results in annual variations with the least amount of time averaging and greatest amplitude. Higher winter growth rates coupled with a constant sampling interval have preferentially captured winter conditions in the geochemical composition of *Diploastrea*'s skeleton. These winter-biased $\delta^{18}O$ time series illustrate that *Diploastrea* is as effective as *Porites* in recording the interannual environmental history of the region, dominated by both sea surface temperature (SST) and SPCZ-related rainfall. Examination of SST and precipitation data suggests that the trend component in *Porites* $\delta^{18}O$ at this site is amplified relative to observed trends in SST and expected trends in $\delta^{18}O_{seawater}$, and that *Diploastrea*-generated $\delta^{18}O$ time series more closely reflects variability on this time scale. Utilizing Singular Spectrum Analysis (SSA) analysis, it is demonstrated that

ACKNOWLEDGEMENTS

This thesis is not only the culmination of my own work, but is the result of the contributions of several people. I am most grateful to Brad Linsley for giving me the opportunity to be part of such an amazing and interesting project, and to do field work in Fiji, a truly incredible experience. Encouraging independent thought and exploration, while at the same time providing essential guidance, his advice through this project has been immeasurable.

I would also like to thank the guru of the isotope lab, Steve Howe. Steve s hard work and dedication to high quality isotope analyses are responsible for most of the data presented here. Thanks are also extended to Peter deMenocal at the Lamont-Doherty Earth Observatory of Columbia University for use of the ICP-AES for Sr/Ca analyses. Additionally Dave Anderson at the NOAA Paleoclimatology Program and Gilbert Compo at the NOAA Climate Diagnostics Center provided invaluable assistance and advice on time series analysis techniques and interpretation of the coral records.

Many thanks to Dave Mucciarone and Tom Potts for their assistance, and camaraderie in the field, and to my committee members Jerry Wellington and Don Rodbell for their input on this thesis.

Funding for this research was provided by the National Oceanic and Atmospheric Administration and the National Science Foundation.

TABLE OF CONTENTS

LIST OF FIGURES

LIST OF TABLES

Assessing the paleoclimatic utility of the Indo-Pacific coral genus *Diploastrea*

in a 225-year oxygen isotope record from Fiji

A thesis presented to the Faculty

of the University at Albany, State University of New York

in partial fulfillment of the requirements

for the degree of

Master of Science

College of Arts and Sciences

Department of Earth and Atmospheric Sciences

Stefan Bagnato

2003

CHAPTER 1

INTRODUCTION TO MAIN PROBLEMS AND OBJECTIVES

Climate change in the tropics plays a pivotal role in global-scale climate on various time scales, from interannual to glacial (e.g., Cole et al., 2000; Lea et al, 2000; Linsley et al., 2000a; Tudhope et al., 2001; Hendy et al., 2002; Seltzer et al., 2002). The interannual El Ni o Southern Oscillation (ENSO), a tropical Pacific phenomenon, is a prime example, affecting climate worldwide. An interdecadal scale pattern of sea surface temperature (SST) variability in the Pacific has been identified (Mantua et al., 1997; Zhang et al., 1997; Power et al., 1999a; Power et al., 1999b; Garreaud and Battisti, 1999; Salinger et al., 2001) that is spatially similar to ENSO but whose forcing (tropical or extratropical) is still poorly understood (Latif and Barnett, 1994). Because continuous measurements of physical ocean properties such as temperature and salinity generally do not span more than 50 years before present in the tropical Pacific, a period likely already affected by human activities, natural variability in such components of the ocean-atmosphere system remain poorly understood. It is therefore necessary to extend these climate records to pre-anthropogenic times with proxy records.

For reconstructing past variability of the tropical surface ocean, massive scleractinian corals probably provide the best annually resolved proxy data because the incorporation of various elements and isotopes into their carbonate skeletons is driven in large part by ocean conditions (e.g., Shen et al., 1992; Fairbanks et al., 1997; Gagan et al., 2000). Coral skeletons incorporate several chemical tracers that have been correlated with important oceanic and atmospheric parameters, including temperature, salinity, rainfall, river runoff, ocean mixing, and anthropogenic influence, depending on the site. The chemistry of coral aragonite skeleton has therefore proven to be a very powerful tool for climate reconstructions on seasonal to millennial time scales (Quinn et al., 1993;

Dunbar et al., 1994; Charles et al., 1997; Linsley et al., 2000a; Tudhope et al., 2001, among many others).

Given the fact that corals grow continuously at rates of several millimeters to a couple of centimeters per year and can live for centuries, living specimens (commonly 200-400 years old) can be used to study the recent past, while fossil coral reef sequences can yield environmental information about the late Quaternary. The formation of annual density bands, couplets of high and low-density material, usually provides an excellent chronology in many corals, yielding absolute age assignments similar to tree rings over the time period of study. However the banding is not always evident and in the absence of distinct annual banding, the annual periodicity of isotopic and/or trace metal analyses can be used to develop a chronology with annual resolution (Alibert and McCulloch, 1997; Charles et al., 1997; Linsley et al., 2000b).

Corals have been successfully used to reconstruct various features of the coupled oceanic-atmospheric system. The $\delta^{18}O$ of massive corals has been used to reconstruct SST, salinity (SSS), and the $\delta^{18}O$ composition of seawater (Dunbar and Wellington, 1981; Cole and Fairbanks, 1990; Cole et al., 1993; Quinn et al., 1993; Linsley et al., 1994; Charles et al., 1997; Linsley et al., 2000b, LeBec et al., 2000). Additionally, past ENSO activity has been identified using Pacific coral $\delta^{18}O$ from equatorial regions (McConnaughey, 1989; Cole and Fairbanks, 1990; Cole et al., 1993; Dunbar et al., 1994; Corr ge et al., 2000; Urban et al., 2000; Tudhope et al., 2001). It has been well documented that the $\delta^{18}O$ of coral skeleton is a function of both temperature and the $\delta^{18}O$ of seawater. At some sites it has been possible to deconvolve temperature and salinity using a salinity-independent temperature proxy in concert with $\delta^{18}O$. The Sr/Ca and

Mg/Ca ratio are highly correlated with SST at some sites and are a common choice (Smith et al., 1979; Beck et al., 1992; deVilliers et al., 1994; McCulloch et al., 1994; Mitsuguchi et al., 1996; Alibert and McCulloch, 1997; Schrag, 1999). Massive corals have proven particularly useful in studying interannual variability, but understanding of decadal changes in ocean properties has had more limited success due to various problems, including a general lack of long coral records.

One common and significant shortcoming of many coral proxy records is their length. It is difficult to evaluate climate variability with decadal and multi-decadal scale periodicity utilizing records which only capture a few cycles. Much coral-based paleoclimate work to date in the Pacific has utilized the genus *Porites*, due to its wide geographic range and high annual growth rate of approximately 1 cm per year. The high growth rate has allowed for extremely high resolution sampling (near monthly or better), but unfortunately the lifespan of this coral genus is generally not sufficient to create proxy records of ocean conditions in excess of ~300 years. The genus *Diploastrea*, however, has a much slower annual growth rate of approximately 4-6 mm per year, which coupled with a denser structure more resistant to boring organisms and grazing fish, promotes a longer lifespan and potentially a temporally longer coral proxy record.

Coral cores of *Diploastrea* and *Porites* were recently retrieved from the same bay in the Fiji Islands, creating a unique opportunity for calibration and comparison. Calibration of *Diploastrea* could provide a means to assess interannual and interdecadal scale variability in the tropical Pacific over a longer multi-century period than would be possible using *Porites*. The objective of this thesis is to calibrate *Diploastrea* coral cores by comparing isotopic data to measured oceanographic data and climate indices and to an existing *Porites* record from the same location. Following calibration, it is demonstrated that *Diploastrea* $\delta^{18}O$ time series faithfully record the interannual, interdecadal, and secular trend scale environmental history of the region, and hold the potential to extend instrumental records and climate indices beyond that possible using the genus *Porites*.

CHAPTER 2

CALIBRATING THE CORAL *DIPLOASTREA HELIOPORA* FOR PALEOCLIMATE RECONSTRUCTION

ABSTRACT

The success of coral-based paleoclimate research in the Pacific remains mostly on interannual time scales, characterization of the globally important El Ni o Southern Oscillation (ENSO) system being a prime example. The principal coral archive utilized in the Pacific for this effort has been the genus *Porites*. The Indo-Pacific coral genus *Diploastrea*, however, due to its slower extension rate, denser structure, and longer lifespan, can potentially preserve geochemical proxy records 2-3 times longer than *Porites* cores of the same length. Before its potential can be realized, *Diploastrea* must first be calibrated and its climate signal assessed. A calibration using two *Diploastrea* cores from Fiji (16… 49 S, 179… 14 E) is presented here that allow for simultaneous calibration and evaluation of the reproducibility of $\delta^{18}O$ at this site. Comparison to a *Porites* $\delta^{18}O$ record from the same location allows for further validation of *Diploastrea* s climate signal, dominated by ENSO and South Pacific Convergence Zone (SPCZ) variability. It is demonstrated that the $\delta^{18}O$ of *Diploastrea* skeletons has the ability to capture interannual climate variability with equal success as *Porites* corals while at the same time have the lifespan necessary to capture interdecadal variability.

INTRODUCTION

The value of coral proxy records in the Pacific is enormous given the short and spatially sparse instrumental climate record, especially in the Western Pacific. The chemistry of coral aragonite has proven to be a very powerful tool in reconstructing various features of the coupled oceanic-atmospheric system including sea surface temperature (SST), sea surface salinity (SSS), and the $\delta^{18}O$ composition of seawater (Dunbar and Wellington. 1981; Cole and Fairbanks, 1990; Cole et al., 1993; Quinn et al., 1993; Linsley et al., 1994; Charles et al., 1997; Linsley et al., 2000b; LeBec et al., 2000).

The coral genus *Porites* has been the primary Pacific coral archive of climate variability to date and evaluation of ENSO-scale variability has been a large success of such coral proxy records (McConnaughey, 1989; Cole and Fairbanks, 1990; Cole et al., 1993; Dunbar et al., 1994; Tudhope et al., 2001). However very few Pacific *Porites* records exist which span more than 100 years (Cole et al., 1993; Linsley et al., 1994; Dunbar et al., 1994; Quinn et al., 1998; Boiseau et al., 1998; Cole et al., 2000; Linsley et al., 2000a; Urban et al., 2000), a significant limitation in addressing climate variability with decadal and multi-decadal periodicity. The massive coral genus *Diploastrea*, however, has a skeletal extension rate 2-3 times slower than *Porites*, which in itself suggests that *Diploastrea* colonies can yield longer proxy records than *Porites* colonies of the same length. Additionally, *Diploastrea* has a dense skeletal structure which is resistant to boring organisms, grazing fish, and the destructive crown-of-thorns starfish, promoting a longer lifespan (Vernon, 1986).

Here the effect of sampling different skeletal elements of *Diploastrea* and sample track width on the amplitude of the seasonal $\delta^{18}O$ cycle is evaluated, and after determining the preferred sampling regime, the $\delta^{18}O$ time series are compared to instrumental climate data and indices. Comparison of both *Diploastrea* cores to the *Porites* record of Linsley et al. (in review) helps to validate the chosen sampling techniques, and illustrates the reproducibility of $\delta^{18}O$ in these Fiji corals. A discussion of *Diploastrea* s ability to accurately resolve both interdecadal and trend-scale climate variability at this site follows in Chapter 4.

STUDY AREA

The Fiji Islands lie in the western subtropical South Pacific and consist of approximately one hundred small islands and two large main islands, Viti Levi and Vanua Levu. Corals were collected from Savusavu Bay, a large bay open to the Koro Sea, on the northern Fijian island of Vanua Levu (16… 49 S, 179… 14 E) (Fig. 1). Four rivers empty into Savusavu Bay, the Ndreke ni wai, the Lango lango, the Vianga, and the Na Tua vou. The average SST in this region is 27.2¡C, with an annual range of about 4¡C. Although Fiji lies significantly south of the equator and outside the heart of the Western Pacific Warm Pool, a region with strong temperature anomalies associated with ENSO, this site is well positioned to record the activity of the SPCZ, and the Southern Oscillation (SO), both globally important climate features. Although *Diploastrea* s geographic range is limited to the Indian and Western Pacific Oceans, the geochemistry of its skeleton, once calibrated, offers additional future potential for studying connections between these two ocean basins, and between ENSO and Asian monsoon variability.

Figure 1. Location map showing Fiji's position in the western subtropical South Pacific and an enlargement of the study area, Savusavu Bay on the northern Fijian island of Vanua Levu.

The axis of SPCZ maximum rainfall for 1958-1998 extends from New Guinea towards French Polynesia, passing between Fiji and Samoa (Fig. 2). The SPCZ is the dominant climatic feature of the Southern Hemisphere subtropics, and its position and activity are modulated by the ENSO and the Interdecadal Pacific Oscillation (IPO) (Trenberth, 1976; Kiladis et al., 1989; Folland et al., 2002). When the SPCZ migrates northward during El Ni o events, drier than average conditions exist in Fiji, while southward displacement of the SPCZ during La Ni a events brings wetter than average conditions (Salinger et al., 1995), thus altering the $\delta^{18}O_{seawater}$. Fiji, lying near the hinge point of Southern Oscillation effects on SST and near the southernmost displacement of the SPCZ, should experience small ENSO-related SST anomalies and relatively large precipitation anomalies on ENSO time scales.

METHODS

Coral Collection and Preparation

In April 1997 a 30 cm coral core (4F1) from a colony of *Diploastrea* was collected by hydraulic drill in ~10 m of water and in December 2001 a 1.3 m coral core (LH) was collected from a second *Diploastrea* colony in 2 m of water, both from the outer edge of Savusavu Bay on the south side of Vanua Levu, Fiji (16… 49 S, 179… 14 E). A 2.3-m-long *Porites* core (1F) (Linsley et al., in review) was collected from the middle of Savusavu Bay in 10 m of water in April 1997. Core preparation and isotope analyses follow the procedures of Linsley et al. (2000b). The cores were washed with fresh water, dried and sectioned into 7-mm-thick slabs along the major growth axes using a band saw.

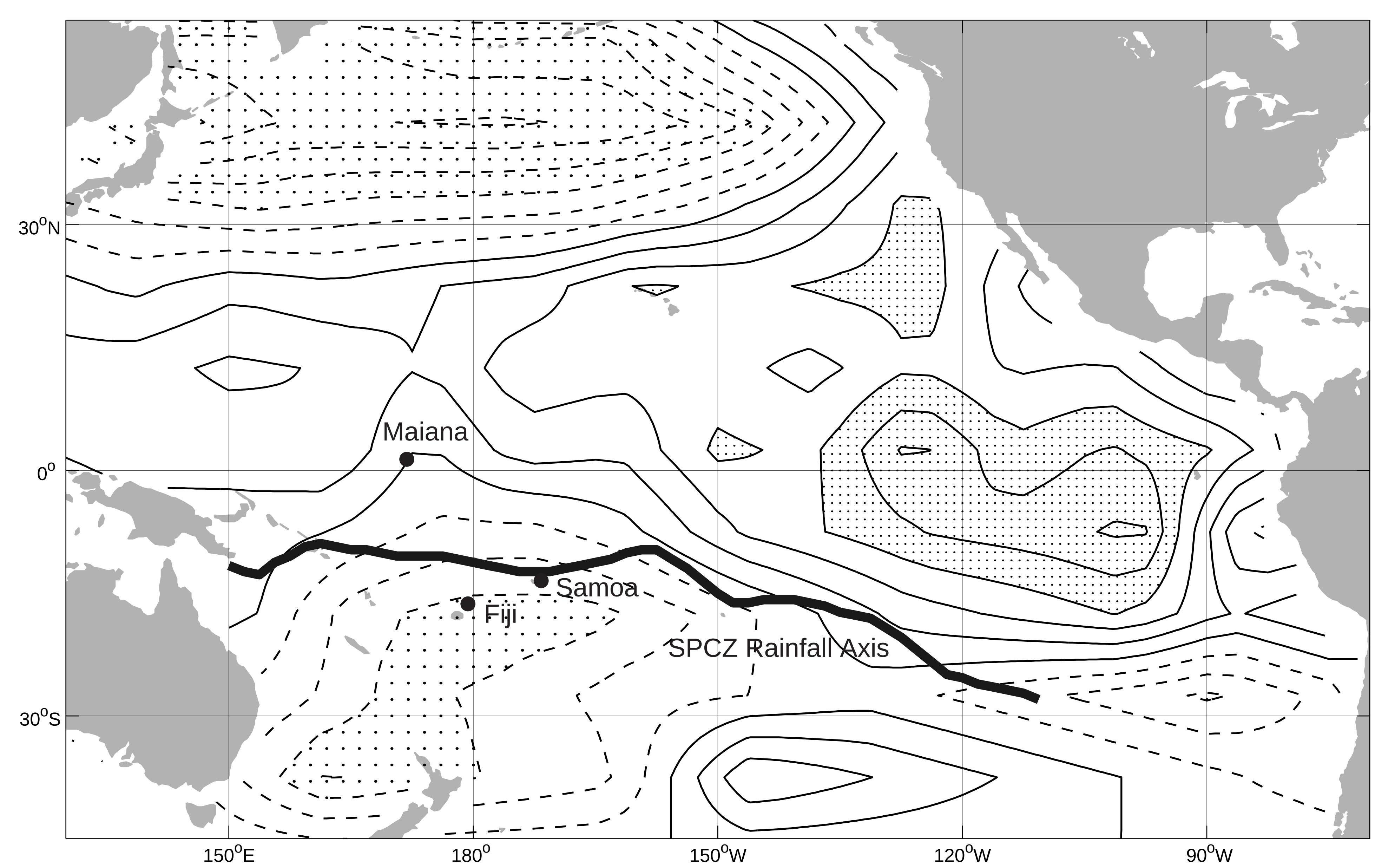

Figure 2. Location of Fiji, Samoa, and Maiana in relationship to the South Pacific Convergence Zone rainfall axis and the spatial pattern of the IPO (from Folland et al., 2002). Background contours show the IPO as a convariance map of the 3rd EOF of low-pass filtered SST anomalies for 1911-1995. The contour interval is 0.04 °C, negative contours are dashed, values <-0.12°C lightly stippled and those >+0.12°C heavily stippled. Figure modified from Folland et al. (2002).

The slabs were then X-rayed to reveal the annual density bands. The slabs were cleaned with deionized water in an ultrasonic bath for approximately 15 minutes to dislodge saw cuttings, then placed in a drying oven at 40…C overnight. Subannual skeletal samples were collected using a Dremel Tool with a 1-mm-diameter round diamond drill bit under a binocular microscope along corallite traces identified both by eye and on the X-ray positives. Each core was sampled at 0.5 mm intervals throughout the upper 50 mm for calibration purposes and at 1 mm intervals below 50 mm. Detailed sampling protocols are discussed in the results section of this chapter.

Stable Isotope Mass Spectrometric Analysis

For each sample, approximately 200 g of coral powder was dissolved in 100% H_3PO_4 at 90…C in a Multiprep sample preparation device and the resulting CO_2 gas was analyzed using a Micromass Optima gas-source triple-collector mass spectrometer at the University at Albany, State University of New York stable isotope laboratory. The total number of subannual samples analyzed from core 4F1 analyzed was 554, with approximately 10% of these being analyzed in duplicate. During the course of analyzing core 4F1, the average standard deviation of the isotopic compositions of international standard NBS-19 was 0.019 for $\delta^{13}C$ and 0.035 for $\delta^{18}O$ (n=100). The average difference between the replicate coral samples analyzed was 0.06 for $\delta^{13}C$ and 0.06 for $\delta^{18}O$ (n=70). The total number of subannual samples analyzed from core LH was 1343, with approximately 10% of these being analyzed in duplicate. During the course of analyzing core LH, the average standard deviation of NBS-19 was 0.015 for $\delta^{13}C$ and 0.034 for $\delta^{18}O$ (n=258). The average difference between replicate samples analyzed was 0.08 for $\delta^{13}C$ and 0.07 for $\delta^{18}O$ (n=174). All data are reported as per mil deviations relative to Vienna Peedee belemnite (VPDB).

ICP-AES Analysis

For each sample, approximately 100 g of coral powder was dissolved in ~2 mL of 2% HNO_3 and introduced as an aerosol to a Jobin-Yvon Panorama inductively coupled plasma atomic emission spectrometer at the Lamont-Doherty Earth Observatory of Columbia University, using procedures similar to those described by Schrag (1999). Measurement of the Sr/Ca ratio used splits of the same samples used for oxygen and carbon isotopic analysis. A total of 235 subannual samples were analyzed from core 4F1, with approximately 10% being analyzed in duplicate. During the course of the analyses, the average relative standard deviation of the replicate samples analyzed was 0.22% (n=18). A total of 245 subannual samples were analyzed from core LH, with approximately 10% being analyzed in duplicate. During the course of the analyses, the average relative standard deviation of the replicate samples analyzed was 0.18% (n=24).

Potential Coral Growth Effects

Coral skeleton is not deposited inorganically; rather it is accomplished through a biologically mediated process which can impart growth effects on skeletal chemistry. For some time, the rate of coral growth has been suspected to affect the $\delta^{18}O$ disequilibrium offset (Land et al., 1975; McConnaughey, 1989; Wellington et al., 1996; deVilliers et al., 1995). This vital effect , if overlooked, can give the appearance of climatic change in an isotopic time series when it is in fact a biological signal. It is therefore a very important consideration when sampling corals, and is most often addressed through careful sampling along the axis of maximum growth, where this effect this thought to be constant (Land et al., 1975; McConnaughey, 1989; Wellington et al., 1996). Coral $\delta^{18}O$ is several parts per mil more depleted than aragonite precipitated in equilibrium with ocean water, and this offset from $\delta^{18}O$ equilibrium is known to shift outside the maximum growth axis (Cohen and Hart, 1997). There is concern, however, that the vital effect may not be constant over the life of a very large/old coral spanning more than a couple of centuries (Barnes et al., 1995) because tissue layer thickness and skeletal density can change through time.

The concern of the stability of the disequilibrium offset over time is well-based. Many coral isotopic time series show a clear trend toward lighter $\delta^{18}O$ values approaching present day (Druffel and Griffin, 1993; Linsley et al., 1994; Quinn et al.,1998; Urban et al., 2000; Hendy et al., 2002), which may or may not be climate-induced. Some researchers have chosen to de-trend their data in order to focus on the interannual and decadal changes in the records. In the hope of avoiding vital effect problems, both *Diploastrea* cores were drilled and sampled as close to the maximum growth axis as was possible. *Diploastrea* corallites grow in much straighter paths than those in *Porites*, facilitating sampling. Core 4F1 was sampled continuously without switching corallites and core LH only required switching sampling paths 3 times, creating nearly uninterrupted records from each core s collection date.

Concern over biological effects on environmental tracers in corals is not limited to stable isotopes. The Sr/Ca ratio of coral aragonite, a common SST proxy, may also be affected by coral growth. Significant correlation between coral skeletal Sr/Ca and SST s at many sites in the tropics has been used as the basis for developing paleo-SST reconstructions over the past several centuries (Beck et al., 1992; deVilliers et al., 1994;

Shen et al., 1996; Alibert and McCulloch, 1997; Linsley et al., 2000a). The underlying assumption for the past ~10 years has been that the coral Sr/Ca ratio is controlled by the same simple thermodynamic laws that govern the precipitation of inorganic aragonite. However the incorporation of Sr and Ca into coral aragonite, like oxygen isotopes, is biologically mediated and not completely understood. The mystery about biological control on aragonite precipitation in corals has begun to raise some doubt about the efficacy of the Sr/Ca ratio in paleoclimate applications. Cohen et al. (2001) report significant variability between daytime calcification rate and nighttime calcification rate, and that the nighttime portion of the skeleton should be sampled because only the chemistry of nighttime skeleton is truly temperature-dependent. Such results fuel a strong controversy about the extent of biological bias that exists in climatic information derived from various tracers in corals. However, the study of Cohen et al. (2001) sampled mostly from within the tissue layer, which has been shown to produce discrepant isotopic and trace metal values. Additionally, their Sr/Ca-SST calibration equation is not significantly different from most bulk sampling studies to warrant drastic changes in the use of this tracer at present. Clearly more work is required to fully understand the effects of complicated coral growth on environmental tracers.

Chronology

The isotopic analyses show a strong and obvious annual cycle, while the density banding in these *Diploastrea* colonies is not distinct over the entire length of the cores, although identified bands do appear to be annual. Therefore, the annual periodicity of skeletal $\delta^{18}O$ was used to develop the chronology for the cores. Because average annual $\delta^{18}O$ amplitude is close to that expected if water temperature was the controlling factor, satellite-derived monthly SST data (1970-2001) from the 2… x 2… grid encompassing Savusavu Bay (Reynolds and Smith, 1994) was used to develop the age models. The $\delta^{18}O$ data were tuned to the SST record by assigning the lowest $\delta^{18}O$ value of each year to the highest SST and the highest $\delta^{18}O$ value of each year to the lowest SST. Age assignments were then linearly interpolated between these two annual anchor points which unavoidably introduces a couple of months of error because corals do not grow uniformly throughout the year. The monthly SST dataset is only available as far back as 1970, so for age assignments before 1970 the lowest $\delta^{18}O$ values were assigned to March and the highest $\delta^{18}O$ values were assigned to August (March and August being the average times of highest and lowest SST respectively from 1970-1997). It should be noted that these temperature extremes do vary from year to year, introducing the potential for additional temporal error on the order of 1 to 2 months in years prior to 1970.

The coral $\delta^{18}O$ data were tuned to the SST record for age assignment, but it is well known that coral skeletal $\delta^{18}O$ is affected by both SST and $\delta^{18}O_{seawater}$. While the Sr/Ca ratio is thought to be a more pure temperature proxy than $\delta^{18}O$ (Beck et al., 1992; deVillers et al., 1994; McCulloch et al., 1994), at this location there is no time lag between the annual cycles in skeletal Sr/Ca and $\delta^{18}O$ (Fig. 3), indicating that corresponding cycles in SST and $\delta^{18}O_{seawater}$ are also coincident. This is consistent with instrumental data from this region. Rainfall data from several sites around Fiji indicate that on average March and August also have the highest and lowest precipitation, respectively. The phase-locked nature of SST and precipitation is confirmed by the correlation coefficients between two SST datasets (Reynolds and Smith, 1994) and precipitation (Kalnay et al., 1996) at this site (r= 0.80 and 0.88 respectively) (Table 1).

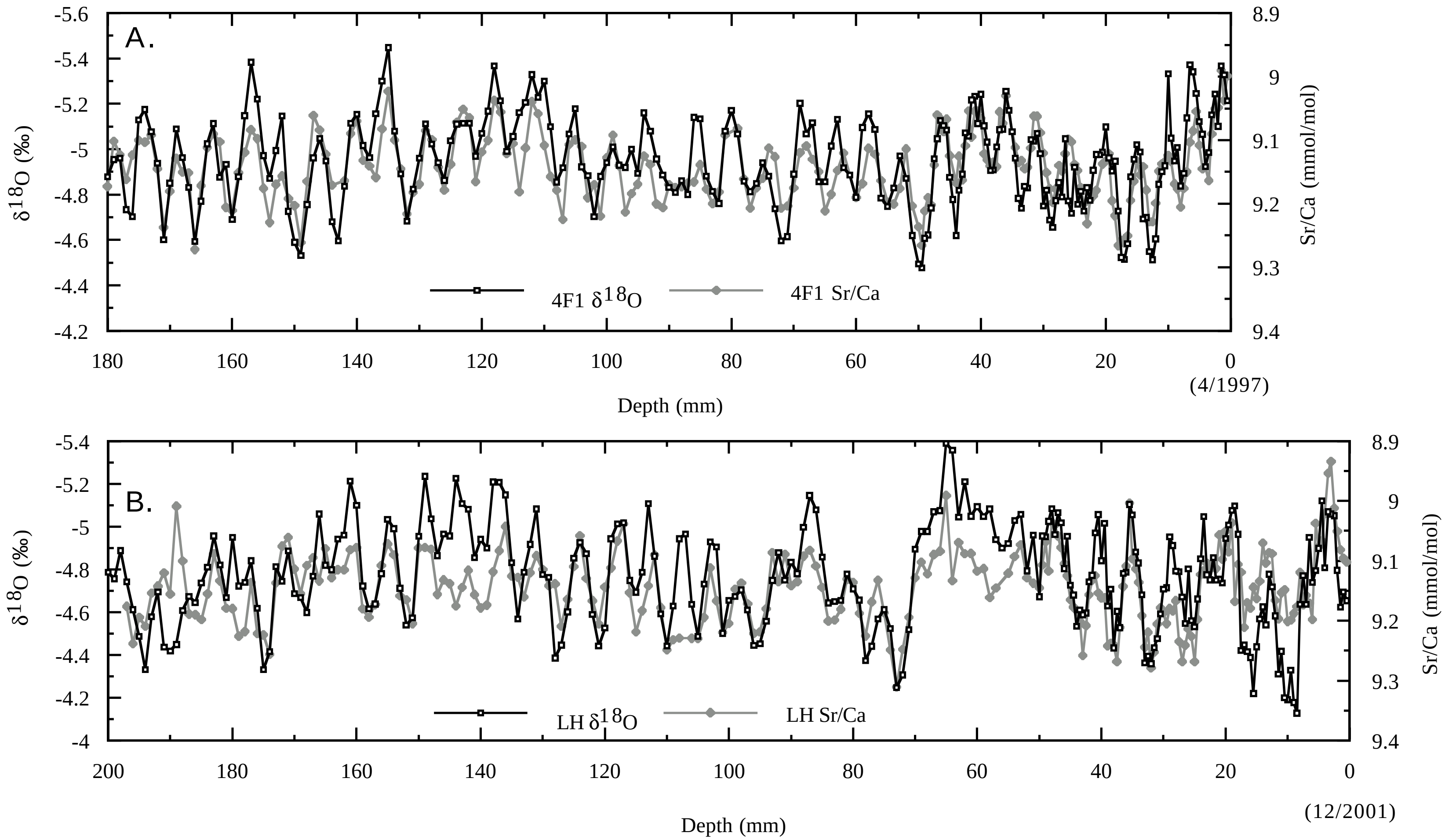

Figure 3. Sr/Ca and $\delta^{18}O$ from the upper 200mm (~35 years) of *Diploastrea* core 4F1 (A) collected in 1997 and LH (B) collected in 2001. The phase-locked relationship between the two tracers indicates that either may be used for age control via tuning to the SST record without conflicting influence from variable seawater chemistry.

Table 1. Correlation matrix for bimonthly Fiji coral and climate data between 1970 and 1997 unless otherwise noted.

	4F1 $\delta^{18}O$	**LH $\delta^{18}O$**	**1F $\delta^{18}O$**	**CAC SST**	**IGOSS SST**	**SSS**	**Precip**
4F1 $\delta^{18}O$	-						
LH $\delta^{18}O$	0.58	-					
1F $\delta^{18}O$	0.54	0.61	-				
CAC SST	-0.63	-0.64	-0.77	-			
IGOSS SST*	-0.75	-0.58	-0.75	0.998	-		
SSS**	0.53	0.56	0.59	-0.42	-0.39	-	
Precipitation	-0.61	-0.62	-0.60	0.80	0.88	-0.34	-

Table 2. Correlation matrix for annual average Fiji coral and climate data between 1970 and 1997 unless otherwise noted.

	4F1 $\delta^{18}O$	**LH $\delta^{18}O$**	**1F $\delta^{18}O$**	**CAC SST**	**IGOSS SST**	**SSS**	**Precip**
4F1 $\delta^{18}O$	-						
LH $\delta^{18}O$	0.45	-					
1F $\delta^{18}O$	0.42	0.52	-				
CAC SST	-0.51	-0.67	-0.75	-			
IGOSS SST*	-0.36	-0.51	-0.37	0.69	-		
SSS**	0.54	0.53	0.88	-0.68	-0.37	-	
Precipitation	-0.55	-0.78	-0.30	0.53	0.53	-0.49	-

* IGOSS SST Data 1982-1997

** SSS Data 1976-1997, from Gouriou and Delcroix (2002)

These correlations, although weaker than bimonthly data, persist for annually averaged data, suggesting that this is a regionally significant relationship (Table 2). This reinforces the assignment of the lowest $\delta^{18}O$ values in a given year to March and that at this location either geochemical tracer will provide comparable age control and seawater chemistry will not affect the choice of SST as the chronology tool. Highly correlated interannual temperature and rainfall at this site is most likely due to the intimate link between the ENSO and the SPCZ (Vincent, 1994; Salinger et al., 1995; Salinger et al., 2001; Folland et al., 2002), producing equally significant SST and precipitation anomalies in the region surrounding Fiji. Thus, both SST and precipitation variability in this region should be recorded by coral $\delta^{18}O$ at this site. For some locations in the Pacific however, extremes in temperature and precipitation or salinity do not necessarily coincide. Clearly, data from both improves confidence in the developed age model, perhaps the most important step in coral-based paleoclimate work.

Linear interpolation between the two subannual tie points of each year allowed for conversion of isotope data to the time domain and is generally considered the most objective method despite the coral s uneven growth rate through the year (Charles et al., 1997). A 1 mm sample interval in the *Diploastrea* cores yields ~5-6 samples per year on average, but due to the inconsistent growth rate this recovery ranged from as low as 2 to as high as 9 samples per year, so the sampling regime cannot accurately be called bimonthly. Because the SST and other climate data are monthly while the coral isotopic data have unequal time steps, all coral and instrumental data presented here were linearly interpolated to 6 points per year using the Timer program from the Arand software package (P. Howell, per. comm.) to facilitate comparison of the records.

RESULTS AND DISCUSSION

Sampling regime effect on the annual cycle

The width of a sampling transect in *Porites* cores usually incorporates 3-4 corallites because the individual polyps are approximately 0.5 mm in diameter. This averaging of endothecal and exothecal material from 3-4 individuals of the colony is unavoidable with bulk sampling methods but is however thought to minimize any geochemical spatial variations in the skeleton. For corals with larger polyps, like *Diploastrea*, there is concern that different skeletal elements in the same time horizon of an individual corallite may show geochemical heterogeneity even when deposited under the same conditions (Land et al., 1975; Dodge et al., 1992; Leder et al., 1996) (Fig. 4). This problem is complicated by the possible complex saw tooth-like pattern of synchronous time horizons (Land et al., 1975; Leder et al., 1996). The recent study of Watanabe et al. (2003), which evaluated this possible sampling effect in *Diploastrea*, was published near the completion of this project, and thus it was necessary to look to other analogous coral genera on which such an evaluation had previously been made. The genus *Montastrea*, a large-polyped, slow-growing Caribbean coral was studied by Dodge et al. (1992) and Leder et al. (1996) and is likely the best published analogue for *Diploastrea*. Dodge et al. (1992) recognized growth differences between endothecal and exothecal material, with lines of skeletal deposition comprising a greater vertical dimension for endothecal than exothecal material. The authors recommend restricted sampling of exothecal material for a more accurate chronology. Leder et al. (1996) noted isotopic variations between skeletal elements of *Montastrea*; the endothecal material showing reduced seasonal amplitude of $\delta^{18}O$ and a more irregular annual cycle, relative

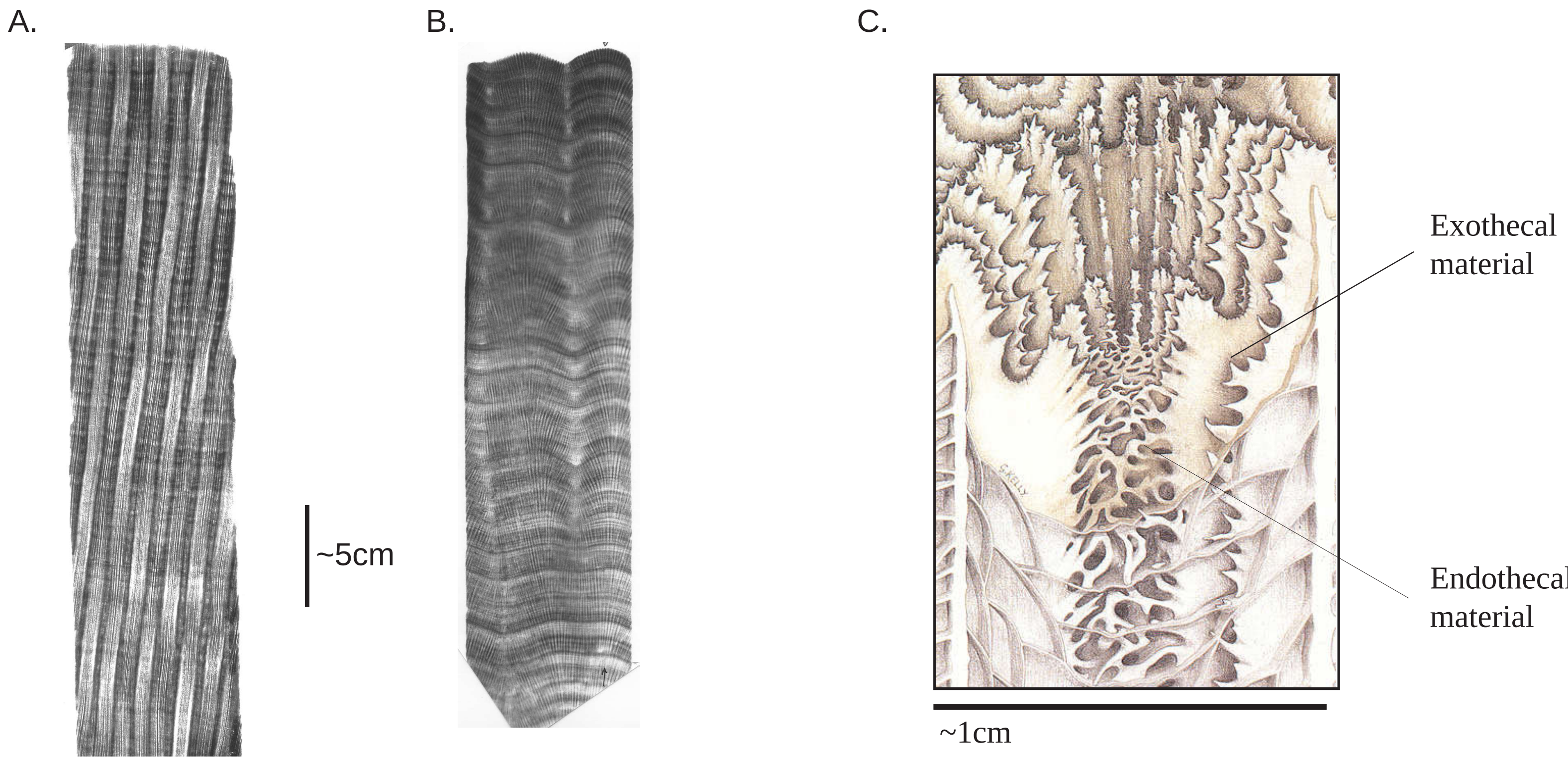

Figure 4. X-radiograph positives of the upper ~30cm of Fiji *Diploastrea* core 4F1 (A) and Fiji *Porites* core 1F (B), both collected in April 1997. The clear inter-genus differences are the much larger corallites in *Diploastrea* relative to *Porites*, and that *Diploastrea* contains 2-3 times as many annual density bands in this interval as *Porites*, the latter creating a longer paleoclimatic record in the same length of core. (C) Sketch of generic corallite showing exothecal and endothecal regions, modified from Vernon (1986). Different skeletal elements can have different isotopic values, even when deposited under the same conditions and complex growth surface geometry can cause time averaging for large-polyped corals like *Diploastrea.* These potential smoothing mechanisms necessitate narrow, single skeletal element sample paths to yield the best possible climate signal using oxygen isotopes.

to time-synchronous exothecal elements. Additionally, stain lines in this coral illustrated that the growth surface is not flat and parallel to the external surface, rather it has a jagged saw tooth pattern, suggesting that wide sampling tracks with a mixture of skeletal elements may result in reduced sensitivity due to time averaging.

To address this sampling concern and to determine the best sampling regime for *Diploastrea*, three time-synchronous sample transects were made in the upper 50 mm of core 4F1, one incorporating only exothecal material, one incorporating endothecal material, and the third incorporating a mixture of exothecal and endothecal material from the full width of a corallite, all at near monthly resolution (0.5 mm sample interval). The isotopic records from the skeletal transects are plotted together versus time in Figure 5, each with their own age model. The exothecal and endothecal transects generally show higher seasonal amplitude than the transect using a mixture of skeletal material. This result is interpreted to be due to the extreme differences in sample track width. Not knowing the exact growth surface geometry of *Diploastrea*, it can only be assumed that the growth surface is similar to that observed in *Montastrea* and other corals (Land et al., 1975; Leder et al., 1996). For the mixed skeletal element transect it was necessary to sample the full corallite width, on the order of 1 cm. Such a wide sampling track increases the amount of time averaging because samples are retrieved perpendicular to the growth axis and therefore cross-cut the jagged growth surface. Meanwhile the single element transects had a width of only 5 and 3 mm for the exothecal and endothecal transects, respectively, greatly reducing the amount of time averaging.

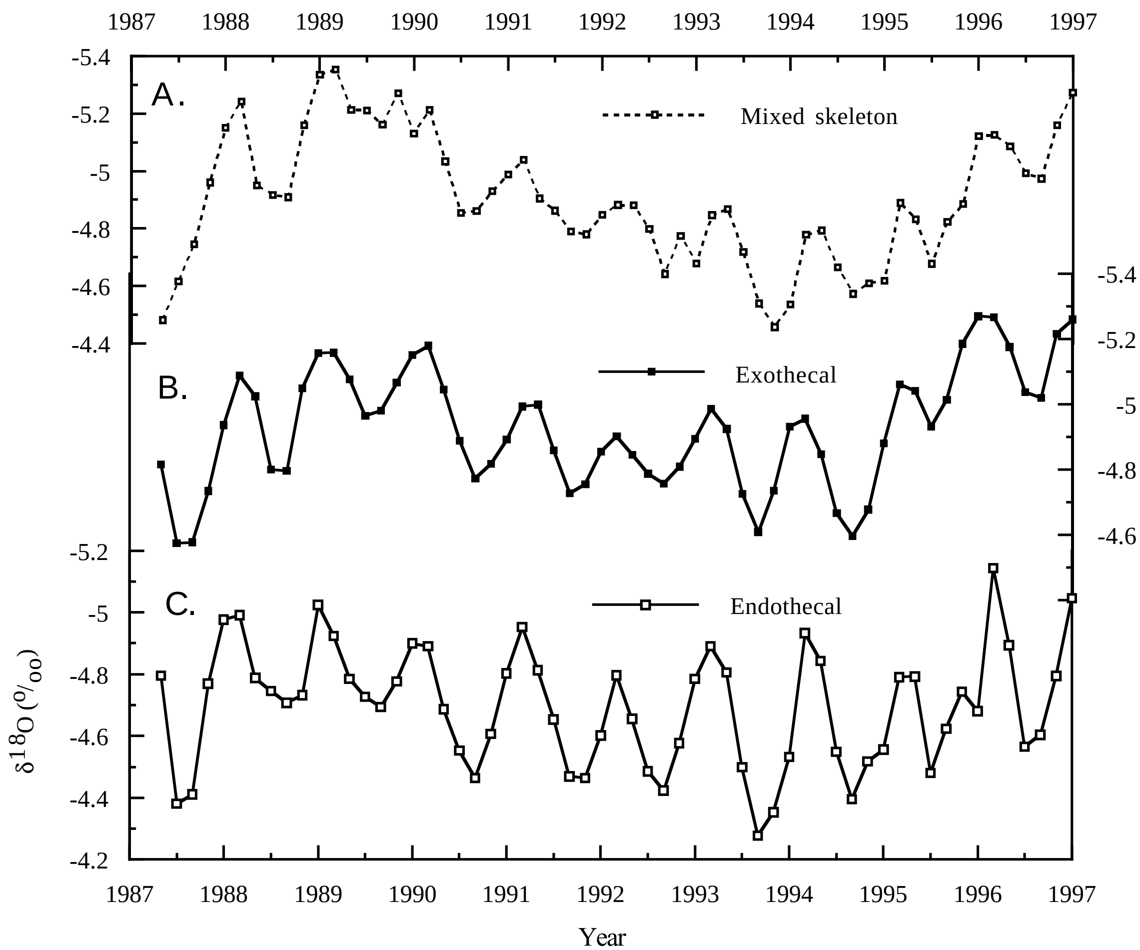

Figure 5. Oxygen isotopic time series from three experimental sample transects in the upper 50 mm of *Diploastrea* core 4F1 utilizing a mixture of skeletal elements (A), exothecal material (B), and endothecal material (C), each with their own age model. Endothecal material seems to yield the largest annual $\delta^{18}O$ amplitude, however the large effect of time averaging indicates that this greater seasonal amplitude may not be due to the inherent nature of endothecal material, but rather the narrow sample path used. This study is not able to distinguish these effects and therefore exothecal skeletal material was used in this study given its recommendation for other large-polyped corals (Dodge et al., 1992; Leder et al., 1996) and its sufficient seasonal amplitude for resolving the interannual and interdecadal signal. However, the recent study of Watanabe et al. (2003) was able to minimize time averaging by using a constant sample path of 2 mm, and suggests that endothecal material may hold the greatest seasonal amplitude for $\delta^{18}O$.

Showing increased amplitude with decreasing sample track width, it is hard to establish whether the inherent heterogeneity of different skeletal regions or the width of sample transects is more important in generating a climate signal with the highest amplitude. It therefore seems necessary to preferentially sample only a single *Diploastrea* skeletal element to more accurately capture the annual cycle, while sampling in as narrow a track as possible to reduce time averaging due to the coral s saw tooth-like growth surface. Although endothecal material yields the largest annual $\delta^{18}O$ amplitude, it was decided to sample both cores using just exothecal material because (1) exothecal material has a more consistent thickness and density and therefore easier to sample (2) all three methods recorded the same interannual signal, and (3) of the preference for analysis of exothecal material in *Montastrea* (the closest possible analogue). In a study too recent to have guided this calibration, Watanabe et al. (2003) examined the spatial heterogeneity of different skeletal elements in *Diploastrea* skeletons from the western Pacific. The authors found that with high resolution sampling (25 samples/year) endothecal material yields the highest seasonal amplitude and recommended preferential sampling of this inner skeletal material to best capture the full annual cycle. The results presented here are consistent with those of Watanabe et al. (2003) but expand on them by pointing out that in generating a long coral proxy record using *Diploastrea*, lower resolution sampling of a single skeletal element will produce as accurate a picture of regional climate variability with fewer samples. Given the promise that Fiji s location holds for capturing ENSO, SPCZ, and IPO-related climate variability of interannual and interdecadal scales, a slight reduction of the amplitude of the annual cycle should not affect major trends (Quinn et al., 1996).

A bias toward winter conditions

It is often assumed, for the purposes of age assignment, that coral skeletal extension rates are constant between subannual tie points each year in the age model, which is most certainly not true, but is generally considered the most objective method (Charles et al., 1997). Density band formation in corals is generally considered to be an annual process. At this location the high density bands are formed in the summer, perhaps due to higher SST and/or greater cloud cover. Conditions in winter months create more optimal growth conditions and low density skeleton forms. For *Diploastrea*, because the sampling interval of the long sample transects is constant at 1 mm, while the growth rate varies at least seasonally, more samples are retrieved per year from the section of skeleton that was growing the fastest, in this case in winter (Fig. 6). Because the sampling interval yields more winter samples than summer, there is preferential capture of the winter months in these *Diploastrea* time series of $\delta^{18}O$. Figure 7, the oxygen isotopic time series since 1970 for core 4F1, along with monthly CAC SST for the 2…x2… grid surrounding Savusavu Bay (Reynolds and Smith, 1994) illustrates this preferential capture of the relative winter SST changes from year to year.

An effect of the seasonal bias is a reduced annual $\delta^{18}O$ amplitude (0.5-0.6) relative to the expected range if SST was the only influence on coral $\delta^{18}O$. Laboratory experiments define the widely recognized 0.22 /…C $\delta^{18}O$ —temperature relationship (Epstein et al., 1953), which given the roughly 4…C annual temperature range in Fiji would produce an expected range of ~0.9 each year. The observed annual range in any given year is about two-thirds of this predicted range based on SST variability, which I interpret to be the result of nearly two-thirds of the samples within a year coming from

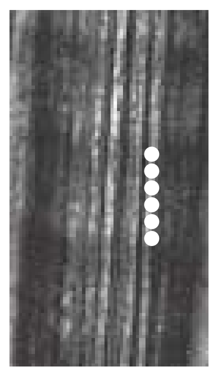

Figure 6. X-radiograph blow-up of one corallite in *Diploastrea* core 4F1. Annual density bands are couplets of high (dark) and low (light) density skeleton. White circles are approximately 1 mm in diameter and represent the constant sampling interval. Due to *Diploastrea*'s variable seasonal growth rate, roughly 2/3 of the samples retrieved from any given year come from the low density band, deposited in winter, thereby introducing a seasonal bias into the $\delta^{18}O$ time series.

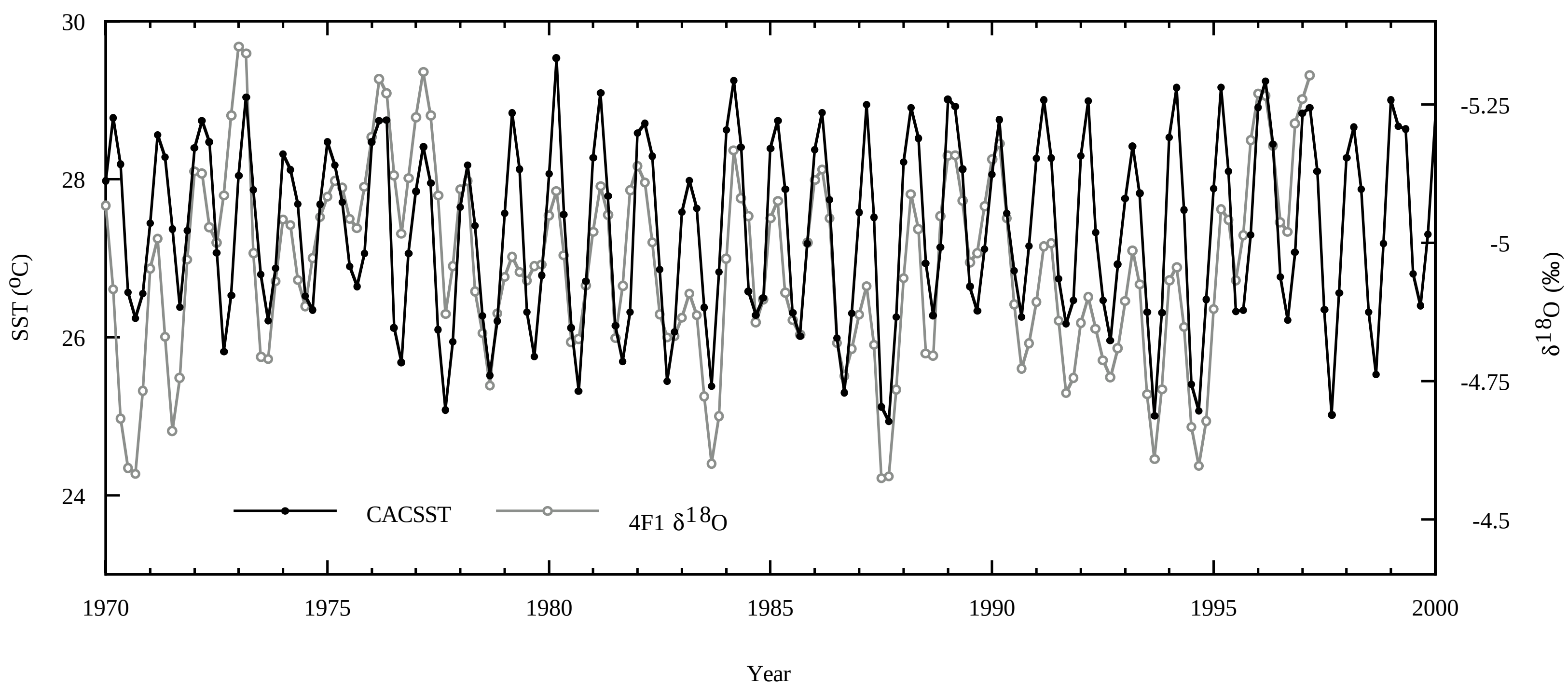

Figure 7. SST data for the 2°x2° grid surrounding Fiji (closed circles) with 4F1 $\delta^{18}O$ (open circles) illustrating that relative changes in winter SST are preferentially captured in the oxygen isotopic composition of *Diploastrea*, while relative summer (peak SST) conditions are not reproduced as well.

the winter portion of the skeleton (the effect may be reduced in endothecal material). Although researchers rarely point out the seasonal bias that corals impart due to their inconsistent growth rates, Leder et al. (1996) recommended a sampling regime of 50 samples per year to accurately capture the annual cycle for this very reason. Recognizing this bias and sacrificing part of the annual cycle with a lower sample resolution, however, is sometimes necessary and useful in generating longer coral records which can contain not only interesting seasonal variability, but interannual and interdecadal variability as well (Quinn et al., 1996; Crowley et al., 1999).

Comparison of Fiji cores and Reproducibility of $\delta^{18}O$

Linsley et al. (1999) note that corals of the same *Porites* species growing in the same location can have different absolute $\delta^{18}O$ values (because skeletal $\delta^{18}O$ is not deposited in equilibrium with seawater) but contain comparable variance. This intra-genus effect is observed for *Diploastrea* as well as inter-genus differences in the average disequilibrium offset when data are plotted together on the same $\delta^{18}O$ scale (Fig. 8). The average $\delta^{18}O$ value for each 1970-1997 coral time series is -4.96 and -4.81 for *Diploastrea* cores 4F1 and LH respectively, and -5.16 for *Porites* 1F of Linsley et al. (in review). Disequilibrium offsets are thought to be relatively constant along the axis of maximum growth (Land et al., 1975; McConnaughey, 1989; Wellington et al., 1996), suggesting that the observed *Diploastrea* intra-genus differences in average $\delta^{18}O$ may indicate that the cores were not retrieved exactly on this axis. Inter-genus differences, as expected, are even larger, but could partially be explained by the sample regime s preference for winter skeleton, which shifts the central tendency toward more positive

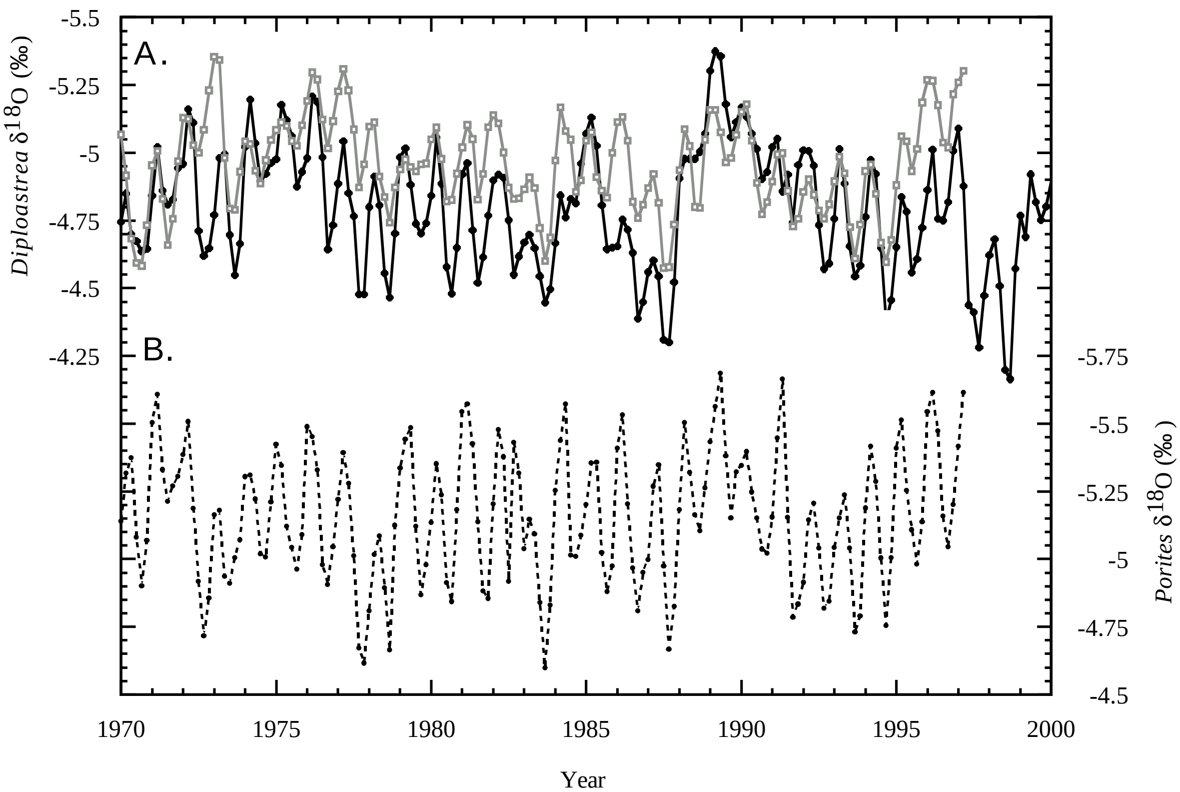

Figure 8. δ^{18}O time series from (A) Fiji *Diploastrea* cores 4F1 (gray squares) and LH (black circles), and (B) Fiji *Porites* core 1F (dashed) showing both intra- and inter-genus differences in the average disequilibrium offset. Additionally, both *Diploastrea* cores have higher average δ^{18}O values than the *Porites* coral because of the sampling regime's preference for winter material and a slower extension rate allowing for aragonite deposition closer to equilibrium with seawater (Land et al., 1975; McConnaughey, 1989; deVilliers et al., 1995).

$\delta^{18}O$ values. Additionally, this may be an inherent inter-genus difference that may stem from *Diploastrea* s slower extension rate, allowing for aragonite deposition closer to equilibrium with seawater (Land et al., 1975; McConnaughey, 1989; deVilliers et al., 1995).

As recommended by Linsley et al. (1999), centering of the data around the mean facilitates comparison of the records, and allows for examination of the common variance in each time series. The mean $\delta^{18}O$ for the period 1945-1995 from each Fiji time series was subtracted from all values, this period being the longest whole year interval common to all three cores. These centered time series (Fig. 9) illustrate that both *Diploastrea* cores share common interannual $\delta^{18}O$ variance over the period of comparison and are positively correlated over the past 30 years (Table 1) despite growing in very different water depths. Reproducibility of coral records remains a considerable concern given the general lack of reliable and continuous site-specific instrumental data to confirm the observed variance. Through the correlation between the two *Diploastrea* records presented here it is demonstrated that the sampling techniques and this new archive itself both yield a reliable and reproducible $\delta^{18}O$ signal.

Given the dominant use of *Porites* over the past 10-20 years in the Pacific, and the general consensus on its dependability for retrospective studies of the surface ocean, the Fiji *Porites* record described in Linsley et al. (in review) proves to be especially useful in further verifying the climate signal contained in both *Diploastrea* records. Correlation coefficients between each *Diploastrea* core and the *Porites* record show that all three Fiji cores are positively correlated over the period of overlap (Tables 1 and 2). Sharing common interannual variance (Fig. 9) is a very promising result given the inherent

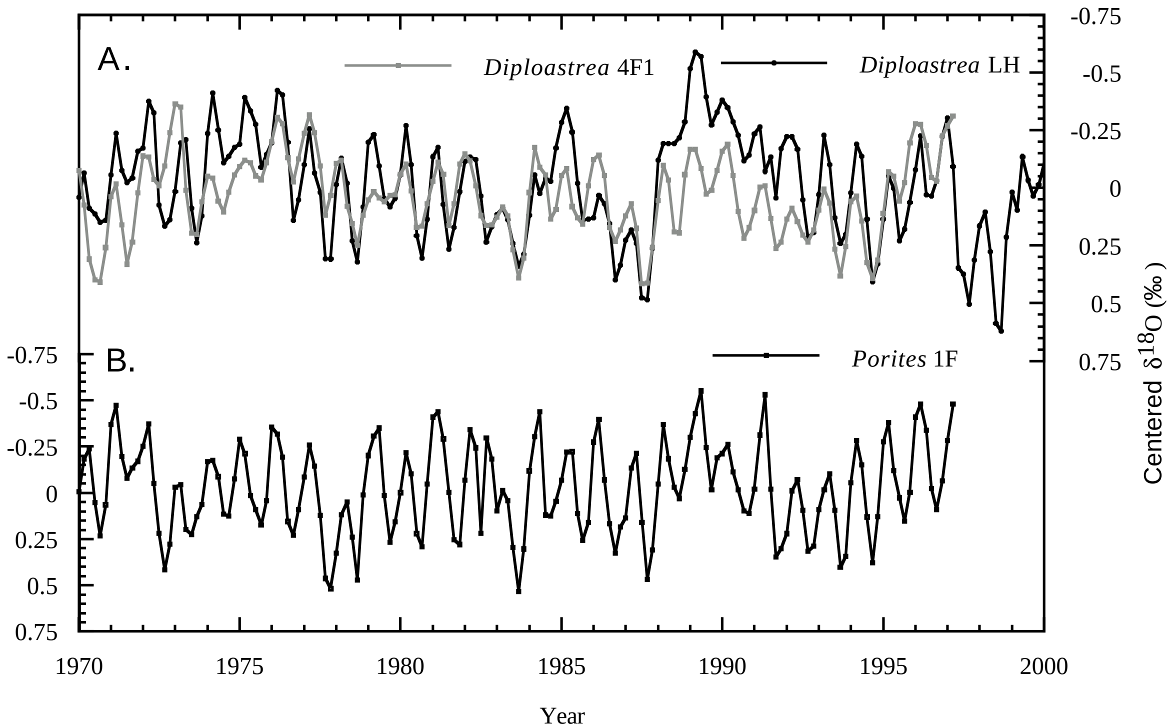

Figure 9. Fiji *Diploastrea* $\delta^{18}O$ (A) and *Porites* (B) $\delta^{18}O$ time series. Coral data were centered by subtracting the 1945-1995 average from all values. All three Fiji cores share common variance over this ~30 year period and demonstrate the reproducibility of the exothecal sampling techniques and that *Diploastrea* skeletons preserve a climate signal as reliable as *Porites* for recording the interannual environmental history of the region.

differences between these genera, the water depths of growth, and the unavoidable reduction of *Diploastrea* s annual amplitude due to the bulk sampling methods. Chapter 4 shows that over the full length of the 225-year time series of *Diploastrea* LH and *Porites* 1F, this inter-genus coherence continues on interannual time scales.

Interpretation of the Fiji Coral δ^{18}O Signal

In this region, SST and precipitation, strongly driven by the ENSO and the SPCZ respectively, dominate the interannual climate signal (Fig. 10). Table 1 documents the correlations between coral δ^{18}O and SST, SSS, and precipitation in this region. Coral δ^{18}O at this site can be explained by this mixed climate signal. Comparison to indices of ENSO and SPCZ activity further illustrate the source of the observed interannual variance. The Ni o-4 SST anomaly index (Kaplan et al., 1998) is equatorial in its coverage (5…N-5…S, 160…E-150…W), but also straddles the dateline and therefore is useful in documenting the SST effect of ENSO activity in the western Pacific. In Figure 10 the two *Diploastrea* records have been averaged for comparison to the climate indices. Such stacking of multiple records is typical of tree-ring paleoclimate studies in order to minimize individual and local biases or noise that could obscure the regional climate signal of interest. Many coral-based paleoclimate studies rely on a single colony from which to derive their proxy data, which may not always be representative of larger scale climate features. Although the sampling regime suppresses the annual cycle, and Fiji is located outside of the region of large ENSO-related SST anomalies, this composite *Diploastrea* δ^{18}O record is still able to capture the major shifts in the Ni o-4 index over the last ~30 years.

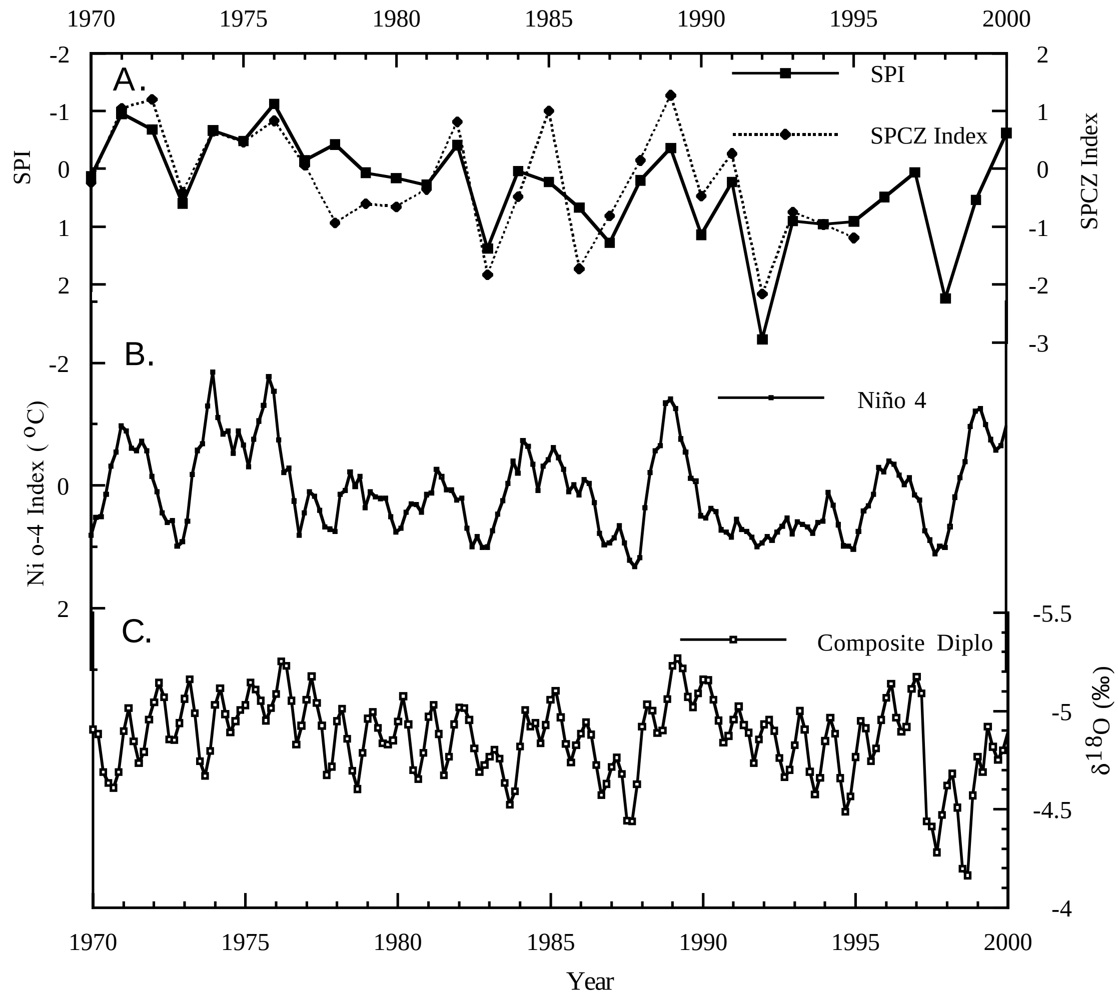

Figure 10. The SPCZ Position Index and the SPCZ rainfall Index (A), the Ni o-4 SST anomaly index (B), and the Fiji *Diploastrea* composite δ^{18}O record (C). Averaging the two *Diploastrea* cores removes individual biases and noise that might otherwise obscure the climate signal, a technique regularly employed in tree-ring climate studies. *Diploastrea* skeletal δ^{18}O captures the major transitions in rainfall and SST-based indices, reliably recording the interannual environmental history of the region, dominated by SPCZ- and ENSO-related precipitation and SST.

The SPCZ Position Index (SPI) defines the position of the SPCZ based on sea level pressure differences between Suva, Fiji, and Apia, Samoa (Folland et al., 2002), where positive values indicate displacement toward Samoa while negative values indicate displacement toward Fiji. The SPCZ rainfall index is the seasonal (December, January, February) average of precipitation station records in the southwest Pacific (17.5…S-22.5…S, 182.5…E-179…W), from the gridded dataset of Dai et al., (1997), as compiled by Deser (2000). These indices, coupled with the Ni o-4 index, demonstrate the interannual link between the activity of the SPCZ and that of the ENSO. While the rainfall-based SPCZ index does not account for evaporation in the South Pacific, the significant match between SPCZ-driven rainfall and coral $\delta^{18}O$ (Table 1, Fig. 10) likely precludes a large evaporation effect on this interannual signal. These climate indices illustrate that this coral genus can reliably capture the climate history of this important region of the Pacific.

Implications

In the South Pacific, temporally short and spatially sparse site-specific instrumental data cannot begin to address long-term variability in ENSO-scale climate dynamics or establish statistically significant conclusions about decadal-scale variability. Intra- and inter-genus reproducibility of coral proxy time series are essential given the lack of reliable climate data against which to test pre-historical variance. Such testing of proxy reproducibility and blending of multiple records is regularly utilized in tree-ring studies of decadal climate variability (D Arrigo et al., 2001; Biondi et al., 2001) and should be employed for comparable coral-based studies to confirm the observed variance. If *Diploastrea* s paleoclimatic utility can be confirmed at additional locations outside of those sampled in this study and by Watanabe et al. (2003), and this new archive s validity further verified, substantial steps can be taken toward knowledge of long-term interannual and decadal climate variability in the Pacific that *Porites*-based proxy records are not long enough to capture.

CONCLUSIONS

Diploastrea skeletal $\delta^{18}O$ from Fiji is influenced by both SST and $\delta^{18}O_{seawater}$ due to the intimately linked ENSO and SPCZ. To best retrieve this mixed climate signal, sampling of *Diploastrea* skeletons for stable isotope analysis should include only a single skeletal element with narrow sample tracks to reduce time averaging, a significant potential problem in such large-polyped corals. Depending on the mode of variance to be studied in a given region, sample interval should be carefully evaluated. A reliable interannual signal is possible with roughly bimonthly sampling of exothecal material, but to best capture the annual cycle, near monthly or better sampling of endothecal material may be necessary given the slow and seasonally variable extension rates. Growing less than a kilometer apart, these *Diploastrea* corals have experienced the same environmental history as the *Porites* coral of Linsley et al. (in review). The equivalence of both *Diploastrea* records illustrates that the chosen sampling regime can yield reproducible results while inter-genus equivalence on interannual time scales over the past ~30 years further verifies that *Diploastrea* can produce viable climate records as effectively as the established coral paleoclimate archive to date. The growth rate and lifespan of *Diploastrea* suggest that continuous proxy records approaching 800 years could potentially be retrieved from the Western Pacific and Indian Ocean in the future.

CHAPTER 3

ENDOLITHIC ALGAE IN *DIPLOASTREA*: A RECORD OF ENSO?

ABSTRACT

Forty five algae bands, likely of the species *Ostreobium quekettii*, are found in the skeleton of a 1.3-m-long *Diploastrea heliopora* coral from Fiji with a recurrence interval between 2 and 8 years. Significant limitations about the nature of algal growth exist which preclude accurate age assignment of the layers, but their very presence in the skeleton suggests a climate link to their colonization and death; their recurrence interval suggesting possible influences from the El Ni o Southern Oscillation (ENSO) system. It is shown that the timing of historical El Ni o events coincides with many of the observed algae layers, but that simple ocean-atmosphere variability may not explain the presence of others. The $\delta^{13}C$ record from this core is not significantly correlated to sunlight availability and/or cloud cover, precluding any connection between the endolithic algae bands and photosynthetic activity of the symbiotic zooxanthellae. Without detailed life cycle, growth information and proper age assignment any relationship between algal presence/absence in the skeletons of *Diploastrea*, or other coral genera, and environmental changes will remain unidentified.

DISCUSSION

A single species of algae, *Ostreobium quekettii*, is the only known species able to survive in the unique environment within the skeleton of living corals. The presence of this algae has been documented in the skeletons of several species of *Porites* (Kanwisher and Wainwright, 1967; Highsmith, 1981; Le Campion-Alsumard et al., 1995; Shashar et al., 1997), as well as *Favia* (Halldal, 1968; Shibata and Haxo, 1969; Fork and Larkum, 1989), *Goniastrea* (Highsmith, 1981), and *Montastrea* (Lukas, 1974). It is believed that the algae live below the coral tissue layer to shade themselves from UV radiation, which is absorbed by various compounds in the coral tissue (Shashar et al., 1997). Additionally the algae gain protection from grazing fish by living below the tissue layer, unlike their vulnerable free-living counterparts on the reef. However, because these algae live below the coral tissue layer, almost all (99.9%) of the incident photosynthetically active radiation (PAR) is absorbed by the symbiotic zooxanthellae before reaching them. Action and absorption spectra indicate that *Ostreobium quekettii* utilize light in the red and near infra-red (Halldal, 1968; Fork and Larkum, 1989), which is not absorbed by the zooxanthellae, allowing them to photosynthesize in a low light environment. Many corals have been found to contain at least one green band of this algae directly below the coral tissue layer, some having a few additional bands deeper in the skeleton. However the number of bands in *Diploastrea* core LH seems to be unprecedented in the literature. Multiple bands were noted in *Porites* corals from Enewetak Atoll, with a periodicity of band formation calculated to be ~1-1.4 years (Highsmith, 1981). Also at Enewetak, Buddemeier et al. (1974) found multiple algae bands in a *Goniastrea* coral 2-2.5 cm apart while the coral growth rate was only 6 mm/yr. Because the bands are obviously not annual the authors have suggested that the algae periodically re-infest corals, although what may trigger this re-infestation remains to be found.

When multiple bands are present it is important to know whether all bands are living or not. Periodic algal re-infestation, indicated by dead lower bands, would suggest some climatic trigger in the re-infestation. Light experiments indicate that incident light is strongly filtered first by zooxanthellae in the coral tissue, leaving 0.1% for the endolithic algae, and that after passing through the first algae band, very little PAR is left (~0.001%) for further photosynthesis, suggesting that only the outer band is active (Halldal, 1968). Additionally Kanwisher and Wainwright (1967), through respiration and light experiments, were able to identify intact chloroplasts only in the outermost band and that lower bands in the coral were green in color due to phaeophytin, a degradation product of chlorophyll, trapped in the skeleton, confirmed by Shibata and Haxo (1969). However, Highsmith (1981) points out an interesting light penetration phenomenon which occurs in corals with high skeletal bulk density. Longer, straighter corallites characteristic of higher skeletal bulk density, a function of corallite wall thickness relative to diameter, allows light to penetrate farther down through light tubes . Corals with lower bulk densities cause more reflections per unit length and light would have to travel farther in thin-walled corallites than in thick-walled corallites to penetrate the same distance into the skeleton.

Highsmith (1981) points out the contradictions in the literature and the enigmatic nature of the algae bands. Most corals contain only one green algae band, directly below the coral tissue, suggesting that the algae grow upwards at pace with the coral. If this is the case, why do some corals contain multiple bands? And if the bands are produced during a particular season, light intensity, oxygen level, or seawater condition, why do not all corals contain multiple bands?

The fact that *Diploastrea* core LH contains multiple algae bands may be due to increased light penetration of the skeleton because it was growing in very shallow water and/or the skeletal density and architecture created light tubes to aid in light penetration. Buddemeier et al. (1974) concluded that algal attack on corals is likely controlled by seasonal and environmental changes. Le Campion-Alsumard et al. (1995) also point out that *Ostreobium quekettii* bands may reflect algal seasonality, although any seasonal influence on coral infestation remains unknown. But if only the outer band was living at the time of core collection, which seems more likely due to light absorption and shading by zooxanthellae, then this core may contain a record of climatically induced algal re-infestation with an El Ni o-like periodicity which may be due to changing light levels, seawater changes, oxygen levels, temperature, or salinity changes.

There are 45 distinct algae bands over the 1.3 m length of *Diploastrea* core LH, most green in color, while a couple are either red or gray in color (Table 3). There is no clear isotopic signature of the algae bands in coral skeletal $\delta^{18}O$ or $\delta^{13}C$, likely because the small amount of algal pigment is diluted in the carbonate powder. The spacing of the algae bands in core LH, every 10-40 mm, translates into every 2-8 years using the average extension rate of 5 mm/yr, with an average spacing between bands of 5 years. This recurrence interval suggests there may be some connection to the ENSO system. Unfortunately, there seems to be no way to accurately assign ages to the algae bands. The age of the skeleton where the algae bands are found at present in the core does not represent the age when the algae band was growing because the algal bands appear to

Table 3. Depth of algae bands in *Diploastrea* core LH and estimated ages

Growth surface-1st algae band offset (years)	Algae Band Depth (mm)	Skeleton Age	Corrected Year
3.31	9	1998.65	2001.96
	18	1997.15	2000.46
	29	1995.21	1998.52
	53	1991.21	1994.52
	74	1987.37	1990.68
	112	1980.35	1983.66
	132	1977.04	1980.35
	152	1973.63	1976.94
	168	1970.79	1974.10
	190	1966.62	1969.93
	214	1962.34	1965.65
	219	1961.11	1964.42
	240	1957.06	1960.37
	256	1954.06	1957.37
	271	1951.21	1954.52

Algae Band Depth (mm)	Skeleton Age	Corrected Year
297	1945.54	1948.84
309	1943.62	1946.93
325	1940.54	1943.84
357	1934.81	1938.12
370	1931.62	1934.93
390	1928.62	1931.93
435	1919.34	1922.65
462	1914.91	1918.22
488	1910.31	1913.62
550	1897.72	1901.02
563	1894.51	1897.82
574	1892.62	1895.93
595	1888.48	1891.79
608	1886.21	1889.52
623	1883.21	1886.52

Algae Band Depth (mm)	Skeleton Age	Corrected Year
640	1880.21	1883.52
660	1876.91	1880.22
689	1871.91	1875.22
744	1861.62	1864.93
840	1846.62	1849.93
878	1840.62	1843.93
917	1834.21	1837.52
951	1829.01	1832.32
1003	1820.37	1823.68
1045	1813.76	1817.07
1060	1811.21	1814.52
1100	1805.62	1808.93
1157	1797.37	1800.68
1190	1792.48	1795.79
1234	1785.34	1788.65

develop several centimeters below the tissue layer and grow at pace with the polyps. Therefore the best estimation of the algal ages adds the time offset between the upper most algae position and the growth surface to the age of the skeleton bearing the algae (Table 3). This correction likely yields a maximum age for the algae bands, assuming that the observed offset represents the maximum depth and lowest light levels under which the algae will grow. The other assumption in this calculation is that the upper band was living at the time of core collection and accurately characterizes the coral tissue-algae band offset distance. If the upper band was dead at core collection these calculations are skewed by an unknown amount. Without in-depth biological examination of the band it cannot be determined if the observed green band is due to chloroplasts in the living algae, or the degradation products of them. However if the algae band growing with the tissue layer never died, then there would only be one band present. It therefore seems that the exact age of algal death, which is what could potentially be climatically related, cannot be determined for this core because the history of the upper algae layer is not known.

This difficulty is evident when the estimated ages of the algae bands are compared to the El Ni o chronology of Quinn et al. (1987), and to the oxygen and carbon isotopic time series (Fig. 11). Most algae bands coincide with either moderate or strong El Ni o events, but there are some bands present during non El Ni o years and some El Ni o years without algae bands. Relative to the δ^{18}O record, interpreted to record rainfall and SST variability, algae bands are present during maximum, minimum, and transitional δ^{18}O values, collectively indicating that perhaps El Ni o-induced cold and dry anomalies are not the only stressor affecting algal activity. The δ^{13}C records from Fiji have been

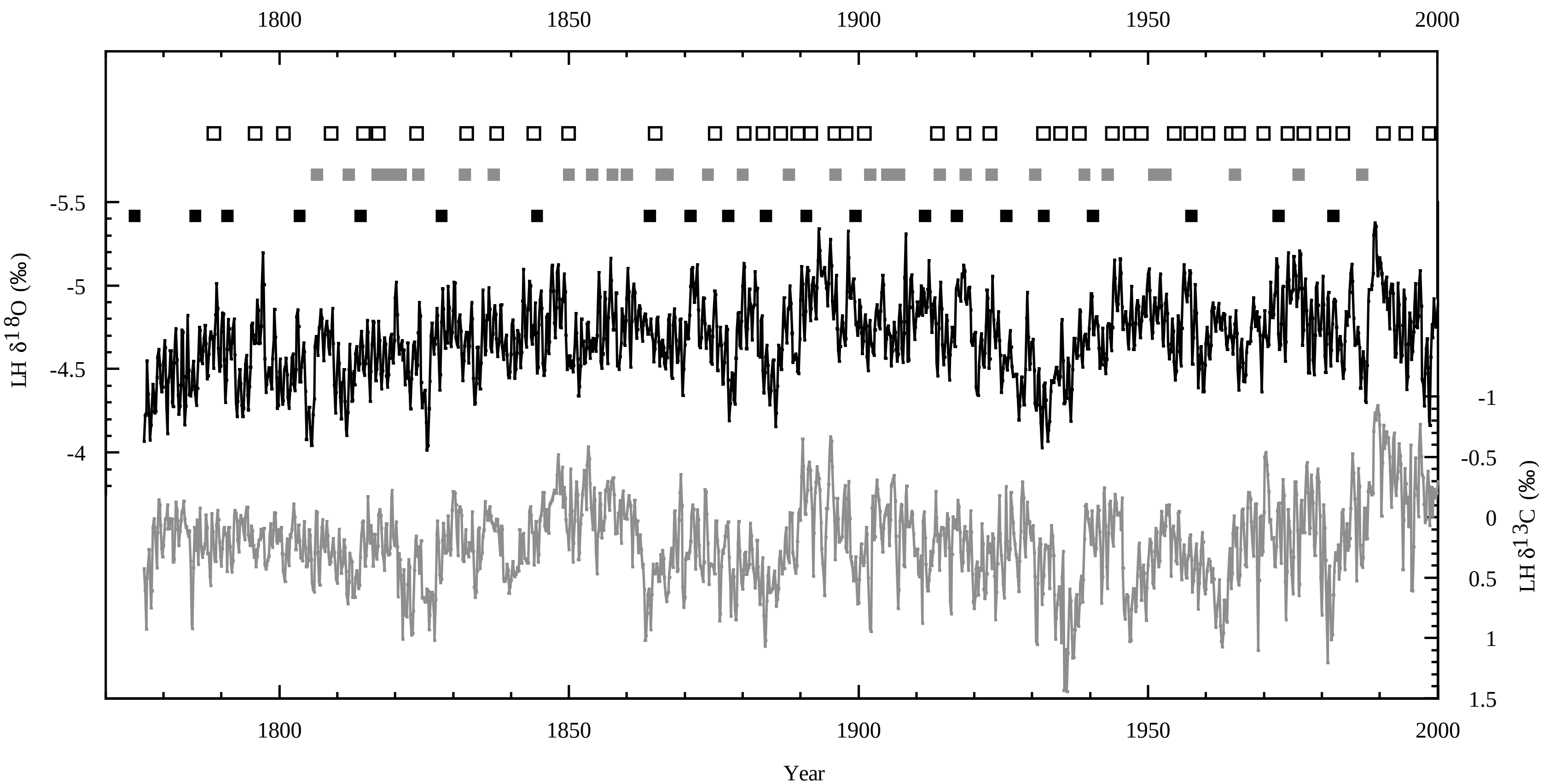

Figure 11. Corrected age of algal bands (open squares), using 3.3 year offset between upper-most band and coral tissue layer, the timing of moderate (gray squares), strong and very strong (black squares) El Ni o events based on the Quinn et al. (1987) chronology, and the *Diploastrea* core LH $\delta^{18}O$ (black) and $\delta^{13}C$ (gray) time series. Algae bands do not produce a distinct signature in the oxygen or carbon isotopic time series. Additionally, difficulty in algal age assignment precludes a clear connection between algal bands and ENSO although the spacing suggests such a connection. It is hard to determine if algal presence is due to El Ni o, La Ni a, high or low SST, salinity, cloud cover, etc.

much more difficult to interpret, with inconsistent annual cycling relative to $\delta^{18}O$, and therefore SST, rainfall, and salinity (r = 0.33 and 0.06 for core LH and 4F1, respectively). However in the upper 30 years of each core there is some evidence that $\delta^{13}C$ may lag the $\delta^{18}O$ record by up to a couple of months with some consistency but in the pre-calibration period this relationship does not persist. Additionally, *Diploastrea* $\delta^{13}C$ shows no clear relationship with cloud cover and/or sunlight availability, with r values equally bleak (0.15 and —0.04 for core LH and 4F1, respectively), although generally more positive $\delta^{13}C$ values occur in austral winter, during times of reduced cloud cover. Such a relationship is expected given the idea that during times of higher photosynthetic activity, zooxanthellae utilize more $^{12}CO_2$, leading to a concentration of $^{13}CO_2$ in the DIC pool from which calcification takes place (Swart et al., 1996). Swart et al. (1996) point out, however, that changes from coral autotrophy to heterotrophy, and changes in the partitioning of ^{13}C between zooxanthellae and coral tissue can also affect the DIC pool available for calcification. Despite the difficulty in interpreting the Fiji *Diploastrea* $\delta^{13}C$ signal, a problem common to coral paleoclimate studies, the estimated algal ages from Table 3 do not consistently coincide with either $\delta^{13}C$ maxima or minima, as with $\delta^{18}O$, questioning the inverse relationship between endolithic algal and coral prosperity.

CONCLUSIONS

The timing of algal death, potentially connected to climatic changes, may not be completely controlled by ENSO-scale variability in physical ocean parameters or sunlight availability, based on the algal chronology calculated here. However only a handful of the many algae bands in this coral cannot be explained by El Ni o activity. The algal chronology created here is certainly inadequate to fully address this issue, with errors up to 4 years in any given age assignment. Additionally it seems that both zooxanthellae and endolithic algae should have some linkage in their activity/prosperity, however the $\delta^{13}C$ record from this coral remains unexplained. The potential climate record in the timing of endolithic algal colonization remains unknown, however band formation in this colony may be unique to the specific shallow, warm water environment of *Diploastrea* core LH, given the lack of such algal re-infestation reported in the literature. Clearly more work is necessary, probably from a biological perspective, to gain a better understanding of how these algae live and die and what controls their infestation into coral skeletons before a climate linkage can be found.

CHAPTER 4

A PALEOCLIMATIC EVALUATION OF THE INDO-PACIFIC CORAL *DIPLOASTREA HELIOPORA* IN FIJI: A PROMISING NEW ARCHIVE OF PACIFIC CLIMATE VARIABILITY

ABSTRACT

A new 225-year oxygen isotope record is presented from the massive coral *Diploastrea* from Fiji that provides a long temperature and rainfall history for an important region with sparse climate records. *Diploastrea* has not previously been utilized for climate reconstructions but may potentially contain longer uninterrupted records of climate than *Porites*, the genus commonly used in Pacific climate studies. Neighboring *Diploastrea* and *Porites* coral $\delta^{18}O$ time series from Fiji are used to show that *Diploastrea* is as effective as *Porites* in recording the interannual environmental history of the region, but potentially more accurate at recording lower-frequency variability. The trend in *Diploastrea* $\delta^{18}O$ at this location is more representative of the long-term trend in regional SST than *Porites*. Additionally, *Diploastrea* faithfully captures climate variability related to the Interdecadal Pacific Oscillation (IPO), and offers evidence supporting the idea that El Ni o Southern Oscillation (ENSO)- and IPO-scale variability are distinct phenomena, although fundamentally linked.

INTRODUCTION

In the tropical Pacific, reliable continuous measurements of physical ocean properties such as sea surface temperature (SST) and sea surface salinity (SSS) generally do not span more than the last 50 years, a period likely already influenced by human activities. Scleractinian corals are uniquely suited for extending the instrumental record to pre-anthropogenic times because climate-driven variability in ocean conditions is in many cases recorded in the chemistry of their aragonite skeletons. Additionally, corals probably provide the best marine archive of changes in SST, SSS and the $\delta^{18}O$ composition of seawater (Dunbar and Wellington, 1981; Cole et al., 1993; Quinn et al., 1993; Linsley et al., 1994; Charles et al., 1997; Linsley et al., 2000b; LeBec et al., 2000, to cite a few) with sufficient time resolution to study in detail phenomena like the ENSO and more recently, interdecadal climate variability.

The coral genus *Porites* has been the primary Pacific coral archive of climate variability for many years. With an annual extension rate of approximately 1 cm per year, near monthly or finer sample resolution is possible. Despite the past success using the genus *Porites* in coral-based paleoclimate reconstruction, several significant limitations of using these archives remain, including interpretation of decadal and trend modes of variance, potential biological artifacts, and the fact that most *Porites* colonies are only 200-300 years in length. Examination of ENSO-scale variability has been the main success of coral proxy records to date but there exist only a few multi-century length Pacific *Porites* records that can begin to address climate variability with decadal and multi-decadal periodicity (Cole et al., 1993; Linsley et al., 1994; Dunbar et al., 1994;

Boiseau et al., 1998; Quinn et al., 1998; Cole et al., 2000; Linsley et al., 2000a; Urban et al., 2000).

The massive coral genus *Diploastrea*, however, has a much slower annual extension rate (4-6 mm/yr), which in itself suggests that *Diploastrea* colonies can yield longer proxy records than *Porites* colonies of the same length. *Diploastrea* has a dense skeletal structure which is rarely damaged by bioeroders, supporting a long lifespan, longer than any other coral in the Faviidae family (Vernon, 1986), with colonies up to 3 meters high known to exist in the western Pacific (T. Quinn, per. comm.). Additionally, *Diploastrea* s presence in the fossil record extends as far back as the Cretaceous, a full 10 million years before *Porites*.

Here three coral cores collected from the same bay in Fiji are used for a unique calibration study, inter-genus comparison, and simultaneous investigation of South Pacific Convergence Zone (SPCZ) activity and Pacific interdecadal climate variability. In Chapter 2 these same corals were used to document the reproducibility of $\delta^{18}O$ at this site over the past 30 years. The 225-year *Diploastrea* time series $\delta^{18}O$ results are discussed here and compared to both multi time-scale indices of climate variability, and to the *Porites* record of Linsley et al. (in review) to document long-term reproducibility of $\delta^{18}O$ and to examine the potential use of *Diploastrea* as a paleoclimate archive. In April 1997 a 30 cm coral core from a colony of *Diploastrea* was collected by hydraulic drill from ~10 m water depth and in December 2001 a 1.3 m coral core was collected from a second colony in 2 m of water, both from the outer edge of Savusavu Bay on the south side of Vanua Levu, Fiji (16… 49 S, 179… 14 E). These *Diploastrea* cores are compared to a 217-year-long *Porites* core collected from the middle of Savusavu Bay in

April 1997 (Linsley et al., in review). Core preparation and isotopic analyses follow the procedures of Linsley et al. (2000a). External precision for $\delta^{18}O$, based on repeated analysis of NBS-19 over the course of this study, is better than 0.04 (1 σ).

METHODS

With no evaluation of *Diploastrea* s paleoclimatic utility in the literature when this calibration work began, the large-polyped, massive Caribbean coral *Montastrea annularis* studied by Leder et al. (1996) was used as the closest analogue on which such an evaluation has been made. For these *Diploastrea* cores, it was determined that sample track width and its affect on time averaging was just as important as the inherent heterogeneity of different skeletal elements on the amplitude of the annual $\delta^{18}O$ cycle. Given the difficulty in separating the effects of each, it was decided to sample only exothecal material following the results of Leder et al. (1996). Recently, however, a detailed study demonstrating *Diploastrea* s skeletal isotope heterogeneity has suggested that endothecal material provides the best climate signal for capturing the annual cycle (Watanabe et al., 2003). The results presented in Chapter 2 are consistent with the conclusions of Watanabe et al. (2003), but it should be pointed out that different sampling methods for Fiji *Diploastrea* all yield comparable interannual signals and should not affect the lower frequency trends discussed here.

Given *Diploastrea* s slow annual extension rate, and the ability to extract useful interannual and interdecadal climate signals from this coral with roughly bimonthly resolution, both *Diploastrea* cores were sampled at 1 mm intervals. At this location high summer SST s (March) slow coral growth and form a high-density band, while lower winter SST s (August) create more optimal growth conditions and low-density band formation. The constant sampling interval therefore yields more samples each year from the faster-growing low-density band. Thus, these Fiji *Diploastrea* time series have a bias toward austral winter given that nearly 2/3 of the samples each year are from winter skeleton, with the annual $\delta^{18}O$ amplitude suppressed by an approximately equal fraction.

The annual periodicity of skeletal $\delta^{18}O$ was used to develop the chronology for the cores presented here. The $\delta^{18}O$ maxima and minima were tuned to those of the 2… x 2… gridded CACSST dataset for this site (Reynolds and Smith, 1994) following the procedures of Linsley et al., (2000b).

Singular Spectrum Analysis (SSA) software written by E. Cook of the Lamont-Doherty Earth Observatory was used in the analysis of the coral $\delta^{18}O$ time series. SSA eigenvectors define the dominant modes of variability in a time series while reconstructed components allow for examination and extraction of the original signal s different frequency components. This technique is described in detail by Vautard and Ghil (1989) and Vautard et al. (1992), and has been used to examine the time scales of ENSO variability (Rasmusson et al., 1990), the recent warming trend in global temperature data (Ghil and Vautard, 1991), and has been applied to coral isotopic time series to identify ENSO-scale variability (Dunbar et al., 1994; Charles et al., 1997; Linsley et al., 2000a).

Wavelet analysis, using the interactive website of Torrence and Compo (1998) (http://paos.colorado.edu/research/wavelets/), was used to further examine the variability in the Fiji coral $\delta^{18}O$ records. Not only can the dominant modes of variability be identified as in SSA, but by decomposing a time series into time-frequency space, their contributions over time can be evaluated, which SSA is not able to do. Wavelet analysis has the unique ability to resolve the time history of the interdecadal components of interest in the Fiji $\delta^{18}O$ records. While SSA uses a set window length whereby small windows tend to coalesce frequencies and large windows separate frequencies, wavelet analysis uses a mother wavelet that is stretched or compressed to change the size of the window, making it possible to analyze a signal at different scales, analogous to a telephoto lens. The result is an analysis technique able to equally resolve both high and low frequencies over time, decomposing a time series into time-frequency space and allowing determination of when different modes of variability are more or less dominant in the time series being analyzed. This technique is described in detail by Hubbard (1998) and by Lau and Weng (1995). Wavelet analysis has not been fully exploited in examining climate data despite the fact that wavelets are well suited to the nonstationary nature of the earth s climate system. Recently, however, wavelet analysis has been used on instrumental data to examine various features of the atmospheric and oceanic systems (Meyers et al., 1993; Weng and Lau, 1994; Foufoula-Georgiou and Kumar, 1994; Torrence and Compo, 1998; Torrence and Webster, 1999). Wavelet analysis has seen much more limited use on paleoclimate records but has had impressive results (Lau and Weng, 1995; Moy et al., 2002), opening the door for paleoclimate applications in the future.

RESULTS AND DISCUSSION

A record of interannual SPCZ-induced climate variability

The coral $\delta^{18}O$ data were tuned to the SST record for age assignment, but it is well known that coral skeletal $\delta^{18}O$ is affected by both SST and $\delta^{18}O_{seawater}$. At this site

SST and precipitation are highly correlated (r = 0.80), as are skeletal $\delta^{18}O$ and Sr/Ca in cores 4F1 and LH (r = 0.75 and 0.56, respectively), suggesting that either tracer is suitable for tuning to the timing of SST changes in developing the chronology. Such a high correlation between SST and precipitation is not unexpected given Fiji s location with respect to the axis of maximum SPCZ rainfall for 1958-1998, which extends from New Guinea towards French Polynesia, passing just north of Fiji. The SPCZ is perhaps the most dominant feature of the Southern Hemisphere subtropics, and its position and activity are modulated by the ENSO and the Interdecadal Pacific Oscillation (IPO) (Kiladis et al., 1989; Vincent, 1994; Folland et al., 2002). When the SPCZ migrates to the northeast during El Ni o events, drier than average conditions exist in Fiji, while southwest displacement of the SPCZ during La Ni a events brings wetter than average conditions (Salinger et al., 1995). Both phases are predicted to alter the $\delta^{18}O_{seawater}$ in the region. Because Fiji lies near the hinge point of the Southern Oscillation and near the position of southernmost displacement of the SPCZ, this region should experience smaller ENSO-related SST anomalies and relatively large precipitation and $\delta^{18}O_{seawater}$ anomalies on ENSO time scales.

Therefore, because coral $\delta^{18}O$ records both $\delta^{18}O_{seawater}$ and SST changes, the rainfall activity of the SPCZ should be amplified in *Diploastrea* skeletal $\delta^{18}O$ relative to SST on these time scales. Coral $\delta^{18}O$ data are compared to two indices of SPCZ activity (Fig. 12), one based on rainfall, and the second based on a sea level pressure gradient. The SPCZ rainfall index is an average of station records for December, January, and February (DJF) (17.5…S-22.5…S, 182.5…E-170…W), from the gridded dataset of Dai et al. (1997), as compiled by Deser (2000). The SPCZ Position Index (SPI) is a station sea

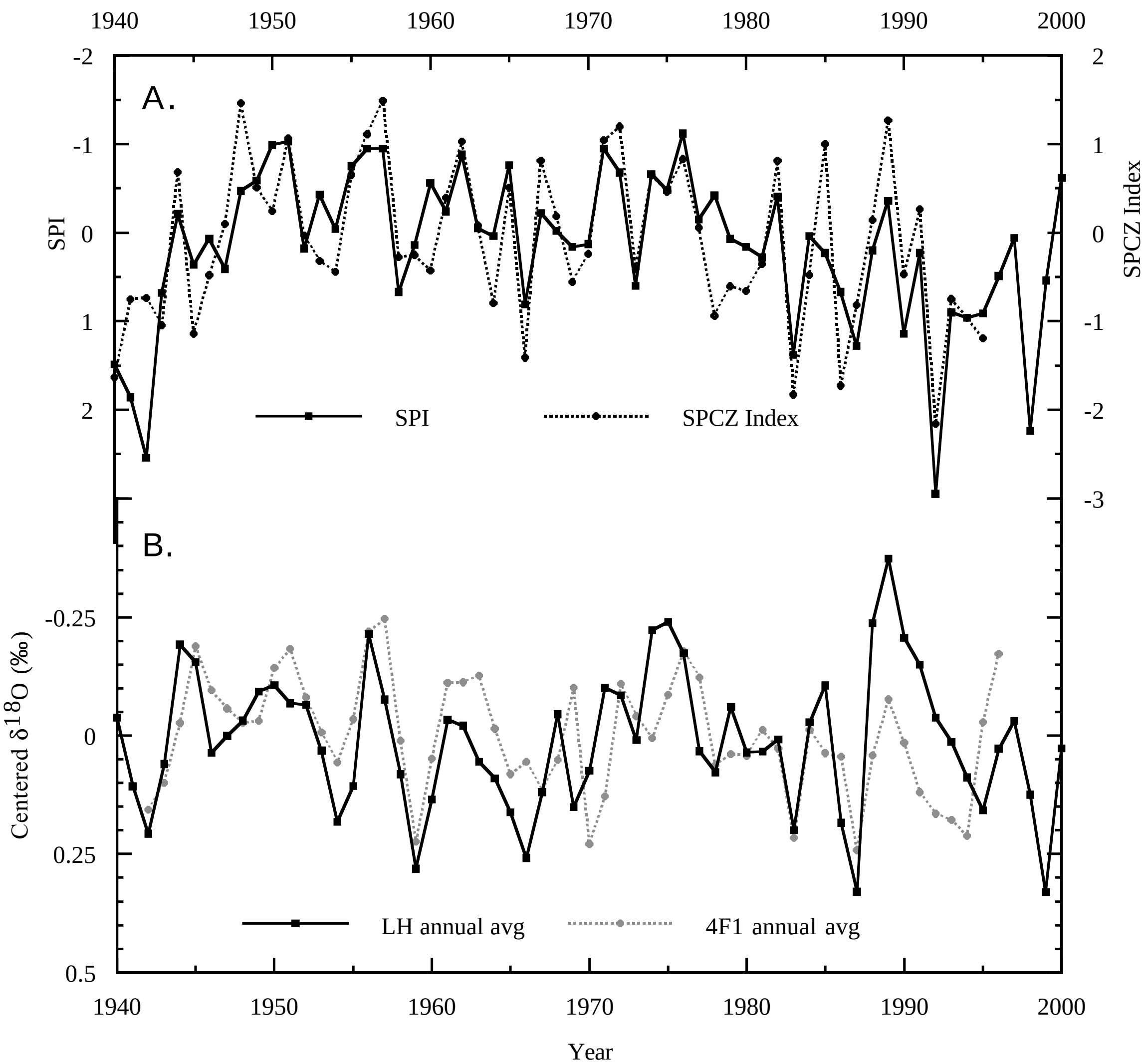

Figure 12. (A) The sea level pressure-based SPCZ Position Index (SPI) of Folland et al. (2002) (solid line) and the rainfall-based SPCZ index of Deser (2000) (dashed line). (B) Annual average skeletal $\delta^{18}O$ for *Diploastrea* core LH (black) and 4F1 (gray). Positive values of the SPI correspond to displacement of the SPCZ toward Samoa while negative values indicate displacement toward Fiji. Positive (negative) values of the SPCZ index correspond to increased (decreased) rainfall over the Fiji region. Movement of the SPCZ toward Fiji, largely associated with ENSO on these interannual time scales, and the large precipitation anomalies which follow, are recorded as negative shifts in the skeletal $\delta^{18}O$ of both *Diploastrea* corals at this site.

level pressure-based index which defines the position of the SPCZ, calculated as the normalized seasonal difference in msl pressure between Suva, Fiji and Apia, Samoa (Folland et al., 2002, and provided by J. Salinger). Annual averaged *Diploastrea* $\delta^{18}O$ accurately record SPCZ activity, capturing nearly all major transitions in both precipitation- and pressure-based indices (Fig. 12), illustrating the region s and *Diploastrea* s sensitivity to SPCZ-induced rainfall on interannual time scales.

Comparison of Fiji cores

The oxygen isotope time series from all three Fiji cores are presented in Figure 13. The 1945-1995 mean $\delta^{18}O$ has been subtracted from all values and the centered series filtered with a running average (14-month window) to highlight the interannual variability and common variance in the cores. Figure 13 shows that both coral genera share the same common interannual variance and are positively correlated over the entire 225-year time series (r = 0.51). One of the noticeable inter-genus differences, however, is the strong trend toward lighter $\delta^{18}O$ values in the Fiji *Porites* record, a feature of many *Porites*-generated coral records (Druffel and Griffin, 1993; Linsley et al., 1994; Quinn et al., 1998; Urban et al., 2000; Hendy et al., 2002). In this *Porites* record, the trend is ~60% greater than the trend in the *Diploastrea* record (Fig. 13). Additionally, the trend in *Diploastrea* is steeper in the first 100 years of the record, and flattens out around 1880, closely following the trend in annual extension rate (Fig. 14). A climatic source of the strong trend component in many coral records is elusive, as is the link between skeletal $\delta^{18}O$ and growth effects (Land et al., 1975; McConnaughey, 1989; Leder et al., 1996; Boiseau et al., 1998; Quinn et al., 1998). The high growth rate of *Porites* colonies relative to *Diploastrea* may account for the stronger trend in the Fiji *Porites* $\delta^{18}O$ time

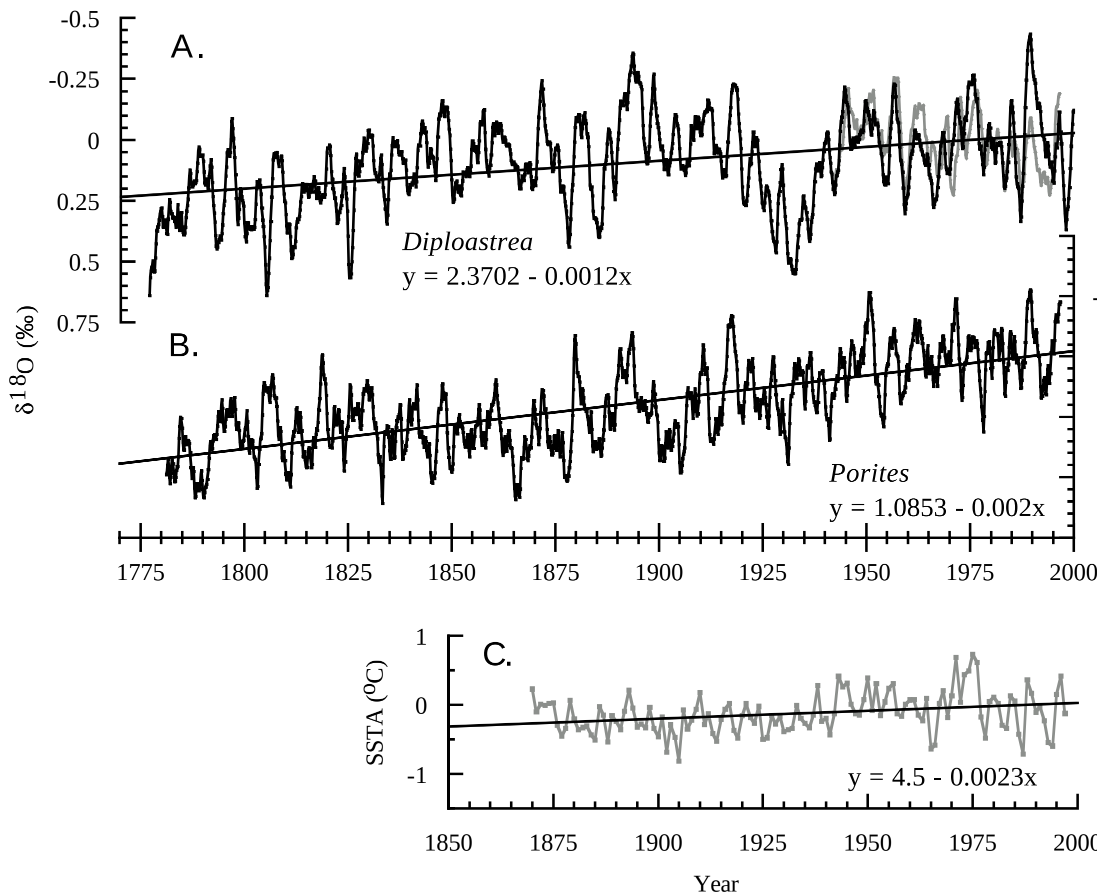

Figure 13. The full $\delta^{18}O$ time series from *Diploastrea* core 4F1 (gray) and LH (black) (A) and *Porites* corals (B). Isotope data have been centered by subtracting the 1945-1995 mean from all values and smoothed with a running average (14 month window) to highlight the shared intra- and inter-genus interannual variance. The long term trend in *Diploastrea* is about half as steep as that for *Porites*. SST anomaly data near Suva, Fiji (Folland et al., in press) (C). Using the working assumption that skeletal $\delta^{18}O$ is controlled solely by SST and that the linear best fit equations shown best represent the observed trends, *Diploastrea* and *Porites* indicate a rise in SST of 0.68^{o} and 1.13^{o}C, respectively, over the period 1875-2000, while SST near Suva has risen only 0.29^{o}C in the same time period. While both corals overestimate the observed rise in SST, *Diploastrea* $\delta^{18}O$ time series may be less influenced by growth effects due to the coral's slower extension rate and may more accurately depict the long-term trend in SST.

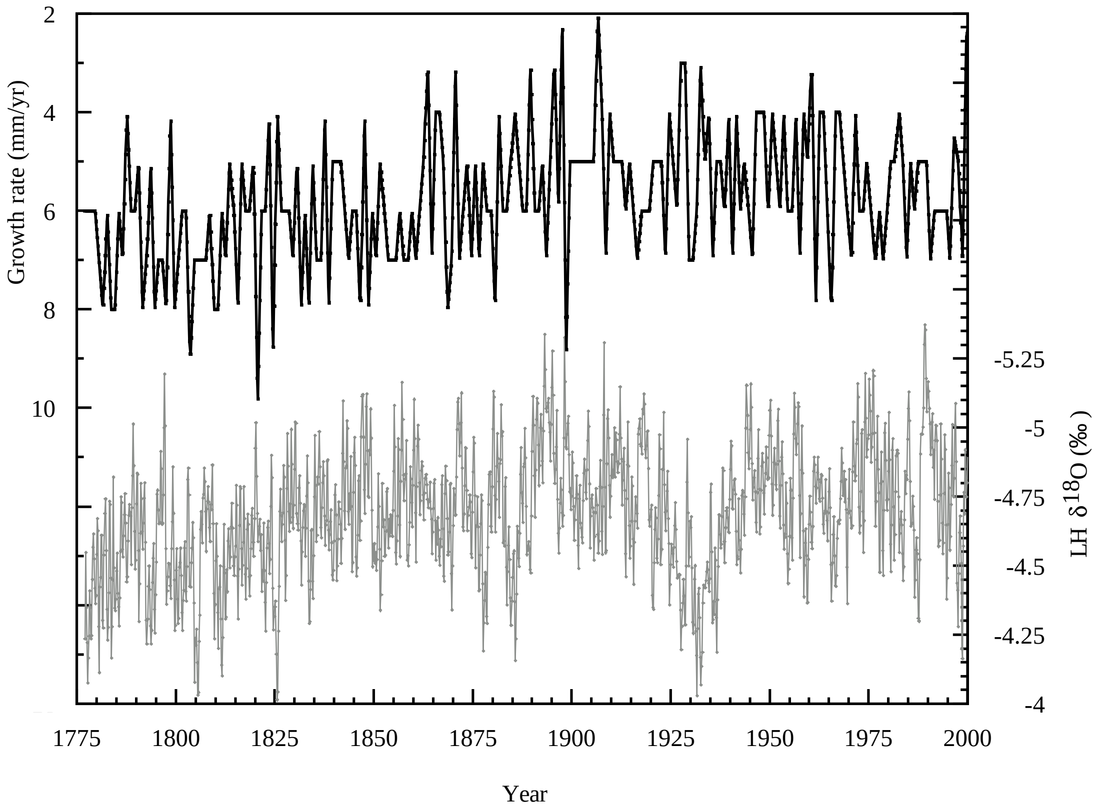

Figure 14. Growth rate (black) and $\delta^{18}O$ (gray) time series for *Diploastrea* core LH. While these two parameters are not highly correlated on an annual scale, both show steeper trends in the pre-1900 section of the core, which then flatten in the twentieth century. The concurrent trends in growth rate and $\delta^{18}O$ suggest that early in the colony's life higher growth rates, and perhaps not climate, produced the observed $\delta^{18}O$ trend in the first approximately 100 years of the record. Such a relationship may explain why *Porites*, which grows faster than *Diploastrea*, may contain a more pronounced $\delta^{18}O$ trend. Quinn et al. (1993) observed a similar growth rate change at the end of the 1800's corresponding to a major shift in $\delta^{18}O$ in a coral from Vanuatu, except with an opposite relationship to growth rate.

series, while the trend in the early part of the *Diploastrea* record may be due to higher extension rates that this coral experienced earlier in its life. Quinn et al. (1993) noted a similar relationship between extension rate and oxygen isotopes in a *Platygyra lamellina* coral from Vanuatu around 1870, suggesting a possible link between growth rate and $\delta^{18}O$ trends. The timing of this change however is interesting and may have climatic significance given the evidence for a fairly abrupt decrease in atmospheric circulation and trade winds coming out of the Little Ice Age (Thompson et al., 1986; Keigwin, 1996; Kreutz et al., 1997; Black et al., 1999) that may have freshened the surface ocean in the South Pacific (Hendy et al., 2002) by reducing evaporation.

If it is assumed, for the purposes of discussion, that coral skeletal $\delta^{18}O$ is purely a function of SST, and a linear best fit equation best represents the long-term trend, *Porites* $\delta^{18}O$ from 1875-2000 translates to a 1.13…C rise in SST and that of *Diploastrea* to a 0.68…C rise, using the widely recognized laboratory calibration of 0.22 /…C (Epstein et al., 1953) (Fig. 13). Meanwhile, examination of long-term SST at Suva, Fiji (Folland et al., in press) indicates a rise in SST of only 0.29…C over the same period, indicating that the $\delta^{18}O$ signals in both coral genera are amplified by some other process. Long-term precipitation at Suva shows a slight decrease over the twentieth century (Vose et al., 1998), indicating that $\delta^{18}O_{seawater}$ may not be implicated in the amplified $\delta^{18}O$ signals despite the strong link between *Diploastrea* $\delta^{18}O$ and SPCZ-related rainfall. This leaves the extension rate as a likely contributor to the observed trends given the similarities of its long-term trend to that of $\delta^{18}O$. Both *Diploastrea* corals have experienced the same environmental history as a neighboring *Porites* colony, contain similar interannual variance, but a lower amplitude $\delta^{18}O$ trend which is most similar to the observed rise in

SST, suggesting that *Diploastrea* s $\delta^{18}O$ time series, due to a slower extension rate, may be more accurately recording the long-term secular trend at this site.

South Pacific interdecadal climate variability

Here it is demonstrated that SST and the position of the SPCZ, important in driving Fiji s interannual climate variability, also affect the interdecadal climate variability at this site. Recently, examination of South Pacific instrumental climate data for the twentieth century has revealed the SPCZ s equally important link to the phasing of the IPO, the Pacific-wide manifestation of the Pacific Decadal Oscillation (PDO) (Folland et al., 2002). With a spatial pattern broadly similar to ENSO, but operating on multi-decadal periods, the positive phase of the IPO would tend to correspond to times of more frequent El Ni os and a northeast displacement of the SPCZ. During the negative phase of the IPO, La Ni a-like conditions persist and the SPCZ is displaced to the southwest (Fig. 2).

Utilizing SSA, the interdecadal components of all three Fiji $\delta^{18}O$ time series have been extracted, with periods between 17 years and the long-term trend, calling this mode of variability the IPO band . A window length (m value) of 300 (~50 years) was used for the 225-year-long *Diploastrea* core LH to resolve the interdecadal components of the $\delta^{18}O$ time series, and because *Diploastrea* core 4F1 is ~60 years long, a proportional m value was set at 108 (~18 years). The IPO band accounts for up to 10% and 21% of the variance in the original 4F1 and LH *Diploastrea* time series respectively (Tables 4 and 5). Both *Diploastrea* $\delta^{18}O$ records align well with each other and both faithfully record the timing of all major transitions of the IPO, while the *Porites* record is only in phase with the IPO and the *Diploastrea* records between ~1880 and 1950 (Fig. 15). This

Table 4. Singular Spectrum Analysis of unfiltered *Diploastrea* 4F1 δ18O time series (m=108).

Eigen vector	Period (years)	Variance (%)	Cummulative Variance (%)
1,2	1	37.05	37.05
3,4,7,8, 11,12,13,14,15	3-9	35.242	72.292
5	56	4.976	77.268
6	24	4.357	81.625
9	13	3.191	84.816
10	10	2.704	87.52

Table 5. Singular Spectrum Analysis of unfiltered *Diploastrea* LH δ18O time series (m=300).

Eigen vector	Period (years)	Variance (%)	Cummulative Variance (%)
1	trend	12.737	12.737
2, 3	1	20.252	32.989
4	83	6.634	39.623
5	42	4.185	43.808
6	33	3.89	47.698
7	24	2.932	50.63
8,9,10,11,12,13,17,18,21,22,23,24,25,26,27,28,29,30	3-9	23.678	74.308
14,15	15-18	3.339	77.647
16, 19,20	11-13	4.048	81.695

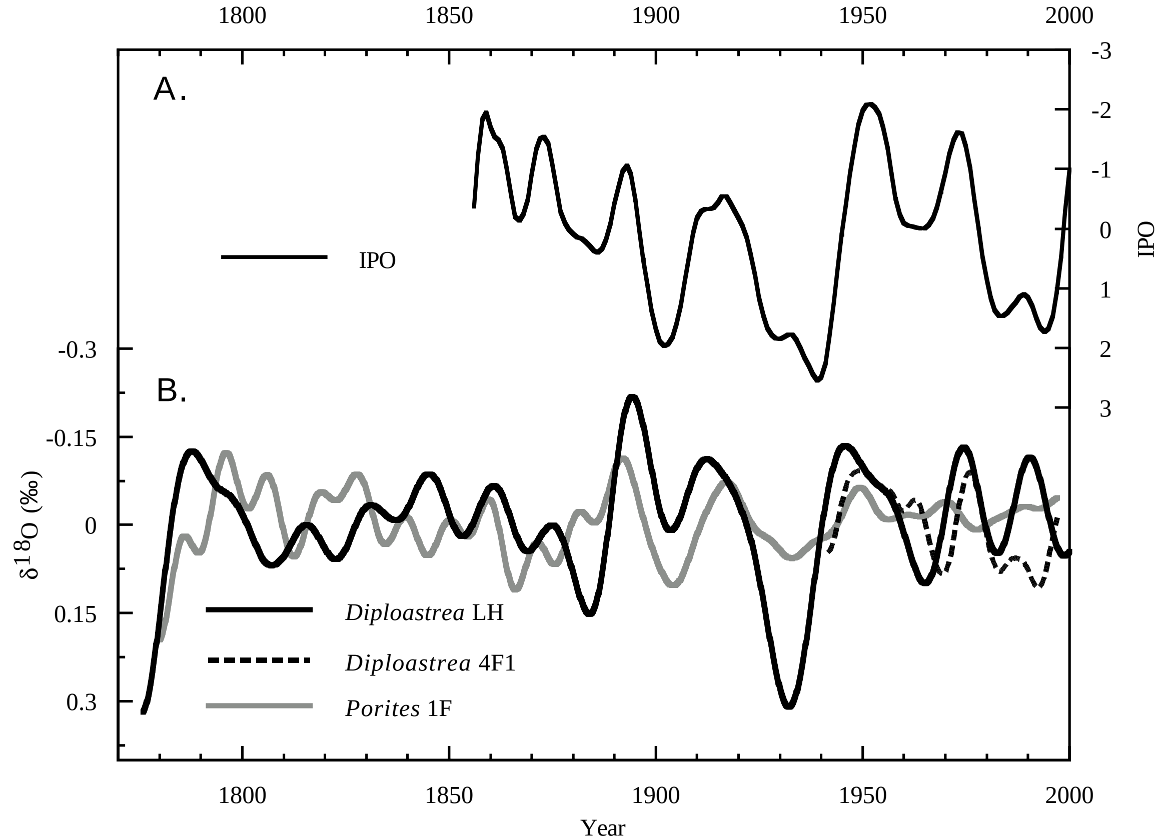

Figure 15. (A) The Interdecadal Pacific Oscillation (IPO) time series which characterizes decadal climate variability in the Pacific. (B) Decadal components of Fiji coral $\delta^{18}O$ time series, extracted using SSA (*Diploastrea* in black, *Porites* in gray). A window length of 50 and 18 years was used for cores LH and 4F1, respectively, and components with periods between 17 years and the long-term trend were combined to create this "IPO band" $\delta^{18}O$ record. *Diploastrea* skeletal $\delta^{18}O$ faithfully records all major transitions of the IPO, an index of Pacific-wide climate variability. The *Porites* record (1F) of Linsley et al. (in review) agrees with the IPO and the *Diploastrea* record only between ~1880 and 1950 and is distinctly out of phase with *Diploastrea* before 1850, indicating stronger interdecadal variability during the period of concordance. Because the IPO is based on SST and the long-term SSTA data show no large decadal changes in this 70-year period, the observed large amplitude decadal variability in these corals must be amplified by $\delta^{18}O_{seawater}$ due to the SPI's stong relationship to the polarity of the IPO (Folland et al., 2002).

analysis alone suggests that the inter-genus differences before 1880 and after 1950 are likely due to weakened IPO-related variability in favor of strengthened ENSO-scale variability.

Wavelet analysis reveals the time history of variability in a climatic time series. The interactive website of Torrence and Compo (1998) was used for examination of the time history of variability in the *Diploastrea* $\delta^{18}O$ record, the Ni o-3 SST anomaly index and the Maiana $\delta^{18}O$ record of Urban et al. (2000). The wavelet power spectra were calculated using the Morlet wavelet with a wavenumber of six and plotted relative to the global wavelet spectrum to examine changes in interdecadal scale variance through time. A red noise background was used to further test the significance of the wavelet spectral estimates, because red noise characterizes the spectra in many climatic time series. The wavelet power spectrum of the long *Diploastrea* isotope record demonstrates that interdecadal variability is strongest between ~1880 and 1950 (Fig. 16), the only period where the *Porites* and *Diploastrea* IPO bands concur (Fig. 15), and a known period of weakened interannual ENSO variability (Torrence and Compo, 1998; Torrence and Webster, 1999). The well-documented ENSO quiet period between 1920 and 1960 is evident in the wavelet power spectrum of the Ni o-3 index (Fig. 17). Such analysis also reveals that decadal and interdecadal variability are present in the tropics, suggesting some degree of connection to IPO-scale variance. Strong decadal variance in the late 1800 s, as observed for Fiji *Diploastrea*, was also observed in a coral record from equatorial Maiana (Urban et al., 2000), clearly visible in the wavelet power spectrum (Fig. 18).

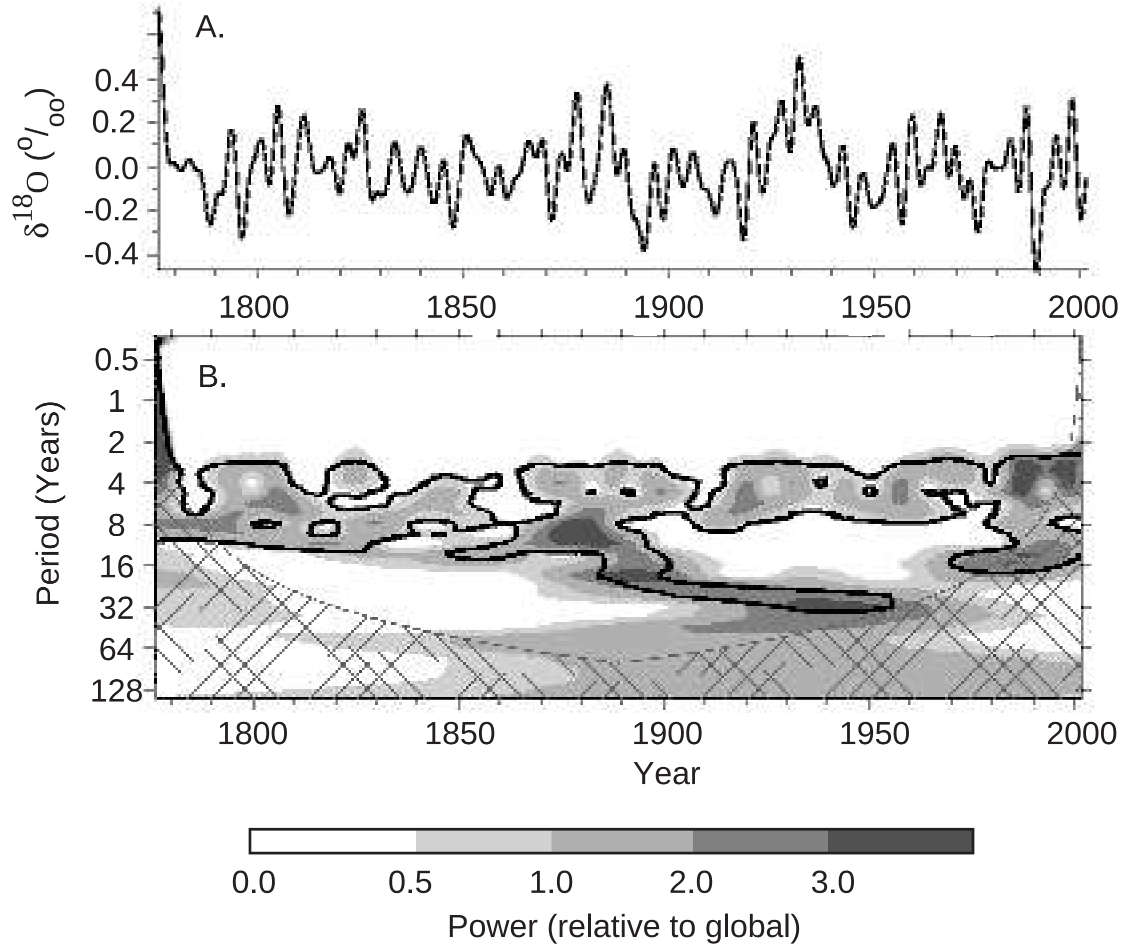

Figure 16. (A) *Diploastrea* LH $\delta^{18}O$ time series with the annual cycle and trend components subtracted using SSA. (B) The wavelet power spectrum calculated using the Morlet wavelet and scaled by the global wavelet spectrum. Black contour is the 10% significance level, using a red-noise background spectrum. The cross-hatched region is the cone of influence, where zero padding on the ends of the time series has reduced the variance. Much of the significant power is concentrated in both the ENSO and IPO bands of variability, with increased IPO-related power between roughly1880 and 1950 in this record. Because IPO variance does not increase at the expense of ENSO variance, rather they occur simultaneously, these modes of variability are likely separate phenomena although the splitting of spectral power around 1880 into both characteristic ENSO and IPO-scale variance suggests are more intimate link between these two modes of variability.

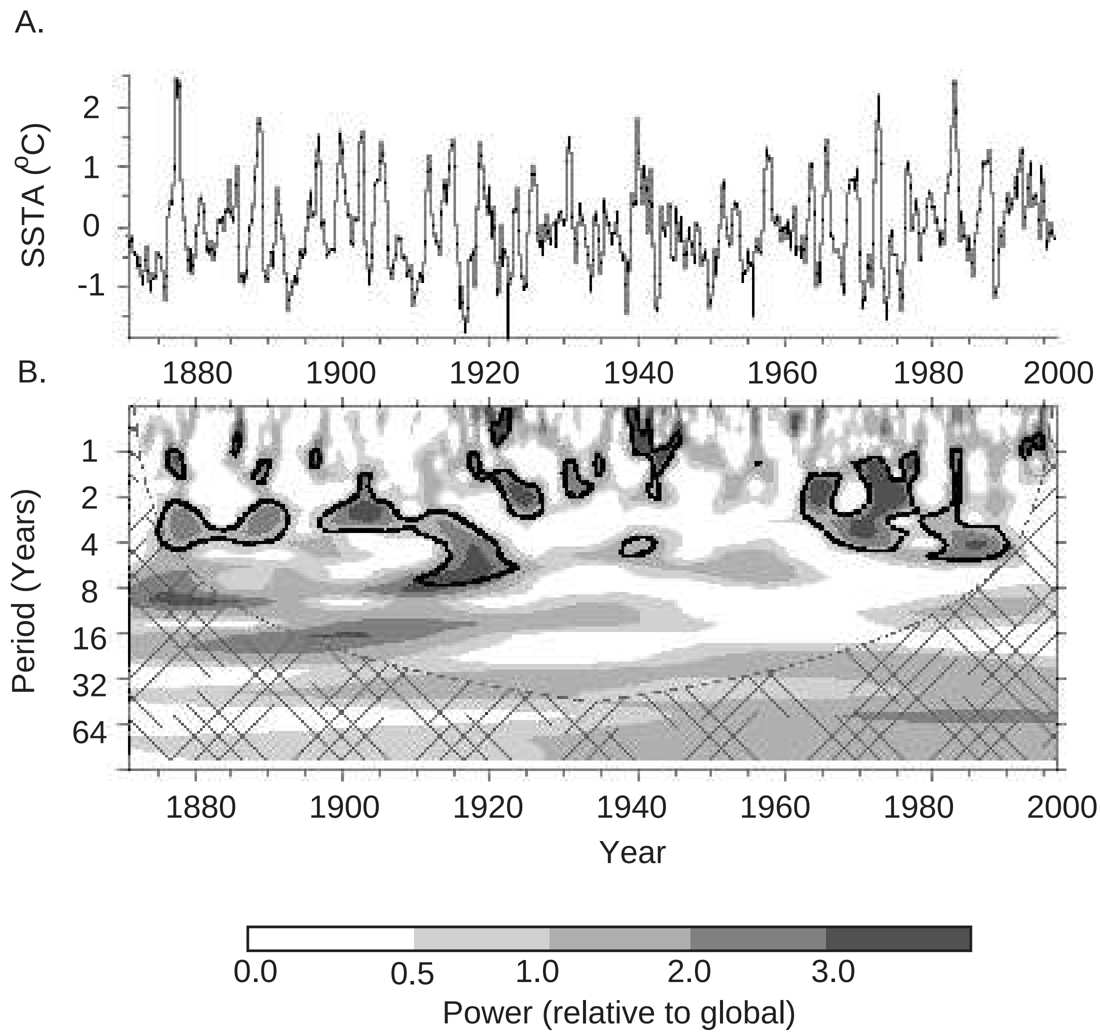

Figure 17. (A) Time series of the Niño-3 SST anomaly Index. (B) The wavelet power spectrum of the Niño-3 SST Index calculated using the Morlet wavelet and scaled by the global wavelet spectrum. Black contour is the 10% significance level, using a red-noise background spectrum. The cross-hatched region is the cone of influence, where zero padding on the ends of the time series has reduced the variance. Most of the significant spectral power lies in the interannual band, with a distinctive quiet period from 1920-1960. Although ENSO is known to operate with a roughly 3-8 year periodicity, there is decadal and interdecadal power centered around the turn of the 20th century, although not within the 10% significance level.

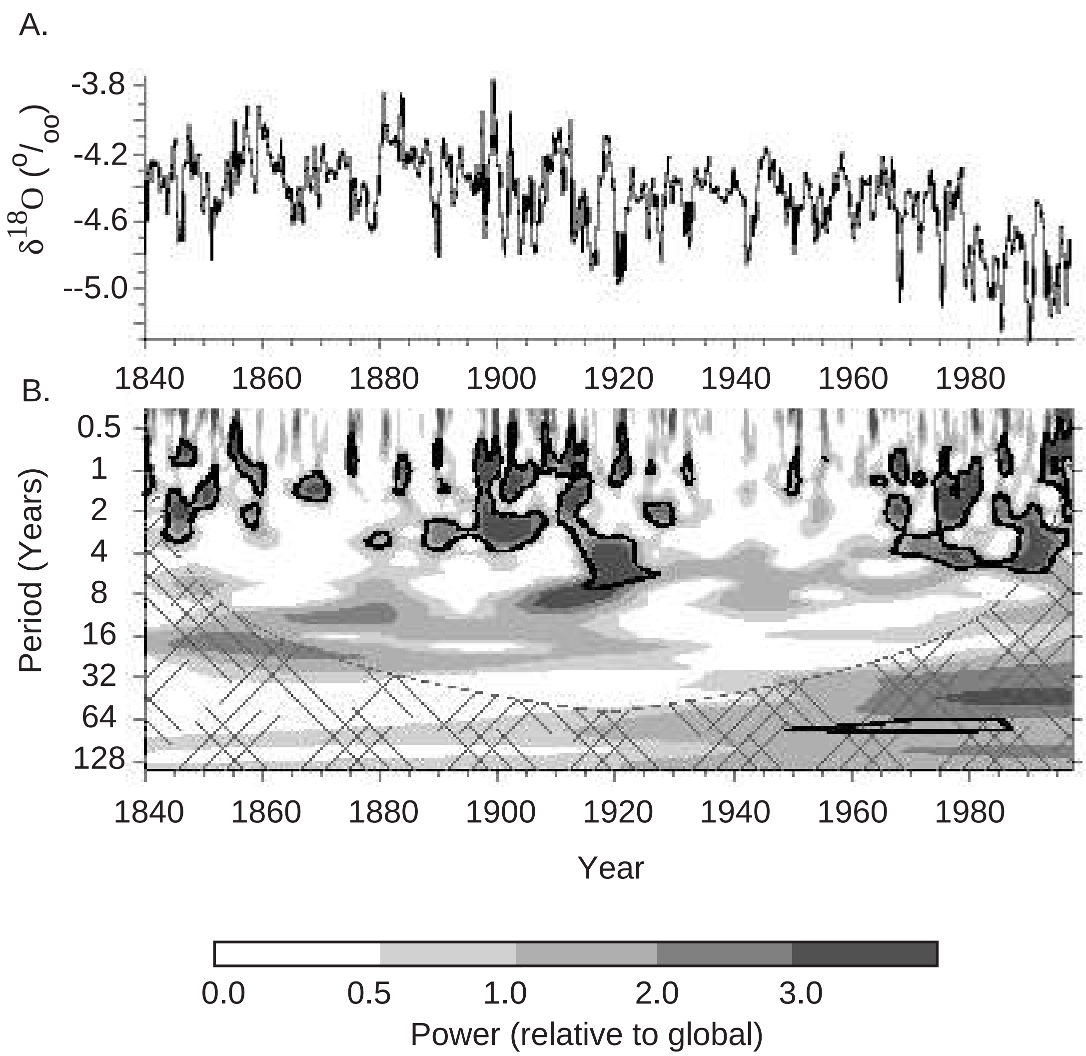

Figure 18. (A) Time series $\delta^{18}O$ results of Urban et al. (2000) from equatorial Maiana. (B) The wavelet power spectrum of Maiana $\delta^{18}O$ of Urban et al. (2000) calculated using the Morlet wavelet and scaled by the global wavelet spectrum. Black contour is the 10% significance level, using a red-noise background spectrum. The cross-hatched region is the cone of influence, where zero padding on the ends of the time series has reduced the variance. Much of the significant power is concentrated in the ENSO band of variability with less significant interdecadal power in the late 1800s, very similar to the Niño-3 index, as expected given Maiana's equatorial location.

Around 1880, ENSO-scale variability in the Fiji *Diploastrea* record splits into two dominant modes, its characteristic interannual signal as well as interdecadal-scale variance. Around 1950, the interdecadal variance starts to bleed back toward ENSO time scales, although this transition occurs near the cone of influence and is not as statistically significant. The fact that the 10% significance (90% confidence) contour encircles the 1880 transition suggests that these modes of variance are not totally separate climate features. However, because IPO-scale power does not increase at the expense of ENSO-scale power, these modes of variability likely operate as separate phenomena. Both oceanic and atmospheric mechanisms that export interannual tropical SST anomalies to higher latitude decadal variability have been described by Alexander et al. (1999) and Alexander et al. (2002) which lend support for a fundamental linkage between ENSO and IPO/PDO variability. Deser and Blackmon (1995), in studying instrumental Pacific SST, noted two significant North Pacific modes, one linked to and one independent of ENSO. Finally, Newman et al. (submitted to J. Climate) note that PDO variance results from a reddened response to atmospheric noise and ENSO anomalies and that such higher latitude decadal variability is significantly dependent upon ENSO. The power spectrum of *Diploastrea* $\delta^{18}O$ cannot specifically address this issue as well as the instrumental record because coral $\delta^{18}O$ is a mixed signal of temperature and salinity/rainfall while Fiji s location records both interannual and interdecadal variability. However the *Diploastrea* $\delta^{18}O$ power spectrum provides support for the tropically forced mechanisms described in the literature and the conclusions of Newman et al. (submitted to J. Climate) on the observed interdecadal variability.

CONCLUSIONS

Interannual climate variability, strongly driven from the tropics, is recorded in *Diploastrea* skeletal $\delta^{18}O$ and is comparable to that recorded in *Porites* $\delta^{18}O$, the backbone of coral-based paleoclimate research for many years. However, the trend component of *Diploastrea* $\delta^{18}O$ is significantly smaller than for *Porites* $\delta^{18}O$. One possible explanation is that the sampling regime preferentially captures winter conditions, and that some feature of austral summer/wet season conditions, suppressed in *Diploastrea* time series, is responsible for the trend to more negative $\delta^{18}O$ in *Porites*. Alternatively, high growth rates alone may impart stronger growth effects on skeletal $\delta^{18}O$. The source of interdecadal climate variability has been elusive to many contemporary studies because short instrumental records in this region contain few realizations of the IPO cycle. *Diploastrea* $\delta^{18}O$ time series faithfully record the same interdecadal mode of Pacific-wide climate variability as is defined by the IPO, with concurrent results from a neighboring *Porites* colony. The discordance in the first 100 and last 50 years of each record provide evidence for weakened IPO-scale variance. The nature of the transitions between ENSO and IPO-scale variance suggests that these modes of variability have a fundamental linkage although they appear to be operating as separate phenomena. It is concluded that *Diploastrea* is a dependable archive of Pacific climate variability due to a combination of winter season sampling bias and inherent inter-genus growth differences. Such features indicate that this coral holds tremendous future potential for additional insight into lower-frequency climate variability, and extending proxy climate records far beyond that which is possible using *Porites*.

CHAPTER 5

CONCLUSIONS AND TOPICS FOR FUTURE WORK

This study has begun the calibration of a new coral genus (*Diploastrea*) for use in Indo-Pacific paleoclimate reconstructions, demonstrating this coral s success in recording interannual through secular trend-scale modes of environmental variance. Additionally, this study has provided a multi-century coral record that contributes to the establishment of a network of long proxy climate records that can collectively provide a spatial reconstruction of long-term tropical and subtropical climate variability. This final chapter summarizes the main conclusions of this study and offers suggestions for future work.

Two *Diploastrea* coral records from Fiji have shown that sampling of a single skeletal element and/or utilizing a narrow sample path yields oxygen isotope values with higher seasonal amplitude and therefore a better climate signal than a sampling regime which includes more than one skeletal element or excessively cross-cuts the uneven growth surface. *Diploastrea* $\delta^{18}O$ time series are biased toward winter conditions because bulk sampling methods at a constant interval preferentially capture skeletal material from the region of fastest growth, which in Fiji occurs during austral winter. This bias would be reduced with a higher density sampling resolution and for in-depth study of the intra-annual variability it is recommended that sampling resolution be finer than monthly, while a viable interannual and interdecadal signal can be extracted with roughly bimonthly sample resolution.

The potential for bands of endolithic algae in coral skeleton to be induced by climate change is significant. The observed recurrence interval of algal bands in the *Diploastrea* skeleton presented here suggests a link to the ENSO system. Detailed knowledge of algal life cycles, and growth regime relative to the coral tissue layer are however necessary to make any significant conclusions about the record of climate change contained in the timing of algal colonization.

Outside the heart of equatorial ENSO-related SST variability, Fiji experiences significant interannual precipitation anomalies associated with SPCZ activity, intimately linked to ENSO and the IPO. On these interannual time scales tropically-driven climate variability, mostly associated with ENSO and the SPCZ, is recorded in *Diploastrea* skeletal $\delta^{18}O$ and is comparable to *Porites*, the primary coral-based paleoclimate archive in the Pacific. Such reproducibility of $\delta^{18}O$ time series both within and between coral genera is crucial in confirming the observed variance in times before instrumental climate records are available for comparison.

The two genera however paint a very different picture of low-frequency climate variability at this site over the last two centuries. The source of the long-term trends in many Pacific *Porites* coral $\delta^{18}O$ records remains unsettled. Such trends usually overestimate any observed long-term rise in SST, precipitation, or salinity. In Fiji, *Diploastrea* skeletal $\delta^{18}O$ has a long-term trend half as steep as that in a neighboring *Porites* record and is more similar to the observed trend in SST for this region, while there is no apparent trend in regional precipitation. Skeletal growth rates are the likely cause of observed inter-genus differences in long-term trend, *Porites* having a growth rate twice as high as *Diploastrea*. Such a relationship fuels the debate over the potential biological artifacts imprinted upon tracers in so many *Porites*-generated coral records. The slow growth rate of *Diploastrea* may provide an archive that is not as clouded by long-term biological artifacts as *Porites*.

The source of interdecadal climate variability has not been fully determined as many studies remain unable to separate the relative importance of tropical versus high latitude forcing. *Diploastrea* $\delta^{18}O$ time series faithfully record the same interdecadal mode of Pacific-wide climate variability as is defined by the IPO, with equal or more success as a neighboring *Porites* colony. Unfortunately data from the two coral genera do not concur in the first 100 years of the $\delta^{18}O$ time series, times without the instrumental IPO index to determine whether one coral genera preferentially captures this interdecadal mode of variability. However, this disagreement in itself may support a breakdown of interdecadal scale climate variability before the late 1800 s, documented by other researchers utilizing both contemporary and proxy climate data. Wavelet analysis of the Fiji coral $\delta^{18}O$ time series may lend some evidence for a tropical forcing of the observed interdecadal variance due to the nature of the transitions between ENSO-scale and interdecadal-scale variance through time, although these modes are observed to operate separately. Because the northern pole of the IPO s spatial response pattern lies in the extreme North Pacific (far north of Hawaiian coral reefs) while the southern pole lies in the South Pacific, coral records from this region are uniquely suited to reconstructing the history of IPO-related climate variability. A more spatially complete reconstruction from this region utilizing multiple archives and proxies is necessary to resolve the source of the observed variability in the Pacific basin or if it is simply low frequency ENSO variability.

Diploastrea s long lifespan and fossil history give this coral great potential in extending our understanding of Pacific climate variability to as much as 600-800 years before present. Before its potential can be fully realized, however, further work is necessary to both confirm and advance the initial results presented here. Not fully appreciating the effect of sample track width, this study is unable to separate its influence from that of heterogeneous skeletal material on the amplitude of the seasonal $\delta^{18}O$ cycle. Future work should specifically address this issue through very high-resolution sampling (micro-milling or ion microprobe techniques) and/or comparison of skeletal elements in equal-width sample transects in a manner similar to Watanabe et al. (2003). Nonetheless, as demonstrated in this study, bulk sampling methods with resolution as low as 6 samples per year can generate records able to accurately resolve both interannual and interdecadal scale variability despite some sacrifice of the annual cycle s amplitude. *Diploastrea* s greatest potential may therefore lie in yielding information about low frequency climate variability over the last several centuries and into windows of the late Quaternary with fossil reef sequences.

REFERENCES

Alexander, M.A., Deser, C., and Timlin, M.S., 1999, The reemergence of SST anomalies in the North Pacific Ocean, *Journal of Climate*, vol. 12, pp. 2419-2433.

Alexander, M.A., Blad , I., Newman, M., Lanzante, J.R., Lau, N.C., and Scott, J.D., 2002, The atmospheric bridge: The influence of ENSO teleconnections on air-sea interaction over the global oceans, *Journal of Climate*, vol. 15, pp. 2205-2231.

Alibert, C. and McCulloch, M.T., 1997, Strontium/calcium ratios in modern *Porites* corals from the Great Barrier Reef as a proxy for sea surface temperature: Calibration of the thermometer and monitoring of ENSO, *Paleoceanography*, vol. 12, pp. 345-363.

Barnes, D.J., Taylor, R.B., and Lough, J.M., 1995, On the inclusion of trace materials into massive coral skeletons. Part II: distortions in skeletal records of annual climate cycles due to growth processes, *Journal of Experimental Marine Biology and Ecology*, vol. 194, pp. 251-275.

Beck, J.W., Edwards, R.L., Ito, E., Taylor, F.W., Recy, J., Rougerie, F., Joannot, P., and Henin, C., 1992, Sea-surface temperature from coral skeletal strontium/calcium ratios, *Science*, vol. 257, pp. 644-647.

Biondi, F., Gershunov, A., and Cayan, D.R., 2001, North Pacific decadal climate variability since 1661, *Journal of Climate*, vol. 14, pp. 5-10.

Black, D.E., Peterson, L.C., Overpeck, J.T., Kaplan, A., Evans, M.N., and Kashgarian, M., 1999, Eight centuries of North Atlantic ocean atmosphere variability, *Science*, vol. 286, pp. 1709-1713.

Boiseau, M., Juillet-Leclerc, A., Yiou, P., Salvat, B., Isdale, P., and Guillaume, M., 1998, Atmospheric and oceanic evidences of El Ni o-Southern Oscillation events in the south central Pacific Ocean from coral stable isotopic records over the last 137 years, *Paleoceanography*, vol. 13, pp. 671-685.

Buddemeier, R.W., Maragos, J.E., and Knutson, D.W., 1974, Radiographic studies of reef coral exoskeletons: Rates and patterns of coral growth, *Journal of Experimental Marine Biology and Ecology*, vol. 14, pp. 179-200.

Charles, C.D., Hunter, D.E., and Fairbanks, R.G., 1997, Interaction between the ENSO and the Asian Monsoon in a coral record of tropical climate, *Science*, vol. 277, pp. 925-928.

Cohen, A.L., and Hart, S.R., 1997, The effect of colony topography on climate signals in coral skeleton, *Geochimica et Cosmochimica Acta*, vol. 61, pp. 3905-3912.

Cohen, A.L., Layne, G.D., and Hart, S.R., 2001, Kinetic control of skeletal Sr/Ca in a symbiotic coral: Implications for the paleotemperature proxy, *Paleoceanography*, vol. 16, pp. 20-26.

Cole, J.E., and Fairbanks, R.G., 1990, The Southern Oscillation recorded in the $\delta^{18}O$ of corals from Tarawa Atoll, *Paleoceanography*, vol. 5, pp. 669-683.

Cole, J.E., Fairbanks, R.G., and Shen, G.T., 1993, Recent variability in the Southern Oscillation: Isotopic results from a Tarawa Atoll coral, *Science*, vol. 260, pp. 1790-1793.

Cole, J.E., Dunbar, R.B., McClanahan, T.R., and Muthiga, N.A., 2000, Tropical Pacific forcing of decadal SST variability in the western Indian Ocean over the past two centuries, *Science*, vol. 287, pp. 617-619.

Corr ge, T., Delcroix, T., R cy, J., Beck, W., Cabioch, G., and LeCornec, F., 2000, Evidence for stronger El Ni o-Southern Oscillation (ENSO) events in a mid-Holocene massive coral, *Paleoceanography*, vol. 15, pp. 465-470.

Crowley, T.J., Quinn, T.M., and Hyde, W.T., 1999, Validation of coral temperature calibrations, *Paleoceanography*, vol. 14, pp. 605-615.

Dai, A., Fung, I.Y., and Del Genio, A.D., 1997, Surface observed global land precipitation variations during 1900-88, *Journal of Climate*, vol. 10, pp. 2943-2962.

D Arrigo, R., Villaba, R., and Wiles, G., 2001, Tree-ring estimates of Pacific decadal climate variability, *Climate Dynamics*, vol. 18, pp. 219-224.

Deser, C. and Blackmon, M.L., 1995, On the relationship between tropical and North Pacific sea surface temperature variations, *Journal of Climate*, vol. 8, pp. 1677-1680.

Deser, C., 2000, Proceedings of the NCAR Summer Colloquium Dynamics of Decadal to Centennual Climate Variability , Boulder, CO.

deVilliers, S., Shen, G.T., and Nelson, B.K., 1994, The Sr/Ca temperature relationship in coralline aragonite: influence of variability in $(Sr/Ca)_{seawater}$ and skeletal growth parameters, *Geochimica et Cosmochimica Acta*, vol. 58, pp. 197-208.

deVilliers, S., Nelson, B.K., and Chivas, A.R., 1995, Biological controls on coral Sr/Ca and $\delta^{18}O$ reconstructions of sea surface temperatures, *Science*, vol. 269, pp. 1247-1249.

Dodge, R.E., Szmant, A.M., Garcia, R., Swart, P.K., Forester, A., and Leder, J.J., 1992, Skeletal structural basis of density banding in the reef coral *Montastrea*

Annularis, *Proceedings of the Seventh International Coral Reef Symposium*, Guam, vol. 1., pp. 186-195.

Druffel, E.R.M., and Griffin, S., 1993, Large variations of surface ocean radiocarbon: Evidence of circulation changes in the southwestern Pacific, *Journal of Geophysical Research*, vol. 98, pp. 20246-20259.

Dunbar, R.B. and Wellington, G.M., 1981, Stable isotopes in a branching coral monitor seasonal temperature variation, *Nature*, vol. 293, pp. 453-455.

Dunbar, R.B., Wellington, G.M., Colgan, M.W., and Glynn, P.W., 1994, Eastern Pacific sea surface temperature since 1600 A.D.: The δ^{18}O record of climate variability in Gal pagos corals, *Paleoceanography*, vol. 9, pp.291-315.

Epstein, S., Buchsbaum, R., Lowenstam, H.A., and Urey, H.C., 1953, Revised carbonate-water isotopic temperature scale, *Geological Society of America Bulletin*, vol. 64, pp. 1315-1326.

Fairbanks, R.G., Evans, M.N., Rubenstone, J.L., Mortlock, R.A., Broad, K., Moore, M.D., and Charles, C.D., 1997, Evaluating climate indices and their geochemical proxies measured in corals, *Coral Reefs*, 16, pp. 93-100.

Folland, C.K., Renwick, J.A., Salinger, M.J., and Mullan, A.B., 2002, Relative influences of the Interdecadal Pacific Oscillation and ENSO on the South Pacific Convergence Zone, *Geophysical Research Letters*, vol. 29, pp. 21-1-21-4.

Folland, C.K., Salinger, M.J., Jiang, N., and Rayner, N.A., (in press), Trends and variations in south Pacific island and ocean surface temperatures, *Journal of Climate*.

Fork, D.C., and Larkum, A.W.D., 1989, Light harvesting in the green alga *Ostreobium* sp., a coral symbiont adapted to extreme shade, *Marine Biology*, vol. 103, pp. 381-385.

Foufoula-Geogiou, E., and Kumar, P., 1994, Wavelets in geophysics, Academic Press, San Diego, California.

Gagan, M.K., Ayliffe, L.K, Beck, J.W., Cole, J.E., Druffel, E.R.M., Dunbar, R.B., and Schrag, D.P., 2000, New views of tropical paleoclimates from corals, *Quaternary Science Reviews*, vol. 19, pp. 45-64.

Garreaud, R.D., and Battisti, D.S., 1999, Interannual (ENSO) and interdecadal (ENSO-like) variability in the southern hemisphere tropospheric circulation, *Journal of Climate*, vol. 12, p. 2113-2123.

Ghil, M., and Vautard, R., 1991, Interdecadal oscillations and the warming trend in global temperature time series, *Nature*, vol. 350, pp. 324-327.

Gouriou, Y., and Delcroix, T., 2002, Seasonal and ENSO variations of sea surface salinity and temperature in the South Pacific Convergence Zone during 1976-2000, *Journal of Geophysical Research*, vol. 107, C12, 8011, doi:101029/2001JC000830.

Halldal, P., 1968, Photosynthetic capacities and photosynthetic action spectra of endozoic algae of the massive coral Favia, *Biological Bulletin*, vol. 134, pp. 411-424.

Hendy, E.J., Gagan, M.K., Alibert, C.A., McCulloch, M.T., Lough, J.M., and Isdale, P.J., 2002, Abrupt decrease in tropical Pacific sea surface salinity at the end of the Little Ice Age, *Science*, vol. 295, pp. 1511-1514.

Highsmith, R.C., 1981, Lime-boring algae in hermatypic coral skeletons, *Journal of Experimental Marine Biology and Ecology*, vol. 55, pp. 267-281.

Hubbard, B.B., 1998, The world according to wavelets: The story of a mathematical technique in the making 2nd ed., A. K. Peters Ltd., Natick, Massachusetts, 330 p.

Kalnay, E., Kanamitsu, M., Kistler, R., Collins, W., Deaven, D., Gandin, L., Iredell, M., Saha, S., White, G., Woollen, J., Zhu, Y., Chelliah, M., Ebisuzaki, W., Higgins, W., Janowiak, J., Mo, K.C., Ropelewski, C., Wang, J., Leetmaa, A., Reynolds, R., Jenne, R., and Joseph, D., 1996, The NCEP/NCAR 40-year reanalysis project, *Bulletin of the American Meteorological Society*, vol. 77, pp. 431-437.

Kanwisher, J.W., and Wainwright, S.A., 1967, Oxygen balance in some reef corals, *Biological Bulletin*, vol. 135, pp. 378-390.

Kaplan, A., Cane, M., Kushnir, Y., Clement, A, Blumenthal, M., and Rajagopalan, B., 1998,   Analyses of global sea surface temperature 1856-1991, *Journal of Geophysical Research*, vol., 103, pp. 18567-18589.

Keigwin, L.D., 1996, The Little Ice Age and Medieval Warm Period in the Sargasso Sea, *Science*, vol. 274, pp. 1504-1508.

Kiladis, G.N., von Storch, H., and van Loon, H., 1989, Origin of the South Pacific Convergence Zone, *Journal of Climate*, vol. 2, pp. 1185-1195.

Kreutz, K.J., Mayewski, P.A, Meeker, L.D., Twickler, M.S., Whitlow, S.I., and Pittalwala, I.I., 1997, Bipolar changes in atmospheric circulation during the Little Ice Age, *Science*, vol. 277, pp. 1294-1296.

Land, L.S., Lang, J.C., and Barnes, D.J., 1975, Extension rate: A primary control on the isotopic composition of West Indian (Jamaican) scleractinian reef coral skeletons, *Marine Biology*, vol. 33, pp. 221-233.

Latif, M., and Barnett, T.P., 1994, Causes of decadal climate variability over the North Pacific and North America, *Science*, vol. 266, p. 634-637.

Lau, K.M., and Weng, H., 1995, Climate signal detection using wavelet transform: How to make a time series sing, *Bulletin of the American Meteorological Society*, vol. 76, pp. 2391-2402.

Lea, D.W., Pak, D.K., and Spero, H.J., 2000, Climate impact of late Quaternary equatorial Pacific sea surface temperature variations, *Science*, vol. 289, pp. 1719-1724.

LeBec, N., Juillet-Leclerc, A., Corr ge, T., Blamart, D., and Delcroix, T., 2000, A coral $\delta^{18}O$ record of ENSO driven sea surface salinity variability in Fiji (south-western tropical Pacific), *Geophysical Research Letters*, vol. 27, pp. 3897-3900.

Le Campion-Alsumard, T., Golubic, S., and Hutchings, P., 1995, Microbial endoliths in skeletons of live and dead corals: *Porites lobata* (Moorea, French Polynesia), *Marine Ecology Progress Series*, vol. 117, pp. 149-157.

Leder, J.J., Swart, P.K., Szmant, A.M., and Dodge, R.E., 1996, The origin and variations in the isotopic record of scleractinian corals: I. Oxygen, *Geochimica et Cosmochimica Acta*, vol. 60, pp. 2857-2870.

Linsley, B.K., Dunbar, R.B., Wellington, G.M., and Mucciarone, D.A., 1994, A coral-based reconstruction of Intertropical Convergence Zone variability over Central

America since 1707, *Journal of Geophysical Research*, vol. 99(C5), pp. 9977-9994.

Linsley, B.K., Messier, R.G., and Dunbar, R.B., 1999, Assessing between-colony oxygen isotope variability in the coral *Porites lobata* at Clipperton Atoll, *Coral Reefs*, vol. 18, pp. 13-27.

Linsley, B.K., Wellington, G.M., and Schrag, D.P., 2000a, Decadal sea surface temperature variability in the subtropical South Pacific from 1726 to 1997 A.D., *Science*, vol. 290, pp. 1145-1148.

Linsley, B.K., Ren, L., Dunbar, R.B., and Howe, S.S., 2000b, El Ni o Southern Oscillation (ENSO) and decadal-scale climate variability at 10…N in the eastern Pacific from 1893 to 1994: A coral-based reconstruction from Clipperton Atoll, *Paleoceanography*, vol. 15, pp. 322-335.

Linsley, B.K., Wellington, G.M., Schrag, D.P., Ren, L., Salinger, M.J., and Tudhope, A.W., in review, Coral evidence for variations in the spatial coherence of South Pacific interdecadal climate variability over the last 300 years, *Climate Dynamics*.

Lukas, K.J., 1974, Two species of the chlorophyte genus *Ostreobium* from skeletons of Atlantic and Caribbean reef corals, *Journal of Phycology*, vol. 10, pp. 331-335.

Mantua, N.J., Hare, S.R., Zhang, Y., Wallace, J.M., and Francis, R.C., 1997, A Pacific interdecadal climate oscillation with impacts in salmon production, *Bulletin of the American Meteorological Society*, vol. 78, pp. 1069-1079.

McConnaughey, T.A., 1989, ^{13}C and ^{18}O isotopic disequilibria in biological carbonates, I, Patterns, *Geochimica et Cosmochimica Acta*, vol.53, pp. 151-162.

McCulloch, M.T., Gagan, M.K., Mortimer, G.E., Chivas, A.R., and Isdale, P.J., 1994, A high-resolution Sr/Ca and $\delta^{18}O$ coral record from the Great Barrier Reef, Australia, and the 1982-83 El Ni o, *Geochimica et Cosmochimica Acta*, vol. 58, pp. 2747-2754.

Meyers, S.D., Kelly, B.G., and O Brien, J.J., 1993, An introduction to wavelet analysis in oceanography and meteorology: With applications to the dispersion of Yanai Waves, *Monthly Weather Review*, vol. 121, pp. 2858-2866.

Mitsuguchi, T., Matsumoto, E., Abe, O., Uchida, T., and Isdale, P.J., 1996, Mg/Ca thermometry in coral skeletons, *Science*, vol. 274, pp. 961-963.

Moy, C.M, Seltzer, G.O., Rodbell, D.T., and Anderson, D.A., 2002, Variability of El Ni o/Southern Oscillation activity at millenni al timescales during the Holocene epoch, *Nature*, vol. 420, pp. 162-165.

Newman, M., Compo, G.P., and Alexander, M.A., submitted, ENSO-forced variability of the Pacific Decadal Oscillation, *Journal of Climate*.

Power, S., Casey, T., Folland, C., Colman, A., and Mehta, V., 1999a, Inter-decadal modulation of the impact of ENSO on Australia, *Climate Dynamics*, vol. 15, pp. 319-324.

Power, S., Tseitkin, F., Mehta, V., Lavery, B., Torok, S., and Holbrook, N., 1999b, Decadal climate variability in Australia during the twentieth century, *International Journal of Climatology*, vol. 19, pp. 169-184.

Quinn, T.M., Taylor, F.W., and Crowley, T.J., 1993, A 173 year stable isotope record from a tropical South Pacific coral, *Quaternary Science Reviews*, vol. 12, pp. 407-418.

Quinn, T.M., Taylor, F.W., Crowley, T.J., and Link, S.M., 1996, Evaluation of sampling resolution in coral stable isotope records: A case study using records from New Caledonia and Tarawa, *Paleoceanography*, vol. 11, pp. 529-542.

Quinn, T.M., Crowley, T.J., Taylor, F.W., Henin, C., Joannot, P., and Join, Y., 1998, A multicentury stable isotope record from a New Caledonia coral: Interannual and decadal sea surface temperature variability in the southwest Pacific since 1657 A.D., *Paleoceanography*, vol. 13, pp. 412-426.

Quinn, W.H., Neal, V.T., and Antunez de Mayolo, S.E., 1987, El Ni o occurrences over the past four and a half centuries, *Journal of Geophysical Research*, vol. 92, pp. 14449-14461.

Rasmusson, E.M., Wang, X., and Ropelewski, C.F., 1990, The biennial component of ENSO variability, *Journal of Marine Systems*, vol. 1, pp. 71-96.

Reynolds, R.W., and Smith, T.M., 1994, Improved global sea surface temperature analyses, *Journal of Climate*, vol. 7, pp. 929-948.

Salinger, M.J., Basher, R.E., Fitzharris, B.B., Hay, J.E., Jones, P.D., Macveigh, J.P., and Schmidely-Leleu, I., 1995, Climate trends in the South-West Pacific, *International Journal of Climatology*, vol. 15, pp. 285-302.

Salinger, M.J., Renwick, J.A., and Mullan, A.B., 2001, The Interdecadal Pacific Oscillation and South Pacific climate, *International Journal of Climatology*, vol. 21, p. 1705-1721.

Schrag, D.P., 1999, Rapid analysis of high-precision Sr/Ca ratios in corals and other marine carbonates, *Paleoceanography*, vol. 14, pp. 97-102.

Seltzer, G.O., Rodbell, D.T., Baker, P.A., Fritz, S.C., Tapia, P.M., Rowe, H.D., and Dunbar, R.B., 2002, Early warming of tropical South America at the last glacial-interglacial transition, *Science*, vol. 296, pp. 1685-1686.

Shashar, N., Banaszak, A.T., Lesser, M.P., and Amrami, D., 1997, Coral endolithic algae: Life in a protected environment, *Pacific Science*, vol. 51, pp. 167-173.

Shen, C.C., Lee, T., Chen, C.Y., Wang, C.H., Dai, C.F., and Li, L.A., 1996, The calibration of D[Sr/Ca] versus sea surface temperature relationship for *Porites* corals, *Geochimica et Cosmochimica Acta*, vol. 60, pp. 3849-3858.

Shen, G.T., Cole, J.E., Lea, D.W., Linn, L.J., McConnaughey, T.A., and Fairbanks, R.G., 1992, Surface ocean variability at Galapagos from 1936-1982: Calibration of geochemical tracers in corals, *Paleoceanography*, vol. 7, pp. 563-588.

Shibata, K., and Haxo, F.T., 1969, Light transmission and spectral distribution through epi- and endozoic algal layers in the brain coral, *Favia*, *Biological Bulletin*, vol. 136, pp. 461-468.

Smith, S.V., Buddemeier, R.W., Redalje, R.C., and Houck, J.E., 1979, Strontium-calcium thermometry in coral skeletons, *Science*, vol. 204, pp. 404-407.

Swart, P.K., Leder, J.J., Szmant, A.M., and Dodge, R.E., 1996, The origin of variations in the isotopic record of scleractinian corals II. Carbon, *Geochimica et Cosmochimica Acta*, vol. 60, pp. 2871-2885.

Thompson, L.G., Mosley-Thompson, E., Dansgaard, W., and Grootes, P.M., 1986, The Little Ice Age as recorded in the stratigraphy of the tropical Quelccaya ice cap, *Science*, vol. 234, pp. 361-364.

Torrence, C., and Compo, G.P., 1998, A practical guide to wavelet analysis, *Bulletin of the American Meteorological Society*, vol. 79, pp. 61-78.

Torrence, C. and Webster, P.J., 1999, Interdecadal changes in the ENSO-Monsoon system, *Journal of Climate*, vol. 12, pp. 2679-2690.

Trenberth, K.E., 1976, Spatial and temporal variations of the Southern Oscillation, *Quarterly Journal of the Royal Meteorological Society*, vol. 102, pp. 639-653.

Tudhope, A.W., Chilcott, C.P., McCulloch, M.T., Cook, E.R., Chappell, J., Ellam, R.M., Lea, D.W., Lough, J.M., and Shimmield, G.B., 2001, Variability in the El Ni o-Southern Oscillation through a glacial-interglacial cycle, *Science*, vol. 291, pp. 1511-1517.

Urban, F.E., Cole, J.E., and Overpeck, J.T., 2000, Influence of mean climate change on climate variability from a 155-year tropical Pacific coral record, *Nature*, vol. 407, pp. 989-993.

Vautard, R., and Ghil, M., 1989, Singular spectrum analysis in nonlinear dynamics, with applications to paleoclimatic time series, *Physica D*, vol. 35, pp. 395-424.

Vautard, R., Yiou, P., and Ghil, M., 1992, Singular spectrum analysis: A toolkit for short, noisy chaotic signals, *Physica D*, vol. 58, pp. 95-126.

Vernon, J.E.N., 1986, Corals of Australia and the Indo-Pacific, University of Hawaii Press, Honolulu, pp. 512-513.

Vincent, D.G., 1994, The South Pacific Convergence Zone (SPCZ): A review, *Monthly Weather Review*, vol. 122, pp. 1949-1970.

Vose, R.S., Peterson, T.C., and Hulme, M., 1998, The Global Historical Climatology Network precipitation database: Version 2.0, In *Proceedings of Ninth Symposium* *on Global Change Studies*, American Meteorological Society, Boston, Massachusetts.

Watanabe, T., Gagan, M.K., Corr ge, T., Scott- Gagan, H., Cowley, J., and Hantoro, W.S., 2003, Oxygen isotope systematics in *Diploastrea heliopora*: New coral archive of tropical paleoclimate, *Geochimica et Cosmochimica Acta*, vol. 67, pp. 1349-1358.

Wellington, G.M., Dunbar, R.B., and Merlen, G., 1996, Calibration of stable isotope signatures in Galapagos corals, *Paleoceanography*, vol. 11, p. 467-480.

Weng, H., and Lau, K.M., 1994, Wavelets, period doubling, and time-frequency localization with application to organization of convection over the tropical western Pacific, *Journal of the Atmospheric Sciences*, vol. 51, pp. 2523-2541.

Zhang, Y., Wallace, J.M., and Battisti, D.S., 1997, ENSO-like interdecadal variability: 1900-93, *Journal of Climate*, vol. 10, p. 1004-1020.

APPENDIX 1

FIJI CORE 4F1 MIXED SKELETON

STABLE ISOTOPE DATA

Depth (mm)	Calendar Year	d^{13}C (‰)	d^{18}O (‰)
0.5	1997.35	-0.186	-5.282
1.0	1997.25	-0.089	-5.175
1.5	1997.14	-0.289	-5.262
2.0	1997.04	-0.188	-5.313
2.5	1996.94	-0.048	-5.208
3.0	1996.83	-0.036	-5.158
3.5	1996.73	-0.006	-5.030
4.0	1996.62	0.010	-4.933
4.5	1996.52	-0.150	-4.966
5.0	1996.42	-0.363	-5.108
5.5	1996.31	-0.406	-5.080
6.0	1996.21	-0.183	-5.151
6.5	1996.10	-0.032	-5.080
7.0	1995.98	0.078	-5.128
7.5	1995.87	0.281	-4.846
8.0	1995.76	0.181	-4.953
8.5	1995.65	0.301	-4.801
9.0	1995.54	0.325	-4.622
9.5	1995.47	0.194	-4.713
10.0	1995.41	0.168	-4.847
10.5	1995.34	0.205	-4.835
11.0	1995.27	0.254	-4.795
11.5	1995.21	0.337	-4.956
12.0	1995.08	0.264	-4.746
12.5	1994.96	0.236	-4.549
13.0	1994.83	0.085	-4.610
13.5	1994.71	0.095	-4.503
14.0	1994.62	-0.191	-4.647
14.5	1994.54	-0.144	-4.592
15.0	1994.46	-0.276	-4.742
15.5	1994.37	-0.228	-4.785
16.0	1994.29	-0.127	-4.801
16.5	1994.21	0.019	-4.830
17.0	1994.08	0.046	-4.668
17.5	1993.96	0.039	-4.464
18.0	1993.83	0.020	-4.456
18.5	1993.71	-0.146	-4.448
19.0	1993.62	-0.224	-4.637
19.5	1993.54	-0.242	-4.706
20.0	1993.46	-0.238	-4.732
20.5	1993.37	-0.432	-4.869
21.0	1993.29	-0.233	-4.866
21.5	1993.21	-0.144	-4.877
22.0	1993.11	-0.038	-4.803
22.5	1993.01	0.027	-4.683
23.0	1992.92	-0.060	-4.644
23.5	1992.82	-0.169	-4.798
24.0	1992.72	-0.239	-4.676
24.5	1992.62	-0.297	-4.613
25.0	1992.52	-0.516	-4.798

Depth (mm)	Calendar Year	d^{13}C (‰)	d^{18}O (‰)
25.5	1992.42	-0.443	-4.800
26.0	1992.32	-0.300	-4.889
26.5	1992.22	-0.163	-4.854
27.0	1992.12	-0.047	-4.903
27.5	1992.02	0.009	-4.865
28.0	1991.92	0.051	-4.765
28.5	1991.81	-0.065	-4.783
29.0	1991.71	-0.207	-4.764
29.5	1991.61	-0.336	-4.827
30.0	1991.51	-0.435	-4.867
30.5	1991.41	-0.436	-4.794
31.0	1991.31	-0.584	-4.944
31.5	1991.21	-0.523	-5.048
32.0	1991.06	-0.371	-5.014
32.5	1990.92	-0.144	-4.951
33.0	1990.77	-0.042	-4.914
33.5	1990.62	-0.084	-4.839
34.0	1990.56	-0.304	-4.853
34.5	1990.50	-0.363	-4.854
35.0	1990.44	-0.481	-4.847
35.5	1990.37	-0.599	-4.943
36.0	1990.31	-0.648	-5.084
36.5	1990.25	-0.670	-5.091
37.0	1990.19	-0.480	-5.151
37.5	1990.12	-0.480	-5.353
38.0	1990.00	0.050	-5.128
38.5	1989.87	0.118	-5.245
39.0	1989.75	-0.071	-5.325
39.5	1989.62	-0.100	-5.075
40.0	1989.53	-0.374	-5.224
40.5	1989.43	-0.517	-5.177
41.0	1989.33	-0.599	-5.213
41.5	1989.23	-0.570	-5.319
42.0	1989.14	-0.354	-5.368
42.5	1989.04	-0.255	-5.453
43.0	1988.94	0.217	-5.147
43.5	1988.83	0.195	-5.160
44.0	1988.73	0.202	-4.961
44.5	1988.62	0.204	-4.871
45.0	1988.54	-0.025	-4.939
45.5	1988.46	-0.202	-4.891
46.0	1988.37	-0.437	-4.902
46.5	1988.29	-0.686	-5.002
47.0	1988.21	-0.891	-5.222
47.5	1988.12	-0.732	-5.263
48.0	1988.01	-0.096	-5.152
48.5	1987.89	0.220	-5.129
49.0	1987.77	0.451	-4.781
49.5	1987.66	0.323	-4.741
50.0	1987.54	0.322	-4.647

APPENDIX 2

FIJI CORE 4F1 ENDOTHECAL SKELETON

STABLE ISOTOPE DATA

Depth (mm)	Calendar Year	$\delta^{13}C$ (‰)	$\delta^{18}O$ (‰)
0.5	1997.35	-0.074	-4.987
1.0	1997.25	-0.148	-4.966
1.5	1997.14	-0.196	-4.921
2.0	1997.04	-0.537	-5.129
2.5	1996.94	-0.181	-4.913
3.0	1996.83	-0.113	-4.792
3.5	1996.73	0.013	-4.763
4.0	1996.62	0.201	-4.491
4.5	1996.56	0.003	-4.622
5.0	1996.50	-0.282	-4.546
5.5	1996.44	-0.490	-4.813
6.0	1996.39	-0.614	-4.932
6.5	1996.33	-0.523	-4.888
7.0	1996.27	-0.398	-5.150
7.5	1996.21	-0.304	-5.254
8.0	1995.98	0.184	-4.637
8.5	1995.76	0.303	-4.793
9.0	1995.54	0.304	-4.398
9.5	1995.47	0.092	-4.536
10.0	1995.41	-0.001	-4.612
10.5	1995.34	-0.005	-4.792
11.0	1995.27	-0.096	-4.797
11.5	1995.21	0.171	-4.797
12.0	1995.08	0.093	-4.777
12.5	1994.96	0.340	-4.438
13.0	1994.83	0.116	-4.519
13.5	1994.71	0.128	-4.342
14.0	1994.62	-0.016	-4.453
14.5	1994.54	-0.105	-4.416
15.0	1994.46	-0.421	-4.693
15.5	1994.37	-0.485	-4.780
16.0	1994.29	-0.543	-4.912
16.5	1994.21	-0.230	-4.994
17.0	1994.08	-0.013	-4.803
17.5	1993.96	0.253	-4.388
18.0	1993.83	0.178	-4.352
18.5	1993.71	0.001	-4.276
19.0	1993.61	-0.057	-4.280
19.5	1993.51	-0.028	-4.481
20.0	1993.41	0.042	-4.755
20.5	1993.31	-0.298	-4.824
21.0	1993.21	-0.191	-4.896
21.5	1993.11	-0.193	-4.883
22.0	1993.01	-0.031	-4.805
22.5	1992.92	0.008	-4.648
23.0	1992.82	0.168	-4.563
23.5	1992.72	0.119	-4.455
24.0	1992.62	0.103	-4.398
24.5	1992.54	-0.162	-4.443
25.0	1992.46	-0.263	-4.532

Depth (mm)	Calendar Year	$\delta^{13}C$ (‰)	$\delta^{18}O$ (‰)
25.5	1992.37	-0.195	-4.656
26.0	1992.29	-0.014	-4.654
26.5	1992.21	-0.088	-4.784
27.0	1992.12	0.080	-4.810
27.5	1992.04	0.233	-4.661
28.0	1991.96	0.253	-4.537
28.5	1991.87	0.044	-4.487
29.0	1991.79	0.076	-4.440
29.5	1991.71	-0.089	-4.423
30.0	1991.58	-0.265	-4.568
30.5	1991.46	-0.322	-4.699
31.0	1991.33	-0.437	-4.814
31.5	1991.21	-0.460	-4.970
32.0	1991.06	-0.267	-4.909
32.5	1990.92	0.170	-4.653
33.0	1990.77	0.259	-4.571
33.5	1990.62	0.156	-4.418
34.0	1990.54	0.023	-4.572
34.5	1990.46	0.153	-4.533
35.0	1990.37	0.171	-4.632
35.5	1990.29	-0.109	-4.746
36.0	1990.21	-0.099	-4.831
36.5	1990.12	0.001	-4.956
37.0	1990.02	0.052	-4.920
37.5	1989.92	0.335	-4.833
38.0	1989.82	0.393	-4.770
38.5	1989.72	0.361	-4.766
39.0	1989.62	0.099	-4.639
39.5	1989.48	-0.332	-4.743
40.0	1989.33	-0.103	-4.785
40.5	1989.19	-0.401	-4.908
41.0	1989.04	-0.449	-5.026
41.5	1988.97	-0.204	-5.022
42.0	1988.90	0.196	-4.927
42.5	1988.83	0.422	-4.727
43.0	1988.76	0.288	-4.796
43.5	1988.69	0.189	-4.746
44.0	1988.62	0.077	-4.643
44.5	1988.46	-0.209	-4.782
45.0	1988.29	-0.371	-4.790
45.5	1988.12	-0.645	-5.061
46.0	1988.05	-0.410	-4.839
46.5	1987.98	-0.527	-5.038
47.0	1987.90	-0.117	-4.924
47.5	1987.83	0.332	-4.766
48.0	1987.76	0.636	-4.512
48.5	1987.69	0.564	-4.405
49.0	1987.61	0.361	-4.427
49.5	1987.54	0.435	-4.282
50.0	1987.47	0.283	-4.463

APPENDIX 3

FIJI CORE 4F1 EXOTHECAL SKELETON

STABLE ISOTOPE AND Sr/Ca DATA

Depth (mm)	Calendar Year	**d**^{13}C (‰)	**d**^{18}O (‰)	Sr/Ca (mmol/mol)
0.5	1997.11	-0.367	-5.213	8.999
1.0	1997.04	-0.270	-5.327	9.038
1.5	1996.97	-0.328	-5.367	8.990
2.0	1996.90	-0.033	-5.101	9.049
2.5	1996.83	-0.135	-5.243	9.050
3.0	1996.76	0.027	-5.151	9.090
3.5	1996.69	0.110	-4.986	9.163
4.0	1996.62	-0.024	-4.924	9.142
4.5	1996.52	-0.342	-5.066	9.145
5.0	1996.42	-0.587	-5.121	9.108
5.5	1996.31	-0.683	-5.246	9.055
6.0	1996.21	-0.232	-5.341	9.085
6.5	1996.04	0.036	-5.372	9.103
7.0	1995.87	0.205	-5.138	9.150
7.5	1995.71	0.299	-4.893	9.176
8.0	1995.54	0.224	-4.838	9.206
8.5	1995.46	-0.047	-5.007	9.177
9.0	1995.37	-0.012	-4.948	9.169
9.5	1995.29	-0.014	-5.049	9.133
10.0	1995.21	0.127	-5.333	9.124
10.5	1995.12	0.300	-4.927	9.134
11.0	1995.04	0.236	-4.901	9.137
11.5	1994.96	-0.057	-4.845	9.149
12.0	1994.87	-0.058	-4.605	9.199
12.5	1994.79	-0.096	-4.513	9.228
13.0	1994.71	-0.255	-4.549	9.229
13.5	1994.58	-0.469	-4.699	9.179
14.0	1994.46	-0.553	-4.692	9.142
14.5	1994.33	-0.666	-4.988	9.154
15.0	1994.21	-0.433	-5.020	9.133
15.5	1994.08	-0.140	-4.956	9.164
16.0	1993.96	-0.153	-4.878	9.195
16.5	1993.83	-0.165	-4.583	9.251
17.0	1993.71	-0.349	-4.514	9.262
17.5	1993.62	-0.289	-4.523	9.258
18.0	1993.54	-0.359	-4.727	9.266
18.5	1993.46	-0.530	-4.947	9.219
19.0	1993.37	-0.504	-4.903	9.195
19.5	1993.29	-0.539	-4.962	9.121
20.0	1993.21	-0.694	-5.098	9.133
20.5	1993.16	-0.360	-4.987	9.138
21.0	1993.11	-0.400	-4.976	
21.5	1993.06	-0.278	-4.977	9.179
22.0	1993.01	-0.387	-4.907	9.187
22.5	1992.96	-0.311	-4.774	9.194
23.0	1992.92	-0.480	-4.830	9.231
23.5	1992.87	-0.457	-4.727	9.200
24.0	1992.82	-0.568	-4.814	9.174
24.5	1992.77	-0.619	-4.758	9.148
25.0	1992.72	-0.652	-4.921	9.138

Depth (mm)	Calendar Year	$\delta^{13}C$ (‰)	$\delta^{18}O$ (‰)	Sr/Ca (mmol/mol)
25.5	1992.67	-0.421	-4.718	9.103
26.0	1992.62	-0.233	-4.772	9.099
26.5	1992.37	-0.172	-5.046	9.122
27.0	1992.12	-0.032	-4.789	9.149
27.5	1992.02	-0.283	-4.853	9.140
28.0	1991.92	-0.304	-4.773	9.177
28.5	1991.81	-0.393	-4.655	9.198
29.0	1991.71	-0.360	-4.688	9.177
29.5	1991.62	-0.692	-4.820	9.151
30.0	1991.54	-0.676	-4.749	9.120
30.5	1991.46	-0.631	-4.980	9.088
31.0	1991.37	-0.541	-5.070	9.062
31.5	1991.29	-0.541	-5.035	9.062
32.0	1991.21	-0.315	-5.043	9.112
32.5	1991.06	-0.355	-4.829	9.143
33.0	1990.92	-0.452	-4.836	9.145
33.5	1990.77	-0.530	-4.740	9.132
34.0	1990.62	-0.505	-4.783	9.135
34.5	1990.50	-0.662	-4.960	9.111
35.0	1990.37	-0.724	-5.077	
35.5	1990.25	-0.658	-5.171	
36.0	1990.12	-0.571	-5.255	9.030
36.5	1990.00	-0.108	-5.088	9.074
37.0	1989.87	0.078	-5.086	9.055
37.5	1989.75	0.147	-5.010	9.142
38.0	1989.62	0.074	-4.908	9.135
38.5	1989.53	-0.238	-4.906	9.141
39.0	1989.43	-0.603	-5.031	9.131
39.5	1989.33	-0.647	-5.103	9.122
40.0	1989.23	-0.777	-5.242	9.066
40.5	1989.14	-0.786	-5.113	9.054
41.0	1989.04	-0.677	-5.234	9.055
41.5	1988.97	-0.331	-5.217	9.095
42.0	1988.90	-0.098	-5.057	9.054
42.5	1988.83	-0.102	-5.072	9.109
43.0	1988.76	0.030	-4.890	9.163
43.5	1988.69	-0.022	-4.820	9.125
44.0	1988.62	-0.029	-4.620	9.167
44.5	1988.54	-0.349	-4.778	
45.0	1988.46	-0.593	-4.877	9.125
45.5	1988.37	-0.985	-5.084	9.067
46.0	1988.29	-0.915	-5.104	9.087
46.5	1988.21	-0.874	-5.126	9.066
47.0	1988.12	-0.413	-5.046	9.060
47.5	1988.03	-0.090	-4.958	9.139
48.0	1987.93	0.296	-4.741	9.202
48.5	1987.83	0.213	-4.622	9.190
49.0	1987.73	0.131	-4.607	9.211
49.5	1987.64	0.157	-4.477	9.265
50.0	1987.54	0.044	-4.494	9.236

Depth (mm)	Calendar Year	d13C (‰)	d18O (‰)	Sr/Ca (mmol/mol)
51	1987.43	-0.072	-4.620	9.204
52	1987.32	0.034	-4.871	9.114
53	1987.21	0.417	-4.971	9.176
54	1986.92	0.506	-4.829	9.201
55	1986.62	0.126	-4.747	9.198
56	1986.48	-0.253	-4.784	9.164
57	1986.35	-0.508	-5.087	9.122
58	1986.21	-0.016	-5.156	9.113
59	1985.92	0.281	-5.096	9.168
60	1985.62	0.089	-4.788	9.190
61	1985.46	-0.380	-4.886	
62	1985.29	-0.258	-4.918	9.120
63	1985.12	0.042	-5.131	9.148
64	1984.96	0.462	-5.014	9.185
65	1984.79	0.256	-4.857	9.211
66	1984.62	-0.081	-4.856	9.150
67	1984.46	-0.384	-5.116	9.130
68	1984.29	-0.287	-5.068	9.109
69	1984.12	-0.052	-5.202	9.120
70	1983.96	0.420	-4.890	9.175
71	1983.79	0.182	-4.615	9.204
72	1983.62	-0.198	-4.596	9.207
73	1983.48	-0.458	-4.738	9.126
74	1983.35	-0.308	-4.882	9.113
75	1983.21	0.083	-4.940	9.160
76	1982.96	0.365	-4.849	9.175
77	1982.71	0.369	-4.813	9.207
78	1982.48	0.005	-4.859	9.161
79	1982.26	-0.320	-5.068	9.082
80	1982.04	-0.168	-5.172	
81	1981.79	0.264	-5.079	9.092
82	1981.54	0.693	-4.761	9.182
83	1981.46	0.254	-4.814	9.200
84	1981.37	0.069	-4.881	9.177
85	1981.29	0.141	-5.134	9.139
86	1981.21	0.554	-5.140	9.166
87	1980.62	0.361	-4.801	9.168
88	1980.56	0.094	-4.862	9.173
89	1980.50	-0.036	-4.810	9.175
90	1980.44	0.418	-4.832	9.170
91	1980.39	0.621	-4.886	9.206
92	1980.33	0.435	-4.957	9.200
93	1980.27	0.000	-5.079	9.138
94	1980.21	-0.018	-5.160	9.125
95	1979.71	0.513	-4.893	9.169
96	1979.58	0.343	-5.001	9.184
97	1979.46	0.167	-4.920	9.213
98	1979.33	-0.059	-4.930	9.140
99	1979.21	-0.072	-5.011	9.092
100	1979.01	0.252	-4.941	9.128

Depth (mm)	Calendar Year	**d**^{13}C (‰)	**d**^{18}O (‰)	Sr/Ca (mmol/mol)
101	1978.82	0.429	-4.880	9.220
102	1978.62	0.168	-4.702	9.170
103	1978.46	-0.287	-4.884	9.191
104	1978.29	-0.265	-4.922	9.110
105	1978.12	-0.445	-5.179	9.099
106	1977.96	0.111	-5.068	9.107
107	1977.79	0.246	-4.919	9.225
108	1977.62	0.128	-4.855	9.179
109	1977.50	-0.214	-5.100	9.157
110	1977.37	-0.376	-5.301	9.108
111	1977.25	-0.253	-5.228	9.058
112	1977.12	0.094	-5.329	9.039
113	1977.00	0.270	-5.206	9.112
114	1976.87	-0.009	-5.161	9.182
115	1976.75	-0.148	-5.056	9.105
116	1976.62	-0.144	-4.990	9.121
117	1976.42	-0.138	-5.213	9.056
118	1976.21	0.209	-5.368	9.037
119	1975.98	0.526	-5.168	9.100
120	1975.76	0.454	-5.070	9.119
121	1975.54	0.413	-4.969	9.165
122	1975.40	-0.152	-5.114	9.065
123	1975.26	-0.136	-5.115	9.051
124	1975.12	0.208	-5.111	9.072
125	1974.79	0.508	-5.037	9.138
126	1974.46	0.770	-4.863	9.179
127	1974.32	0.465	-4.941	9.143
128	1974.18	-0.002	-5.023	9.099
129	1974.04	-0.168	-5.112	9.085
130	1973.87	0.151	-4.961	9.169
131	1973.71	0.272	-4.825	9.182
132	1973.54	0.252	-4.683	9.216
133	1973.40	0.133	-4.891	9.145
134	1973.26	0.214	-5.080	9.100
135	1973.12	0.108	-5.448	9.023
136	1972.93	0.380	-5.301	9.082
137	1972.73	0.290	-5.157	9.159
138	1972.54	0.335	-4.963	9.141
139	1972.33	0.053	-5.016	9.132
140	1972.12	-0.105	-5.154	9.070
141	1971.93	0.276	-5.115	9.090
142	1971.73	0.607	-4.837	9.164
143	1971.54	0.415	-4.596	
144	1971.40	0.108	-4.680	9.171
145	1971.26	-0.089	-4.948	9.122
146	1971.12	0.051	-5.047	9.084
147	1970.98	0.608	-4.962	9.061
148	1970.85	0.685	-4.756	9.165
149	1970.71	0.520	-4.531	9.261
150	1970.48	0.298	-4.590	9.203

Depth (mm)	Calendar Year	$\delta^{13}C$ (‰)	$\delta^{18}O$ (‰)	Sr/Ca (mmol/mol)
151	1970.26	0.059	-4.726	9.192
152	1970.04	0.383	-5.146	9.156
153	1969.79	0.431	-4.994	9.170
154	1969.54	0.432	-4.872	9.230
155	1969.40	0.023	-4.972	9.176
156	1969.26	-0.153	-5.221	9.098
157	1969.12	-0.046	-5.383	9.084
158	1968.93	0.378	-5.148	9.119
159	1968.73	0.491	-4.879	9.151
160	1968.54	0.364	-4.690	9.211
161	1968.40	-0.015	-4.934	9.206
162	1968.26	-0.046	-4.876	9.103
163	1968.12	-0.182	-5.113	9.090
164	1967.93	0.300	-5.024	9.112
165	1967.73	0.359	-4.771	9.172
166	1967.54	0.365	-4.594	9.272
167	1967.40	0.002	-4.831	9.151
168	1967.26	0.029	-4.963	9.150
169	1967.12	0.589	-5.089	9.129
170	1966.83	0.919	-4.850	9.180
171	1966.54	0.440	-4.601	9.238
172	1966.40	-0.023	-4.939	9.145
173	1966.26	-0.151	-5.077	9.092
174	1966.12	0.037	-5.175	9.103
175	1965.83	-0.043	-5.130	9.100
176	1965.54	0.217	-4.703	9.123
177	1965.40	-0.029	-4.734	9.162
178	1965.26	0.113	-4.960	9.123
179	1965.12	0.374	-4.954	9.102
180	1964.83	0.571	-4.879	9.173
181	1964.54	0.365	-4.806	9.198
182	1964.40	0.119	-4.822	9.184
183	1964.26	-0.127	-5.199	
184	1964.12	0.417	-5.333	9.132
185	1963.83	0.842	-4.956	9.157
186	1963.54	0.465	-4.889	9.223
187	1963.33	0.051	-5.300	9.109
188	1963.12	0.323	-5.320	9.124
189	1962.83	0.434	-5.100	
190	1962.54	0.437	-4.924	
191	1962.40	0.045	-5.060	
192	1962.26	-0.148	-5.106	
193	1962.12	-0.054	-5.304	
194	1961.93	0.265	-5.133	
195	1961.73	0.280	-5.026	
196	1961.54	0.373	-4.900	
197	1961.33	0.250	-5.172	
198	1961.12	0.317	-5.287	
199	1960.93	0.414	-5.065	
200	1960.73	0.320	-4.897	

Depth (mm)	Calendar Year	**d**^{13}C (‰)	**d**^{18}O (‰)
201	1960.54	0.065	-4.819
202	1960.12	-0.218	-5.031
203	1959.98	0.064	-5.030
204	1959.83	0.550	-4.782
205	1959.69	0.517	-4.641
206	1959.54	0.252	-4.562
207	1959.44	0.019	-4.726
208	1959.33	0.087	-4.859
209	1959.23	0.404	-4.763
210	1959.12	0.276	-4.862
211	1958.54	0.173	-4.780
212	1958.40	0.076	-4.812
213	1958.26	-0.151	-5.081
214	1958.12	-0.182	-5.286
215	1957.83	0.087	-5.268
216	1957.54	0.297	-5.022
217	1957.40	0.041	-5.153
218	1957.26	-0.272	-5.320
219	1957.12	-0.196	-5.427
220	1956.93	0.237	-5.270
221	1956.73	0.325	-5.275
222	1956.54	0.129	-5.081
223	1956.40	-0.091	-5.096
224	1956.26	-0.226	-5.162
225	1956.12	-0.169	-5.349
226	1955.98	0.011	-5.260
227	1955.83	0.003	-4.960
228	1955.69	-0.034	-4.920
229	1955.54	-0.095	-4.865
230	1955.12	-0.353	-5.199
231	1954.93	-0.089	-5.054
232	1954.73	0.178	-4.842
233	1954.54	0.327	-4.699
234	1954.44	0.064	-4.756
235	1954.33	-0.232	-4.774
236	1954.23	-0.442	-4.934
237	1954.12	-0.528	-5.328
238	1954.01	0.068	-5.097
239	1953.89	0.154	-4.915
240	1953.77	0.338	-4.921
241	1953.66	0.158	-4.901
242	1953.54	0.081	-4.885
243	1953.33	-0.007	-4.986
244	1953.12	0.350	-5.178
245	1952.83	0.694	-4.953
246	1952.54	0.732	-4.765
247	1952.44	0.455	-4.845
248	1952.33	-0.047	-5.260
249	1952.23	-0.177	-5.365
250	1952.12	-0.018	-5.398

Depth (mm)	Calendar Year	**d**^{13}C (‰)	**d**^{18}O (‰)
251	1951.83	0.386	-5.037
252	1951.54	0.331	-4.963
253	1951.40	0.140	-5.137
254	1951.26	-0.060	-5.339
255	1951.12	0.046	-5.422
256	1950.93	0.428	-5.240
257	1950.73	0.313	-5.065
258	1950.54	0.288	-4.796
259	1950.33	-0.043	-5.175
260	1950.12	-0.029	-5.406
261	1949.83	0.296	-5.008
262	1949.54	0.310	-4.784
263	1949.44	0.112	-4.808
264	1949.33	-0.156	-5.083
265	1949.23	0.002	-5.107
266	1949.12	0.097	-5.268
267	1948.93	0.457	-5.112
268	1948.73	0.532	-4.963
269	1948.54	0.292	-4.682
270	1948.40	-0.170	-4.975
271	1948.26	-0.248	-5.016
272	1948.12	-0.166	-5.317
273	1947.93	0.425	-5.079
274	1947.73	0.312	-4.941
275	1947.54	0.255	-4.738
276	1947.40	-0.071	-5.006
277	1947.26	-0.147	-5.237
278	1947.12	-0.015	-5.267
279	1946.93	0.342	-5.110
280	1946.73	0.409	-4.972
281	1946.54	0.221	-4.865
282	1946.33	-0.133	-5.036
283	1946.12	-0.254	-5.328
284	1945.83	0.117	-5.241
285	1945.54	0.459	-4.920
286	1945.46	0.082	-5.043
287	1945.37	-0.301	-5.223
288	1945.29	-0.309	-5.254
289	1945.21	0.073	-5.347
290	1945.12	0.403	-5.387
291	1944.83	0.479	-4.977
292	1944.54	0.387	-4.893
293	1944.12	0.090	-5.137
294	1943.93	0.324	-5.078
295	1943.73	0.415	-4.779
296	1943.54	0.294	-4.761
297	1943.12	0.006	-5.033
298	1942.98	0.214	-4.899
299	1942.83	0.473	-4.858
300	1942.69	0.462	-4.815
301	1942.54	0.126	-4.686
302	1942.33	-0.072	-4.883
303	1942.12	-0.006	-4.887
304	1941.54	0.193	-4.793

APPENDIX 4

FIJI CORE LH EXOTHECAL SKELETON

STABLE ISOTOPE AND Sr/Ca DATA

Depth (mm)	Calendar Year	**d**^{13}C (‰)	**d**^{18}O (‰)	Sr/Ca (mmol/mol)
0.5	2001.96	-0.168	-4.654	9.102
1.0	2001.79	-0.223	-4.694	9.096
1.5	2001.63	-0.244	-4.623	9.081
2.0	2001.46	-0.469	-4.796	9.051
2.5	2001.29	-0.707	-5.051	9.012
3.0	2001.13	-0.540	-5.059	8.935
3.5	2000.96	-0.656	-5.069	8.954
4.0	2000.79	-0.458	-4.808	9.022
4.5	2000.21	-0.667	-5.120	9.066
5.0	2000.01	-0.307	-4.898	9.077
5.5	1999.82	-0.194	-4.794	9.037
6.0	1999.63	-0.153	-4.740	9.198
6.5	1999.29	-0.250	-4.949	9.171
7.0	1999.14	0.036	-4.636	9.157
7.5	1999.00	-0.257	-4.770	9.174
8.0	1998.85	-0.244	-4.637	9.119
8.5	1998.71	0.095	-4.128	9.176
9.0	1998.65	0.055	-4.178	9.188
9.5	1998.60	-0.533	-4.329	9.199
10.0	1998.54	-0.174	-4.191	9.201
10.5	1998.48	-0.281	-4.201	9.149
11.0	1998.43	-0.505	-4.417	9.153
11.5	1998.37	-0.309	-4.311	9.197
12.0	1998.32	-0.410	-4.583	9.166
12.5	1998.26	-0.397	-4.719	9.088
13.0	1998.21	-0.230	-4.777	9.086
13.5	1998.11	-0.184	-4.541	9.104
14.0	1998.01	0.008	-4.625	9.070
14.5	1997.91	0.075	-4.568	9.134
15.0	1997.81	0.034	-4.438	9.163
15.5	1997.71	-0.066	-4.220	9.144
16.0	1997.60	-0.177	-4.388	9.179
16.5	1997.48	-0.352	-4.416	9.170
17.0	1997.37	-0.601	-4.447	9.211
17.5	1997.26	0.101	-4.421	9.119
18.0	1997.15	-0.618	-4.964	9.106
18.5	1997.04	-0.840	-5.097	9.168
19.0	1996.93	-0.646	-5.075	9.036
19.5	1996.83	-0.569	-5.007	9.085
20.0	1996.73	-0.186	-4.945	9.050
20.5	1996.63	0.106	-4.737	9.097
21.0	1996.56	-0.180	-4.755	9.057
21.5	1996.49	-0.248	-4.749	9.113
22.0	1996.42	-0.287	-4.855	9.105
22.5	1996.35	-0.264	-4.751	9.114
23.0	1996.28	-0.203	-4.775	9.104
23.5	1996.21	-0.569	-5.047	9.116
24.0	1995.98	-0.154	-4.849	9.123
24.5	1995.76	0.437	-4.662	9.198
25.0	1995.54	0.848	-4.531	9.269

Depth (mm)	Calendar Year	$\delta^{13}C$ (‰)	$\delta^{18}O$ (‰)	Sr/Ca (mmol/mol)
25.0	1995.54	0.848	-4.531	9.269
25.5	1995.50	0.576	-4.560	9.226
26.0	1995.45	0.075	-4.802	9.214
26.5	1995.41	-0.176	-4.548	9.241
27.0	1995.37	-0.214	-4.670	9.268
27.5	1995.33	-0.625	-4.790	9.235
28.0	1995.29	-0.431	-4.792	9.167
28.5	1995.25	-0.187	-4.911	9.184
29.0	1995.21	-0.082	-4.952	9.180
29.5	1995.12	0.003	-4.714	9.205
30.0	1995.04	0.209	-4.707	9.187
30.5	1994.96	-0.062	-4.592	9.178
31.0	1994.87	-0.150	-4.477	9.206
31.5	1994.79	-0.187	-4.434	9.252
32.0	1994.71	0.056	-4.359	9.279
32.5	1994.64	-0.249	-4.394	9.219
33.0	1994.56	-0.212	-4.364	9.244
33.5	1994.49	-0.288	-4.681	9.192
34.0	1994.42	-0.302	-4.830	9.136
34.5	1994.35	-0.409	-4.882	9.113
35.0	1994.28	-0.401	-5.055	9.096
35.5	1994.21	-0.226	-5.103	9.004
36.0	1994.11	0.386	-4.786	9.109
36.5	1994.01	0.452	-4.781	9.143
37.0	1993.91	0.160	-4.528	9.211
37.5	1993.81	-0.175	-4.604	9.268
38.0	1993.71	-0.312	-4.433	9.240
38.5	1993.61	-0.629	-4.708	9.237
39.0	1993.51	-0.507	-4.628	9.242
39.5	1993.41	-0.554	-5.016	9.162
40.0	1993.31	-0.631	-4.840	9.162
40.5	1993.21	-0.547	-5.056	9.154
41.0	1993.12	-0.207	-4.971	9.125
41.5	1993.04	-0.329	-4.772	9.132
42.0	1992.96	-0.314	-4.742	9.157
42.5	1992.88	-0.127	-4.596	9.208
43.0	1992.79	-0.236	-4.588	9.258
43.5	1992.71	-0.362	-4.611	9.201
44.0	1992.63	-0.242	-4.534	9.183
44.5	1992.56	-0.570	-4.680	9.177
45.0	1992.50	-0.688	-4.726	9.165
45.5	1992.44	-0.968	-4.954	9.125
46.0	1992.38	-0.656	-4.804	9.105
46.5	1992.31	-0.635	-5.017	9.078
47.0	1992.25	-0.642	-5.065	9.059
47.5	1992.19	-0.375	-4.963	9.040
48.0	1992.13	-0.255	-5.083	9.035
48.5	1992.02	-0.033	-5.024	9.117
49.0	1991.92	-0.265	-4.952	9.068
49.5	1991.81	-0.416	-4.956	9.107
50.0	1991.71	-0.444	-4.672	9.145

Depth (mm)	Calendar Year	d13C (‰)	d18O (‰)	Sr/Ca (mmol/mol)
51	1991.54	-0.666	-4.960	9.137
52	1991.37	-0.637	-4.793	9.128
53	1991.21	-0.729	-5.057	9.073
54	1991.01	-0.622	-5.028	9.093
55	1990.82	-0.569	-4.921	9.121
56	1990.63	-0.810	-4.899	
57	1990.54	-0.675	-4.939	9.145
58	1990.46	-0.246	-5.082	9.161
59	1990.38	0.074	-5.047	9.113
60	1990.29	-0.090	-5.093	9.117
61	1990.21	-0.285	-5.048	9.088
62	1990.13	-0.704	-5.209	9.088
63	1989.63	-0.949	-5.045	9.070
64	1989.33	-0.808	-5.357	9.133
65	1989.04	-0.906	-5.388	8.991
66	1988.90	-0.195	-5.074	9.084
67	1988.76	-0.206	-5.069	9.090
68	1988.63	-0.182	-4.977	9.122
69	1988.13	-0.295	-4.977	9.102
70	1987.98	-0.202	-4.895	9.128
71	1987.83	0.180	-4.519	9.194
72	1987.68	0.210	-4.307	9.248
73	1987.54	-0.042	-4.248	9.311
74	1987.37	-0.198	-4.524	9.248
75	1987.21	0.311	-4.612	9.187
76	1987.01	0.418	-4.568	9.132
77	1986.82	0.387	-4.441	9.168
78	1986.63	0.193	-4.373	9.225
79	1986.49	-0.300	-4.656	9.187
80	1986.35	-0.429	-4.709	9.136
81	1986.21	-0.184	-4.779	9.131
82	1986.01	0.573	-4.655	9.181
83	1985.82	-0.109	-4.650	9.199
84	1985.63	-0.162	-4.643	9.200
85	1985.46	-0.430	-4.857	9.145
86	1985.29	-0.555	-5.079	9.109
87	1985.13	-0.310	-5.145	9.082
88	1984.88	0.158	-4.997	9.092
89	1984.63	0.252	-4.780	9.135
90	1984.49	0.275	-4.834	9.141
91	1984.35	0.050	-4.749	9.089
92	1984.21	0.083	-4.879	9.135
93	1984.06	0.355	-4.748	9.086
94	1983.92	0.540	-4.558	9.180
95	1983.77	-0.048	-4.452	9.219
96	1983.63	-0.069	-4.444	9.221
97	1983.42	-0.013	-4.610	9.172
98	1983.21	0.357	-4.704	9.137
99	1983.04	0.618	-4.674	9.147
100	1982.87	0.181	-4.655	9.204

Depth (mm)	Calendar Year	$\delta^{13}C$ (‰)	$\delta^{18}O$ (‰)	Sr/Ca (mmol/mol)
101	1982.71	0.370	-4.501	9.220
102	1982.37	0.258	-4.905	9.167
103	1982.04	0.571	-4.928	9.112
104	1981.79	1.063	-4.732	9.194
105	1981.54	0.959	-4.487	9.230
106	1981.37	0.418	-4.637	9.229
107	1981.21	0.358	-4.966	
108	1981.01	1.238	-4.943	9.229
109	1980.82	0.767	-4.628	9.232
110	1980.63	0.251	-4.442	9.248
111	1980.49	0.069	-4.592	9.178
112	1980.35	-0.135	-4.861	9.090
113	1980.21	0.167	-5.108	9.142
114	1979.96	0.939	-4.787	9.183
115	1979.71	0.060	-4.693	9.219
116	1979.46	-0.366	-4.748	9.153
117	1979.21	-0.437	-5.018	9.039
118	1979.06	-0.048	-5.013	9.067
119	1978.92	0.370	-4.943	9.112
120	1978.77	0.278	-4.527	9.144
121	1978.63	0.223	-4.442	9.205
122	1978.46	-0.223	-4.590	9.167
123	1978.29	-0.210	-4.873	9.129
124	1978.13	-0.398	-4.925	9.058
125	1978.02	0.023	-4.853	9.110
126	1977.92	0.324	-4.601	9.164
127	1977.81	0.090	-4.446	9.209
128	1977.71	-0.119	-4.386	9.138
129	1977.54	-0.458	-4.762	9.141
130	1977.37	-0.446	-4.776	9.114
131	1977.21	-0.336	-5.082	9.091
132	1977.04	0.177	-4.917	9.120
133	1976.87	-0.034	-4.786	9.160
134	1976.71	0.233	-4.568	9.128
135	1976.57	-0.144	-4.831	9.125
136	1976.43	-0.141	-5.148	9.043
137	1976.29	-0.054	-5.207	9.083
138	1976.12	0.778	-5.208	9.119
139	1975.96	0.604	-4.900	9.174
140	1975.79	-0.056	-4.940	9.179
141	1975.63	-0.233	-4.855	9.156
142	1975.49	-0.299	-5.081	9.116
143	1975.35	-0.353	-5.108	9.145
144	1975.21	0.257	-5.225	9.175
145	1974.98	0.660	-4.956	9.138
146	1974.76	0.383	-4.965	9.132
147	1974.54	0.140	-4.864	9.156
148	1974.33	0.034	-5.036	9.081
149	1974.13	-0.090	-5.235	9.078
150	1973.96	0.613	-4.954	9.078

Depth (mm)	Calendar Year	**d**^{13}C (‰)	**d**^{18}O (‰)	Sr/Ca (mmol/mol)
151	1973.79	0.918	-4.573	9.205
152	1973.63	0.419	-4.540	9.165
153	1973.49	-0.244	-4.712	9.159
154	1973.35	-0.320	-4.990	9.090
155	1973.21	-0.254	-5.033	9.072
156	1973.01	0.396	-4.780	9.108
157	1972.82	0.142	-4.638	9.173
158	1972.63	-0.184	-4.615	9.194
159	1972.49	-0.106	-4.722	9.180
160	1972.35	-0.082	-5.100	9.078
161	1972.21	0.196	-5.213	9.081
162	1972.01	0.408	-4.960	9.115
163	1971.82	0.405	-4.942	9.115
164	1971.63	0.102	-4.798	9.128
165	1971.38	0.222	-4.819	9.080
166	1971.13	-0.018	-5.059	9.133
167	1970.96	0.055	-4.768	9.095
168	1970.79	-0.313	-4.599	9.108
169	1970.57	-0.390	-4.668	9.155
170	1970.35	-0.543	-4.686	9.114
171	1970.13	-0.486	-4.886	9.061
172	1970.00	-0.041	-4.744	9.076
173	1969.87	0.181	-4.812	9.137
174	1969.74	0.517	-4.415	9.256
175	1969.62	0.183	-4.331	9.224
176	1969.41	-0.153	-4.619	9.221
177	1969.21	0.263	-4.840	9.136
178	1969.06	1.206	-4.739	9.218
179	1968.91	0.951	-4.722	9.226
180	1968.76	-0.063	-4.950	9.180
181	1968.62	-0.139	-4.669	9.179
182	1968.41	-0.087	-4.821	9.134
183	1968.21	0.349	-4.956	9.088
184	1968.01	0.205	-4.811	9.155
185	1967.81	0.014	-4.736	9.198
186	1967.62	-0.205	-4.644	9.190
187	1967.21	-0.204	-4.673	9.189
188	1967.01	0.411	-4.608	9.100
189	1966.81	0.394	-4.449	9.009
190	1966.62	0.163	-4.418	9.155
191	1966.41	-0.032	-4.437	9.120
192	1966.21	-0.132	-4.695	9.142
193	1965.91	0.436	-4.579	9.154
194	1965.62	0.586	-4.332	9.209
195	1965.51	0.551	-4.487	9.194
196	1965.41	0.162	-4.612	9.238
197	1965.31	0.063	-4.742	9.176
198	1965.21	0.249	-4.888	
199	1965.06	0.215	-4.756	
200	1964.91	-0.044	-4.787	

Depth (mm)	Calendar Year	d^{13}C (‰)	d^{18}O (‰)
201	1964.76	0.020	-4.609
202	1964.62	0.192	-4.583
203	1964.48	0.510	-4.678
204	1964.34	0.619	-4.685
205	1964.21	0.246	-4.842
206	1964.01	0.303	-4.701
207	1963.81	0.537	-4.690
208	1963.62	0.976	-4.594
209	1963.41	0.760	-4.695
210	1963.21	0.623	-4.825
211	1962.91	1.094	-4.835
212	1962.62	1.016	-4.714
213	1962.48	0.877	-4.747
214	1962.34	0.507	-4.805
215	1962.21	0.623	-4.907
216	1961.62	0.935	-4.710
217	1961.41	0.581	-4.848
218	1961.21	0.395	-4.897
219	1961.11	0.470	-4.891
220	1961.01	0.528	-4.865
221	1960.91	0.592	-4.658
222	1960.81	0.396	-4.639
223	1960.72	0.409	-4.616
224	1960.62	0.318	-4.509
225	1960.21	0.413	-4.778
226	1959.91	0.669	-4.598
227	1959.62	0.542	-4.322
228	1959.48	0.148	-4.372
229	1959.34	0.115	-4.529
230	1959.21	0.258	-4.648
231	1958.91	0.441	-4.556
232	1958.62	0.826	-4.354
233	1958.48	0.366	-4.672
234	1958.34	0.211	-4.818
235	1958.21	0.307	-5.045
236	1957.62	0.649	-4.483
237	1957.48	0.306	-4.800
238	1957.34	0.147	-5.074
239	1957.21	0.136	-5.102
240	1957.06	0.302	-5.064
241	1956.91	0.336	-4.944
242	1956.76	0.354	-4.943
243	1956.62	0.578	-4.882
244	1956.21	0.194	-5.161
245	1956.01	0.355	-4.993
246	1955.81	0.531	-4.719
247	1955.62	0.401	-4.454
248	1955.41	0.025	-4.715
249	1955.21	-0.163	-4.870
250	1955.06	0.323	-4.678

Depth (mm)	Calendar Year	**d**^{13}C (‰)	**d**^{18}O (‰)
251	1954.91	0.469	-4.504
252	1954.76	0.265	-4.476
253	1954.62	0.138	-4.417
254	1954.41	0.137	-4.641
255	1954.21	-0.030	-4.867
256	1954.06	0.528	-4.629
257	1953.91	0.423	-4.566
258	1953.76	-0.112	-4.659
259	1953.62	-0.095	-4.512
260	1953.41	0.034	-4.752
261	1953.21	-0.142	-4.963
262	1952.91	0.163	-4.865
263	1952.62	0.115	-4.592
264	1952.48	0.037	-4.695
265	1952.34	-0.060	-4.864
266	1952.21	0.084	-5.077
267	1952.01	0.357	-5.036
268	1951.81	0.416	-4.850
269	1951.62	0.256	-4.753
270	1951.41	0.022	-4.827
271	1951.21	0.203	-4.938
272	1951.01	0.586	-4.884
273	1950.81	0.536	-4.703
274	1950.62	0.298	-4.678
275	1950.41	0.146	-4.885
276	1950.21	0.240	-5.109
277	1949.91	0.458	-5.045
278	1949.62	0.930	-4.773
279	1949.41	0.506	-4.845
280	1949.21	0.389	-4.966
281	1949.06	0.410	-4.835
282	1948.91	0.717	-4.835
283	1948.76	0.658	-4.752
284	1948.62	0.296	-4.655
285	1948.41	0.150	-4.847
286	1948.21	0.424	-4.920
287	1947.91	0.867	-4.837
288	1947.62	0.544	-4.603
289	1947.41	0.626	-4.627
290	1947.21	0.699	-5.020
291	1946.91	1.151	-4.833
292	1946.62	0.692	-4.580
293	1946.41	0.630	-4.716
294	1946.21	0.653	-4.851
295	1945.91	0.921	-4.807
296	1945.62	0.319	-4.725
297	1945.54	-0.040	-4.800
298	1945.45	-0.323	-4.966
299	1945.37	0.022	-5.021
300	1945.29	0.197	-5.137
301	1945.21	-0.044	-5.199

Depth (mm)	Calendar Year	**d**^{13}C (‰)	**d**^{18}O (‰)
301	1945.21	-0.044	-5.199
302	1944.91	-0.022	-4.908
303	1944.62	-0.021	-4.841
304	1944.41	-0.191	-4.963
305	1944.21	-0.190	-5.178
306	1944.06	0.281	-5.092
307	1943.91	0.177	-4.863
308	1943.76	0.126	-4.652
309	1943.62	-0.063	-4.590
310	1943.41	-0.182	-4.760
311	1943.21	0.007	-4.776
312	1943.01	0.601	-4.767
313	1942.81	0.386	-4.537
314	1942.62	-0.031	-4.454
315	1942.48	-0.282	-4.576
316	1942.34	-0.247	-4.576
317	1942.21	0.429	-4.800
318	1942.01	0.736	-4.525
319	1941.81	0.257	-4.536
320	1941.62	0.078	-4.494
321	1941.41	-0.166	-4.725
322	1941.21	0.029	-4.815
323	1940.91	0.355	-4.809
324	1940.62	0.204	-4.686
325	1940.54	0.206	-4.702
326	1940.45	0.130	-4.715
327	1940.37	-0.302	-4.924
328	1940.29	0.235	-4.947
329	1940.21	0.249	-4.976
330	1939.91	0.073	-4.797
331	1939.62	0.004	-4.586
332	1939.21	-0.158	-4.713
333	1939.01	0.159	-4.703
334	1938.81	0.557	-4.631
335	1938.62	0.748	-4.471
336	1938.51	0.503	-4.553
337	1938.41	0.399	-4.795
338	1938.31	0.595	-4.861
339	1938.21	0.668	-4.897
340	1937.91	1.002	-4.585
341	1937.62	0.565	-4.560
342	1937.41	0.787	-4.654
343	1937.21	1.160	-4.733
344	1937.01	1.173	-4.505
345	1936.81	0.972	-4.364
346	1936.62	0.599	-4.128
347	1936.41	0.588	-4.453
348	1936.21	1.038	-4.628
349	1936.01	1.466	-4.322
350	1935.81	1.051	-4.377

Depth (mm)	Calendar Year	$\delta^{13}C$ (‰)	$\delta^{18}O$ (‰)
351	1935.62	1.230	-4.281
352	1935.51	1.571	-4.286
353	1935.41	0.615	-4.345
354	1935.31	0.184	-4.612
355	1935.21	0.350	-4.798
356	1935.01	1.062	-4.787
357	1934.81	0.571	-4.418
358	1934.62	0.579	-4.405
359	1934.21	0.784	-4.522
360	1934.01	1.030	-4.482
361	1933.81	0.602	-4.444
362	1933.62	0.221	-4.415
363	1933.21	-0.002	-4.439
364	1933.06	0.754	-4.174
365	1932.91	0.341	-4.209
366	1932.76	0.200	-4.072
367	1932.62	0.261	-4.067
368	1932.21	0.214	-4.423
369	1931.91	0.593	-4.388
370	1931.62	0.749	-3.958
371	1931.48	0.138	-4.213
372	1931.34	0.176	-4.243
373	1931.21	0.200	-4.511
374	1931.01	0.512	-4.463
375	1930.81	1.113	-4.267
376	1930.62	0.993	-4.252
377	1930.48	0.406	-4.304
378	1930.34	0.311	-4.475
379	1930.21	0.073	-4.705
380	1930.06	0.048	-4.606
381	1929.91	0.144	-4.689
382	1929.76	0.227	-4.637
383	1929.62	0.075	-4.481
384	1929.48	0.032	-4.503
385	1929.34	0.043	-4.670
386	1929.21	-0.127	-4.961
387	1929.06	-0.121	-4.951
388	1928.91	0.312	-4.588
389	1928.76	0.342	-4.422
390	1928.62	0.088	-4.218
391	1928.41	-0.353	-4.340
392	1928.21	-0.196	-4.472
393	1927.62	0.688	-4.171
394	1927.41	0.329	-4.467
395	1927.21	0.329	-4.471
396	1926.62	0.017	-4.455
397	1926.51	-0.054	-4.508
398	1926.41	-0.236	-4.561
399	1926.31	-0.199	-4.654
400	1926.21	0.239	-4.749

Depth (mm)	Calendar Year	**d**^{13}C (‰)	**d**^{18}O (‰)
401	1925.91	0.397	-4.602
402	1925.62	0.158	-4.474
403	1925.51	-0.244	-4.555
404	1925.41	-0.331	-4.478
405	1925.31	0.375	-4.586
406	1925.21	0.698	-4.596
407	1924.62	0.282	-4.338
408	1924.48	0.109	-4.622
409	1924.34	-0.205	-4.656
410	1924.21	0.095	-4.861
411	1923.62	0.919	-4.606
412	1923.51	0.522	-4.702
413	1923.41	0.270	-4.652
414	1923.31	0.147	-4.837
415	1923.21	0.059	-5.110
416	1923.01	0.438	-4.849
417	1922.81	0.193	-4.850
418	1922.62	0.326	-4.463
419	1922.48	0.283	-4.513
420	1922.34	0.139	-4.916
421	1922.21	0.429	-5.028
422	1921.91	0.704	-4.638
423	1921.62	0.576	-4.486
424	1921.48	0.160	-4.536
425	1921.34	0.022	-4.669
426	1921.21	0.439	-4.731
427	1920.91	0.413	-4.591
428	1920.62	0.690	-4.292
429	1920.48	0.319	-4.359
430	1920.34	0.413	-4.366
431	1920.21	0.629	-4.724
432	1919.91	0.807	-4.696
433	1919.62	0.403	-4.633
434	1919.48	0.076	-4.672
435	1919.34	-0.079	-4.842
436	1919.21	0.231	-4.990
437	1919.01	0.448	-4.989
438	1918.81	0.251	-4.930
439	1918.62	0.070	-4.878
440	1918.48	0.184	-4.930
441	1918.34	0.072	-5.082
442	1918.21	0.147	-5.141
443	1918.01	0.365	-5.050
444	1917.81	0.450	-5.070
445	1917.62	0.234	-4.851
446	1917.48	0.106	-4.948
447	1917.34	-0.078	-4.933
448	1917.21	-0.207	-5.042
449	1917.01	0.106	-5.001
450	1916.81	0.008	-4.974

Depth (mm)	Calendar Year	**d**^{13}C (‰)	**d**^{18}O (‰)
451	1916.62	0.107	-4.522
452	1916.48	0.084	-4.719
453	1916.34	-0.016	-4.713
454	1916.21	0.144	-4.790
455	1916.06	0.739	-4.645
456	1915.91	0.883	-4.688
457	1915.76	0.515	-4.496
458	1915.62	0.121	-4.403
459	1915.41	-0.069	-4.743
460	1915.21	0.032	-4.867
461	1915.06	0.442	-4.701
462	1914.91	0.127	-4.607
463	1914.76	0.154	-4.541
464	1914.62	0.062	-4.522
465	1914.41	0.100	-4.739
466	1914.21	0.068	-5.059
467	1914.01	0.456	-4.874
468	1913.81	0.108	-4.729
469	1913.62	0.231	-4.370
470	1913.51	0.034	-4.524
471	1913.41	-0.167	-4.672
472	1913.31	-0.229	-4.804
473	1913.21	0.133	-4.939
474	1912.91	0.230	-4.852
475	1912.62	0.434	-4.695
476	1912.48	0.255	-4.920
477	1912.34	0.428	-4.945
478	1912.21	0.497	-5.191
479	1911.91	0.653	-4.887
480	1911.62	0.338	-4.829
481	1911.41	0.045	-4.914
482	1911.21	-0.186	-5.026
483	1911.01	0.911	-4.812
484	1910.81	0.256	-5.021
485	1910.62	0.439	-4.765
486	1910.51	0.558	-4.859
487	1910.41	0.101	-4.773
488	1910.31	0.569	-4.835
489	1910.21	0.257	-4.921
490	1909.62	0.322	-4.655
491	1909.41	-0.004	-4.895
492	1909.21	-0.072	-5.072
493	1908.91	0.095	-5.018
494	1908.62	0.025	-4.463
495	1908.48	0.088	-4.562
496	1908.34	-0.251	-4.737
497	1908.21	-0.382	-5.359
498	1908.06	0.403	-5.177
499	1907.91	0.422	-4.854
500	1907.76	0.367	-4.594

Depth (mm)	Calendar Year	**d**^{13}C (‰)	**d**^{18}O (‰)
501	1907.62	-0.091	-4.515
502	1907.21	-0.119	-4.904
503	1907.01	0.592	-4.799
504	1906.81	0.775	-4.568
505	1906.62	0.357	-4.540
506	1906.21	-0.354	-4.801
507	1905.62	-0.253	-4.495
508	1905.48	0.066	-4.727
509	1905.34	0.259	-4.706
510	1905.21	-0.106	-4.761
511	1904.91	-0.098	-4.736
512	1904.62	-0.012	-4.530
513	1904.51	-0.026	-4.778
514	1904.41	0.080	-4.916
515	1904.31	0.095	-5.031
516	1904.21	0.316	-5.087
517	1903.62	-0.081	-4.711
518	1903.21	-0.305	-4.904
519	1903.06	-0.318	-4.838
520	1902.91	0.028	-4.835
521	1902.76	0.279	-4.650
522	1902.62	0.136	-4.551
523	1902.48	-0.231	-4.612
524	1902.34	-0.162	-4.639
525	1902.21	0.952	-4.622
526	1901.91	0.901	-4.863
527	1901.62	0.420	-4.415
528	1901.48	0.095	-4.602
529	1901.34	0.070	-4.752
530	1901.21	0.251	-4.846
531	1900.91	0.417	-4.702
532	1900.62	0.342	-4.570
533	1900.48	0.199	-4.740
534	1900.34	0.331	-4.866
535	1900.21	0.469	-4.951
536	1899.91	0.810	-4.668
537	1899.62	0.453	-4.803
538	1899.48	0.303	-4.762
539	1899.34	0.462	-4.891
540	1899.21	0.548	-5.048
541	1898.91	0.394	-5.002
542	1898.62	0.314	-4.908
543	1898.48	-0.040	-4.934
544	1898.34	-0.298	-5.150
545	1898.21	-0.276	-5.389
546	1898.11	0.019	-5.238
547	1898.01	0.288	-4.990
548	1897.91	0.283	-4.737
549	1897.81	0.237	-4.670
550	1897.72	-0.221	-4.652

Depth (mm)	Calendar Year	$\delta^{13}C$ (‰)	$\delta^{18}O$ (‰)
551	1897.62	-0.307	-4.634
552	1897.21	0.157	-4.839
553	1896.62	0.207	-4.520
554	1896.48	-0.021	-4.634
555	1896.34	-0.170	-4.711
556	1896.21	0.024	-5.096
557	1896.01	0.371	-4.936
558	1895.81	-0.011	-4.841
559	1895.62	-0.214	-4.786
560	1895.41	-0.577	-5.000
561	1895.21	-0.719	-5.311
562	1894.62	-0.014	-4.841
563	1894.51	-0.079	-4.988
564	1894.41	-0.057	-4.968
565	1894.31	0.230	-5.035
566	1894.21	0.677	-5.111
567	1893.62	0.221	-5.053
568	1893.41	-0.088	-5.084
569	1893.21	-0.441	-5.416
570	1893.09	-0.101	-5.194
571	1892.97	-0.442	-5.138
572	1892.85	-0.434	-5.020
573	1892.74	-0.348	-4.838
574	1892.62	-0.244	-4.775
575	1892.41	-0.177	-4.960
576	1892.21	0.628	-5.058
577	1892.01	-0.064	-5.010
578	1891.81	-0.257	-4.847
579	1891.62	-0.433	-4.772
580	1891.41	-0.481	-5.062
581	1891.21	-0.260	-5.134
582	1891.06	-0.127	-5.038
583	1890.91	-0.147	-5.021
584	1890.76	0.076	-4.697
585	1890.62	-0.272	-4.665
586	1890.48	-0.449	-4.853
587	1890.34	-0.667	-4.998
588	1890.21	-0.431	-5.162
589	1890.01	0.031	-4.930
590	1889.81	-0.080	-4.654
591	1889.62	-0.013	-4.415
592	1889.41	0.355	-4.542
593	1889.21	0.475	-4.593
594	1888.62	0.274	-4.536
595	1888.48	-0.089	-4.745
596	1888.34	0.048	-4.880
597	1888.21	-0.146	-5.032
598	1888.01	0.375	-4.871
599	1887.81	0.326	-4.857
600	1887.62	0.264	-4.590

Depth (mm)	Calendar Year	**d**^{13}C (‰)	**d**^{18}O (‰)
601	1887.48	0.056	-4.751
602	1887.34	0.154	-4.750
603	1887.21	0.427	-4.951
604	1887.01	0.416	-4.846
605	1886.81	0.472	-4.593
606	1886.62	0.345	-4.466
607	1886.41	0.234	-4.575
608	1886.21	0.570	-4.704
609	1886.01	0.671	-4.408
610	1885.81	0.742	-4.217
611	1885.62	0.508	-4.136
612	1885.48	0.435	-4.410
613	1885.34	0.520	-4.554
614	1885.21	0.587	-4.566
615	1884.62	0.626	-4.260
616	1884.48	0.379	-4.406
617	1884.34	0.477	-4.513
618	1884.21	0.613	-4.659
619	1883.91	1.190	-4.537
620	1883.62	0.736	-4.323
621	1883.48	0.269	-4.524
622	1883.34	0.392	-4.817
623	1883.21	0.598	-4.843
624	1883.01	0.729	-4.572
625	1882.81	0.549	-4.592
626	1882.62	0.364	-4.582
627	1882.48	0.163	-5.053
628	1882.34	0.476	-4.958
629	1882.21	0.609	-5.134
630	1882.01	0.489	-4.886
631	1881.81	0.416	-4.870
632	1881.62	0.213	-4.611
633	1881.48	0.144	-4.838
634	1881.34	0.020	-4.879
635	1881.21	0.381	-5.008
636	1880.62	0.479	-4.588
637	1880.51	0.298	-4.712
638	1880.41	0.226	-5.008
639	1880.31	0.329	-5.142
640	1880.21	0.378	-5.174
641	1880.06	0.587	-5.024
642	1879.91	0.609	-4.953
643	1879.76	0.473	-4.641
644	1879.62	0.421	-4.615
645	1879.48	0.253	-4.649
646	1879.34	0.029	-4.839
647	1879.21	0.089	-4.856
648	1879.01	0.719	-4.733
649	1878.81	0.862	-4.548
650	1878.62	0.732	-4.205

Depth (mm)	Calendar Year	$\delta^{13}C$ (‰)	$\delta^{18}O$ (‰)
651	1878.48	0.451	-4.336
652	1878.34	0.433	-4.467
653	1878.21	0.454	-4.502
654	1878.01	0.838	-4.381
655	1877.81	0.512	-4.285
656	1877.62	0.269	-4.161
657	1877.48	-0.002	-4.480
658	1877.34	0.093	-4.733
659	1877.21	0.051	-4.782
660	1876.91	0.203	-4.598
661	1876.62	0.315	-4.378
662	1876.51	0.264	-4.400
663	1876.41	0.318	-4.464
664	1876.31	0.433	-4.695
665	1876.21	0.776	-4.779
666	1876.01	0.894	-4.644
667	1875.81	0.214	-4.646
668	1875.62	0.182	-4.441
669	1875.48	0.005	-4.808
670	1875.34	-0.007	-4.941
671	1875.21	0.479	-4.997
672	1874.91	0.402	-4.773
673	1874.62	0.396	-4.482
674	1874.51	0.410	-4.513
675	1874.41	0.219	-4.728
676	1874.31	0.445	-4.734
677	1874.21	0.637	-4.767
678	1874.01	0.232	-4.715
679	1873.81	-0.059	-4.679
680	1873.62	-0.262	-4.609
681	1873.48	-0.223	-4.802
682	1873.34	0.358	-4.923
683	1873.21	0.549	-4.962
684	1872.91	0.430	-4.718
685	1872.62	0.395	-4.609
686	1872.41	0.109	-4.667
687	1872.21	-0.122	-5.156
688	1872.06	0.096	-5.049
689	1871.91	0.641	-4.975
690	1871.76	0.240	-4.922
691	1871.62	-0.001	-4.887
692	1871.48	-0.078	-5.035
693	1871.34	-0.105	-5.109
694	1871.21	-0.065	-5.096
695	1871.06	0.159	-5.090
696	1870.91	0.257	-4.854
697	1870.76	0.309	-4.794
698	1870.62	0.354	-4.631
699	1870.21	0.275	-4.814
700	1869.91	0.829	-4.576

Depth (mm)	Calendar Year	**d**13C (‰)	**d**18O (‰)
701	1869.62	0.522	-4.294
702	1869.51	-0.049	-4.435
703	1869.41	-0.378	-4.690
704	1869.31	-0.350	-4.833
705	1869.21	-0.259	-4.838
706	1869.01	-0.001	-4.627
707	1868.81	0.479	-4.542
708	1868.62	0.438	-4.540
709	1868.41	0.021	-4.772
710	1868.21	-0.174	-4.869
711	1868.11	0.151	-4.852
712	1868.01	0.400	-4.790
713	1867.91	0.527	-4.529
714	1867.81	0.355	-4.423
715	1867.72	0.181	-4.527
716	1867.62	0.326	-4.399
717	1867.41	0.422	-4.810
718	1867.21	0.615	-4.854
719	1867.01	0.640	-4.567
720	1866.81	0.703	-4.601
721	1866.62	0.606	-4.470
722	1866.21	0.221	-4.701
723	1866.01	0.479	-4.574
724	1865.81	0.287	-4.666
725	1865.62	0.607	-4.471
726	1865.41	0.472	-4.808
727	1865.21	0.372	-4.821
728	1864.91	0.477	-4.660
729	1864.62	0.446	-4.520
730	1864.51	0.392	-4.690
731	1864.41	0.380	-4.548
732	1864.31	0.716	-4.753
733	1864.21	0.983	-4.820
734	1864.01	0.739	-4.735
735	1863.81	0.577	-4.733
736	1863.62	0.666	-4.703
737	1863.21	1.122	-4.834
738	1862.91	0.377	-4.809
739	1862.62	0.420	-4.638
740	1862.41	0.154	-4.846
741	1862.21	0.130	-4.885
742	1862.01	0.308	-4.852
743	1861.81	-0.004	-4.724
744	1861.62	0.188	-4.674
745	1861.41	-0.120	-4.898
746	1861.21	-0.183	-5.055
747	1861.06	0.491	-4.890
748	1860.91	0.290	-5.000
749	1860.76	-0.001	-4.602
750	1860.62	-0.145	-4.469

Depth (mm)	Calendar Year	$\delta^{13}C$ (‰)	$\delta^{18}O$ (‰)
751	1860.48	-0.130	-4.729
752	1860.34	-0.184	-4.947
753	1860.21	-0.155	-5.143
754	1860.06	0.064	-4.999
755	1859.91	-0.056	-4.802
756	1859.76	0.053	-4.783
757	1859.62	-0.011	-4.572
758	1859.48	-0.027	-4.757
759	1859.34	-0.219	-4.807
760	1859.21	-0.206	-4.910
761	1859.01	0.236	-4.663
762	1858.81	-0.176	-4.567
763	1858.62	0.052	-4.477
764	1858.48	-0.051	-4.548
765	1858.34	0.135	-4.481
766	1858.21	0.071	-4.994
767	1858.06	0.254	-4.850
768	1857.91	-0.044	-4.810
769	1857.76	-0.311	-4.818
770	1857.62	-0.334	-4.695
771	1857.41	-0.295	-4.931
772	1857.21	-0.276	-5.192
773	1857.09	-0.158	-5.116
774	1856.97	-0.028	-4.855
775	1856.85	-0.158	-4.845
776	1856.74	-0.173	-4.618
777	1856.62	-0.388	-4.473
778	1856.48	-0.207	-4.679
779	1856.34	-0.238	-4.912
780	1856.21	-0.033	-5.031
781	1856.01	0.111	-4.687
782	1855.81	0.029	-4.581
783	1855.62	0.219	-4.481
784	1855.51	-0.112	-4.541
785	1855.41	-0.097	-4.591
786	1855.31	-0.232	-5.033
787	1855.21	0.096	-5.141
788	1855.01	0.136	-4.852
789	1854.81	0.504	-4.684
790	1854.62	0.212	-4.582
791	1854.48	-0.202	-4.698
792	1854.34	-0.275	-4.612
793	1854.21	0.150	-4.728
794	1854.06	-0.034	-4.577
795	1853.91	0.008	-4.654
796	1853.76	-0.153	-4.682
797	1853.62	-0.345	-4.507
798	1853.41	-0.592	-4.724
799	1853.21	-0.570	-4.868
800	1853.09	-0.160	-4.577

Depth (mm)	Calendar Year	$\delta^{13}C$ (‰)	$\delta^{18}O$ (‰)
801	1852.97	-0.037	-4.642
802	1852.85	-0.243	-4.532
803	1852.74	-0.549	-4.574
804	1852.62	-0.276	-4.506
805	1852.48	-0.285	-4.693
806	1852.34	-0.201	-4.622
807	1852.21	-0.036	-4.870
808	1852.01	0.038	-4.527
809	1851.81	0.322	-4.382
810	1851.62	0.360	-4.325
811	1851.48	-0.277	-4.600
812	1851.34	-0.297	-4.703
813	1851.21	-0.243	-4.880
814	1850.91	0.140	-4.541
815	1850.62	0.415	-4.473
816	1850.51	0.006	-4.544
817	1850.41	-0.426	-4.581
818	1850.31	-0.391	-4.487
819	1850.21	-0.099	-4.597
820	1850.01	0.279	-4.515
821	1849.81	0.093	-4.585
822	1849.62	0.132	-4.467
823	1849.48	0.001	-4.742
824	1849.34	-0.144	-4.950
825	1849.21	-0.300	-5.112
826	1849.01	-0.065	-4.902
827	1848.81	-0.456	-4.921
828	1848.62	-0.200	-4.691
829	1848.48	-0.197	-4.763
830	1848.34	-0.326	-4.897
831	1848.21	-0.675	-5.155
832	1848.09	-0.214	-5.065
833	1847.97	-0.393	-5.081
834	1847.85	-0.200	-4.893
835	1847.74	-0.204	-4.746
836	1847.62	-0.232	-4.649
837	1847.41	-0.220	-4.870
838	1847.21	-0.154	-5.122
839	1846.91	-0.130	-5.111
840	1846.62	-0.090	-4.573
841	1846.55	0.102	-4.608
842	1846.48	0.143	-4.588
843	1846.41	-0.152	-4.848
844	1846.34	0.015	-4.834
845	1846.28	0.300	-4.793
846	1846.21	-0.106	-4.855
847	1845.91	0.205	-4.509
848	1845.62	-0.288	-4.453
849	1845.48	-0.191	-4.547
850	1845.34	-0.064	-4.855

Depth (mm)	Calendar Year	$\delta^{13}C$ (‰)	$\delta^{18}O$ (‰)
851	1845.21	-0.026	-4.978
852	1845.01	0.003	-4.919
853	1844.81	0.339	-4.750
854	1844.62	0.380	-4.433
855	1844.48	0.108	-4.486
856	1844.34	0.028	-4.696
857	1844.21	0.126	-4.947
858	1844.01	0.409	-4.703
859	1843.81	0.095	-4.769
860	1843.62	0.136	-4.610
861	1843.51	-0.044	-4.672
862	1843.41	0.162	-4.849
863	1843.31	-0.166	-5.042
864	1843.21	-0.156	-5.067
865	1843.01	0.375	-4.863
866	1842.81	0.380	-4.854
867	1842.62	0.361	-4.559
868	1842.48	0.337	-4.723
869	1842.34	0.361	-4.855
870	1842.21	0.126	-5.141
871	1842.01	0.141	-4.927
872	1841.81	0.403	-4.564
873	1841.62	0.206	-4.492
874	1841.48	0.086	-4.678
875	1841.34	0.448	-4.701
876	1841.21	0.409	-4.764
877	1840.91	0.465	-4.527
878	1840.62	0.496	-4.430
879	1840.48	0.471	-4.727
880	1840.34	0.356	-4.795
881	1840.21	0.454	-4.799
882	1839.91	0.548	-4.501
883	1839.62	0.643	-4.440
884	1839.48	0.402	-4.471
885	1839.34	0.382	-4.574
886	1839.21	0.486	-4.713
887	1838.91	0.545	-4.639
888	1838.62	0.498	-4.542
889	1838.51	0.123	-4.606
890	1838.41	-0.054	-4.780
891	1838.31	0.111	-4.917
892	1838.21	0.352	-4.959
893	1838.06	0.210	-4.667
894	1837.91	0.177	-4.659
895	1837.76	0.058	-4.639
896	1837.62	-0.004	-4.543
897	1837.41	0.026	-4.785
898	1837.21	0.120	-4.896
899	1836.91	0.062	-4.763
900	1836.62	0.031	-4.570

Depth (mm)	Calendar Year	**d**^{13}C (‰)	**d**^{18}O (‰)
901	1836.51	-0.007	-4.646
902	1836.41	-0.026	-4.598
903	1836.31	-0.107	-4.937
904	1836.21	-0.065	-5.037
905	1836.01	0.024	-4.796
906	1835.81	-0.034	-4.826
907	1835.62	-0.054	-4.539
908	1835.51	-0.144	-4.596
909	1835.41	-0.046	-4.540
910	1835.31	0.149	-4.868
911	1835.21	0.135	-5.027
912	1835.01	0.288	-4.764
913	1834.81	0.348	-4.512
914	1834.62	0.450	-4.338
915	1834.48	0.028	-4.462
916	1834.34	0.089	-4.629
917	1834.21	0.399	-4.679
918	1833.91	0.703	-4.302
919	1833.62	0.556	-4.289
920	1833.51	0.305	-4.436
921	1833.41	0.141	-4.503
922	1833.31	-0.101	-4.892
923	1833.21	0.243	-4.942
924	1833.06	0.365	-4.782
925	1832.91	0.087	-4.712
926	1832.76	0.318	-4.572
927	1832.62	0.329	-4.517
928	1832.51	0.253	-4.714
929	1832.41	0.356	-4.723
930	1832.31	0.276	-4.721
931	1832.21	0.060	-4.713
932	1831.91	0.369	-4.608
933	1831.62	0.348	-4.396
934	1831.48	-0.078	-4.624
935	1831.34	-0.049	-4.716
936	1831.21	-0.169	-4.856
937	1831.09	0.073	-4.773
938	1830.97	-0.086	-4.787
939	1830.85	0.315	-4.612
940	1830.74	0.324	-4.723
941	1830.62	0.031	-4.602
942	1830.48	-0.128	-4.705
943	1830.34	-0.201	-5.013
944	1830.21	-0.212	-5.063
945	1829.91	-0.215	-4.759
946	1829.62	0.358	-4.611
947	1829.51	0.308	-4.667
948	1829.41	0.340	-4.726
949	1829.31	0.092	-4.911
950	1829.21	-0.082	-5.083

Depth (mm)	Calendar Year	$\delta^{13}C$ (‰)	$\delta^{18}O$ (‰)
951	1829.01	0.270	-4.653
952	1828.81	0.287	-4.732
953	1828.62	0.302	-4.589
954	1828.41	0.036	-4.777
955	1828.21	0.068	-4.998
956	1828.06	0.510	-4.932
957	1827.91	0.509	-4.556
958	1827.76	0.567	-4.387
959	1827.62	0.434	-4.369
960	1827.41	0.041	-4.762
961	1827.21	0.009	-4.916
962	1827.06	0.481	-4.728
963	1826.91	0.973	-4.642
964	1826.76	1.058	-4.659
965	1826.62	0.660	-4.553
966	1826.41	0.633	-4.779
967	1826.21	0.596	-4.775
968	1826.06	0.690	-4.495
969	1825.91	0.987	-4.326
970	1825.76	0.883	-4.209
971	1825.62	0.469	-3.960
972	1825.41	0.690	-4.056
973	1825.21	0.707	-4.379
974	1824.91	0.661	-4.340
975	1824.62	0.666	-4.255
976	1824.54	0.294	-4.354
977	1824.45	0.059	-4.508
978	1824.37	0.316	-4.740
979	1824.29	0.346	-4.913
980	1824.21	0.584	-4.936
981	1824.06	0.133	-4.809
982	1823.91	0.411	-4.581
983	1823.76	0.246	-4.475
984	1823.62	0.110	-4.470
985	1823.41	0.258	-4.665
986	1823.21	0.729	-4.658
987	1822.91	1.057	-4.525
988	1822.62	0.753	-4.210
989	1822.48	0.356	-4.394
990	1822.34	0.337	-4.464
991	1822.21	0.486	-4.711
992	1822.01	0.823	-4.442
993	1821.81	0.807	-4.489
994	1821.62	0.733	-4.380
995	1821.51	0.394	-4.615
996	1821.41	0.678	-4.604
997	1821.31	1.111	-4.542
998	1821.21	0.730	-4.675
999	1820.91	0.376	-4.630
1000	1820.62	0.287	-4.580

Depth (mm)	Calendar Year	**d**^{13}C (‰)	**d**^{18}O (‰)
1001	1820.54	0.574	-4.672
1002	1820.45	0.771	-4.715
1003	1820.37	0.345	-4.763
1004	1820.29	0.123	-4.899
1005	1820.21	0.007	-5.064
1006	1820.09	0.098	-4.935
1007	1819.97	0.278	-4.923
1008	1819.85	0.217	-4.669
1009	1819.74	0.289	-4.684
1010	1819.62	0.057	-4.428
1011	1819.48	-0.285	-4.612
1012	1819.34	-0.193	-4.708
1013	1819.21	0.237	-4.711
1014	1818.91	0.327	-4.501
1015	1818.62	0.275	-4.369
1016	1818.48	0.019	-4.475
1017	1818.34	0.069	-4.646
1018	1818.21	0.454	-4.701
1019	1818.01	0.364	-4.642
1020	1817.81	0.288	-4.474
1021	1817.62	0.027	-4.349
1022	1817.41	-0.050	-4.561
1023	1817.21	-0.090	-4.850
1024	1817.06	0.182	-4.623
1025	1816.91	0.324	-4.532
1026	1816.76	0.361	-4.475
1027	1816.62	0.262	-4.409
1028	1816.48	0.121	-4.588
1029	1816.34	0.294	-4.777
1030	1816.21	0.467	-4.822
1031	1815.91	0.001	-4.573
1032	1815.62	0.259	-4.254
1033	1815.48	0.049	-4.497
1034	1815.34	-0.190	-4.704
1035	1815.21	0.043	-4.904
1036	1815.09	0.441	-4.576
1037	1814.97	0.276	-4.571
1038	1814.85	0.395	-4.531
1039	1814.74	0.445	-4.547
1040	1814.62	0.067	-4.405
1041	1814.41	0.004	-4.573
1042	1814.21	0.101	-4.740
1043	1814.06	0.276	-4.694
1044	1813.91	0.405	-4.564
1045	1813.76	0.692	-4.504
1046	1813.62	0.535	-4.488
1047	1813.41	0.431	-4.631
1048	1813.21	0.463	-4.639
1049	1813.01	0.663	-4.402
1050	1812.81	0.609	-4.495

Depth (mm)	Calendar Year	**d**^{13}C (‰)	**d**^{18}O (‰)
1051	1812.62	0.682	-4.255
1052	1812.48	0.320	-4.317
1053	1812.34	0.353	-4.457
1054	1812.21	0.254	-4.677
1055	1812.06	0.414	-4.580
1056	1811.91	0.710	-4.374
1057	1811.76	0.717	-4.124
1058	1811.62	0.598	-4.091
1059	1811.41	0.333	-4.180
1060	1811.21	0.114	-4.513
1061	1811.06	0.368	-4.463
1062	1810.91	0.395	-4.368
1063	1810.76	0.410	-4.460
1064	1810.62	0.488	-4.070
1065	1810.54	0.411	-4.299
1066	1810.45	0.109	-4.374
1067	1810.37	0.038	-4.506
1068	1810.29	0.163	-4.569
1069	1810.21	0.227	-4.686
1070	1810.01	0.546	-4.528
1071	1809.81	0.501	-4.342
1072	1809.62	0.399	-4.200
1073	1809.48	0.272	-4.435
1074	1809.34	0.168	-4.629
1075	1809.21	0.270	-4.956
1076	1809.09	0.157	-4.691
1077	1808.97	0.369	-4.707
1078	1808.85	0.364	-4.745
1079	1808.74	0.396	-4.611
1080	1808.62	0.388	-4.574
1081	1808.21	0.045	-4.801
1082	1808.09	0.006	-4.764
1083	1807.97	0.305	-4.723
1084	1807.85	0.310	-4.725
1085	1807.74	0.155	-4.608
1086	1807.62	0.279	-4.512
1087	1807.48	-0.026	-4.728
1088	1807.34	0.080	-4.798
1089	1807.21	0.165	-4.888
1090	1807.06	0.473	-4.769
1091	1806.91	0.687	-4.744
1092	1806.76	0.387	-4.746
1093	1806.62	0.234	-4.502
1094	1806.51	-0.016	-4.647
1095	1806.41	-0.178	-4.674
1096	1806.31	-0.011	-4.703
1097	1806.21	0.210	-4.711
1098	1806.01	0.620	-4.327
1099	1805.81	0.590	-4.216
1100	1805.62	0.520	-3.984

Depth (mm)	Calendar Year	$\delta^{13}C$ (‰)	$\delta^{18}O$ (‰)
1101	1805.41	0.223	-4.070
1102	1805.21	0.032	-4.277
1103	1805.09	0.231	-4.260
1104	1804.97	0.394	-4.199
1105	1804.85	0.388	-4.268
1106	1804.74	0.440	-4.088
1107	1804.62	0.382	-4.070
1108	1804.48	0.229	-4.416
1109	1804.34	0.036	-4.596
1110	1804.21	0.028	-4.683
1111	1804.06	0.351	-4.587
1112	1803.91	0.371	-4.530
1113	1803.76	0.295	-4.494
1114	1803.62	0.357	-4.389
1115	1803.51	0.213	-4.409
1116	1803.41	0.081	-4.524
1117	1803.31	0.059	-4.827
1118	1803.21	0.196	-4.908
1119	1803.09	0.216	-4.751
1120	1802.97	0.155	-4.833
1121	1802.85	0.301	-4.505
1122	1802.74	0.105	-4.459
1123	1802.62	-0.077	-4.310
1124	1802.48	-0.116	-4.425
1125	1802.34	-0.040	-4.587
1126	1802.21	0.086	-4.603
1127	1802.01	0.165	-4.415
1128	1801.81	0.145	-4.370
1129	1801.62	0.484	-4.232
1130	1801.48	0.281	-4.348
1131	1801.34	0.175	-4.457
1132	1801.21	0.258	-4.577
1133	1801.01	0.535	-4.514
1134	1800.81	0.495	-4.493
1135	1800.62	0.422	-4.248
1136	1800.51	0.325	-4.294
1137	1800.41	0.171	-4.274
1138	1800.31	0.058	-4.412
1139	1800.21	0.097	-4.579
1140	1800.01	0.202	-4.497
1141	1799.81	0.093	-4.261
1142	1799.62	0.257	-4.268
1143	1799.48	0.181	-4.480
1144	1799.34	-0.030	-4.677
1145	1799.21	-0.097	-4.862
1146	1799.09	0.064	-4.851
1147	1798.97	0.110	-4.598
1148	1798.85	0.235	-4.590
1149	1798.74	0.309	-4.425
1150	1798.62	0.158	-4.350

Depth (mm)	Calendar Year	$\delta^{13}C$ (‰)	$\delta^{18}O$ (‰)
1151	1798.48	0.036	-4.442
1152	1798.34	0.169	-4.506
1153	1798.21	0.311	-4.522
1154	1797.62	0.441	-4.346
1155	1797.54	0.396	-4.503
1156	1797.45	0.380	-4.641
1157	1797.37	0.149	-4.916
1158	1797.29	0.025	-5.114
1159	1797.21	0.145	-5.243
1160	1797.01	0.167	-5.015
1161	1796.81	0.091	-4.729
1162	1796.62	0.217	-4.631
1163	1796.51	0.180	-4.646
1164	1796.41	0.198	-4.687
1165	1796.31	0.241	-4.902
1166	1796.21	0.297	-4.982
1167	1796.01	0.416	-4.658
1168	1795.81	0.252	-4.656
1169	1795.62	0.359	-4.653
1170	1795.48	0.213	-4.711
1171	1795.34	0.122	-4.769
1172	1795.21	-0.033	-4.843
1173	1795.06	0.344	-4.537
1174	1794.91	0.069	-4.478
1175	1794.76	0.301	-4.325
1176	1794.62	0.068	-4.222
1177	1794.48	-0.109	-4.363
1178	1794.34	-0.083	-4.579
1179	1794.21	-0.109	-4.617
1180	1794.09	0.212	-4.356
1181	1793.97	0.172	-4.466
1182	1793.85	0.156	-4.270
1183	1793.74	-0.103	-4.253
1184	1793.62	0.103	-4.192
1185	1793.21	-0.066	-4.512
1186	1793.06	0.317	-4.465
1187	1792.91	0.236	-4.369
1188	1792.76	0.144	-4.256
1189	1792.62	-0.027	-4.198
1190	1792.48	-0.034	-4.320
1191	1792.34	-0.057	-4.568
1192	1792.21	-0.097	-4.813
1193	1792.06	0.261	-4.772
1194	1791.91	0.502	-4.708
1195	1791.76	0.411	-4.610
1196	1791.62	0.381	-4.537
1197	1791.41	0.140	-4.692
1198	1791.21	-0.006	-4.824
1199	1791.11	0.229	-4.761
1200	1791.01	0.466	-4.627

Depth (mm)	Calendar Year	$\delta^{13}C$ (‰)	$\delta^{18}O$ (‰)
1201	1790.91	0.304	-4.543
1202	1790.81	0.097	-4.408
1203	1790.72	0.160	-4.381
1204	1790.62	0.126	-4.216
1205	1790.41	0.046	-4.811
1206	1790.21	0.220	-4.862
1207	1790.01	0.410	-4.738
1208	1789.81	0.316	-4.496
1209	1789.62	0.163	-4.487
1210	1789.41	-0.093	-4.728
1211	1789.21	-0.002	-5.079
1212	1789.06	0.245	-4.840
1213	1788.91	0.546	-4.807
1214	1788.76	0.201	-4.627
1215	1788.62	0.237	-4.444
1216	1788.48	0.100	-4.721
1217	1788.34	-0.079	-4.692
1218	1788.21	0.584	-4.732
1219	1788.01	0.498	-4.689
1220	1787.81	0.273	-4.579
1221	1787.62	0.309	-4.422
1222	1787.48	0.047	-4.445
1223	1787.34	-0.041	-4.644
1224	1787.21	0.209	-4.780
1225	1786.62	0.343	-4.510
1226	1786.51	0.280	-4.557
1227	1786.41	-0.001	-4.578
1228	1786.31	-0.099	-4.776
1229	1786.21	0.021	-4.800
1230	1786.01	0.411	-4.563
1231	1785.81	-0.020	-4.364
1232	1785.62	0.373	-4.256
1233	1785.48	0.120	-4.367
1234	1785.34	0.066	-4.387
1235	1785.21	0.289	-4.562
1236	1785.01	0.922	-4.487
1237	1784.81	0.878	-4.368
1238	1784.62	0.188	-4.329
1239	1784.51	0.104	-4.337
1240	1784.41	0.163	-4.413
1241	1784.31	0.157	-4.517
1242	1784.21	0.163	-4.923
1243	1784.06	0.031	-4.552
1244	1783.91	0.147	-4.300
1245	1783.76	0.026	-4.263
1246	1783.62	0.001	-4.118
1247	1783.51	-0.135	-4.414
1248	1783.41	-0.131	-4.711
1249	1783.31	-0.041	-4.725
1250	1783.21	-0.078	-4.834

Depth (mm)	Calendar Year	$\delta^{13}C$ (‰)	$\delta^{18}O$ (‰)
1251	1783.06	0.051	-4.468
1252	1782.91	-0.006	-4.308
1253	1782.76	0.219	-4.253
1254	1782.62	0.238	-4.220
1255	1782.41	0.010	-4.435
1256	1782.21	-0.166	-4.747
1257	1782.06	-0.028	-4.730
1258	1781.91	0.280	-4.633
1259	1781.76	0.407	-4.457
1260	1781.62	0.349	-4.183
1261	1781.51	0.038	-4.276
1262	1781.41	-0.146	-4.460
1263	1781.31	0.065	-4.657
1264	1781.21	-0.019	-4.697
1265	1781.06	0.085	-4.388
1266	1780.91	0.106	-4.564
1267	1780.76	0.084	-4.301
1268	1780.62	-0.198	-4.020
1269	1780.51	0.014	-4.252
1270	1780.41	-0.010	-4.452
1271	1780.31	0.023	-4.681
1272	1780.21	0.064	-4.702
1273	1780.01	0.226	-4.551
1274	1779.81	0.339	-4.375
1275	1779.62	0.232	-4.360
1276	1779.41	-0.061	-4.464
1277	1779.21	-0.167	-4.622
1278	1779.06	-0.096	-4.600
1279	1778.91	0.449	-4.522
1280	1778.76	0.392	-4.388
1281	1778.62	0.141	-4.177
1282	1778.41	0.037	-4.281
1283	1778.21	-0.037	-4.461
1284	1778.06	0.424	-4.273
1285	1777.91	0.883	-4.207
1286	1777.76	0.634	-4.130
1287	1777.62	0.373	-4.050
1288	1777.48	0.249	-4.251
1289	1777.34	0.392	-4.327
1290	1777.21	0.389	-4.630
1291	1777.01	0.946	-4.236
1292	1776.81	0.569	-4.223
1293	1776.62	0.378	-4.014